A MATHEMATICAL MODEL DEVELOPMENT FOR SIMULATING IN-STREAM PROCESSES OF NON-POINT SOURCE POLLUTANTS

By

Joy Tuoyo Adu

Student No: 216075524

Submitted in fulfilment of the academic requirements for the degree of

Doctor of Philosophy in Civil Engineering

College of Agriculture, Engineering and Science,

University of KwaZulu-Natal,

Howard College Campus, Durban.

December 2018

SUPERVISOR: Dr Muthukrishna vellaisamy Kumarasamy

EXAMINER'S COPY

DECLARATION

Supervisor:

As the candidate's Supervisor I agree/do not agree to the submission of this dissertation.

Signed …...……. (Dr Muthukrishna Vellaisamy Kumarasamy) Date.……

Candidate:

I, **Joy Tuoyo Adu**, declare that:

1. The research reported in this thesis, except where otherwise indicated, is my original research.

2. This thesis has not been submitted for any degree or examination at any other university.

3. This thesis does not contain other persons' data, pictures, graphs or other information, unless specifically acknowledged as being sourced from other persons.

4. This thesis does not contain other persons' writing, unless specifically acknowledged as being sourced from other researchers. Where other written sources have been quoted, then:

a. Their words have been re-written, but the general information attributed to them has been referenced
b. Where their exact words have been used, then their writing has been placed in italics and inside quotation marks and referenced.

5. This thesis does not contain text, graphics or tables copied and pasted from the Internet, unless specifically acknowledged, and the source being detailed in the thesis and in the References sections.

…….. ……

Joy Tuoyo Adu Date

ACKNOWLEDGEMENTS

My utmost appreciation and sincere gratitude go to my supervisor Dr Muthukrishna vellaisamy Kumarasamy for his consistent guidance, constructive feedback and suggestions, encouragement, kindness and financial support which has contributed to the success of this work. Dr Sam thank you so much for believing in me.

My thanks go to Water Research Commission of South Africa for giving funding to support this study. Also, my immense appreciation goes to Prof Kenneth Bencala and Prof Robert Runkel for providing me with data from their research.

I wish to express my sincere appreciation to the following individuals Ooma Chetty, Naomi Njovbu, Kayode Olowe, Dagmawit Badge, Thabani Mbutho, Kenneth Njibana, Peter Mmopane, Ope Makinde, and Deji Ogunode, Thank you for your constant support and encouragement during my study.

To my beautiful children, Moyinoluwa, Mosopefoluwa and Mofehintoluwa, thank you for enduring my absence and supporting my dreams, you are indeed my joy.

To my family, my loving mother, Rose-Margret Scott-Emuakpor, my amazing big brothers Bemigho and Henry and to my most awesome baby sister Irene. Thank you for being my support in more ways than I can mention. Your prayers have seen me through.

ABSTRACT

In coming years, chronic water stress is inevitable owing to the unavailability of fresh water. This situation is occasioned by rapid urbanisation, climate change, rising food demand, and production. The increasing rate of water scarcity associated with water pollution problems, makes water quality management an issue of great concern. Rivers owe their existence to the relationship of rainfalls, soil properties and land use within a catchment. The entire hydrological processes that occur in the catchment area has a direct effect on occurrences and quality of the rivers there-in. A principal part of the hydrological cycle is runoff generation. Runoff characterises soil erosion, sediment transport, pollutants and chemicals all otherwise referred to as non-point source pollutants and released into water bodies. Most non-point source pollutants are generated from agricultural fields, informal settlements, mining fields, industrial areas, and roads. These sources produce increased nutrient concentrates (sewage effluent from informal settlements and fertilisers from agricultural fields) and toxic substances which alter the water quality in uncertain quantities. This affects aquatic biota and ultimately human health negatively.

Non-point source pollution is a major source of water quality degradation globally and is the single most significant threat to subsurface and surface sources of usable water. Developed countries, unlike many developing countries, have long sought ways to stop the release of non-point source pollution directly into natural rivers through the establishment of best management practices but unfortunately with little success in actual practice. Numerous non-point source models exist which are basically watershed based and are limited to simulate the in-stream processes of non-point source pollution in water channels. Most existing non-point source models are site-specific, cumbersome to manipulate, need high-level operational skills and extensive data sets. Consequently, these models are difficult to use in areas apart from where they were developed and with limited data sets, as is the case with developing countries. Hence, to develop a non-point source pollution model that would adequately and effectively, simulate non-point source pollution in water bodies, towards restoring good river health is needed. This is required to enhance the proper monitoring and remediation of water sources affected by Non-Point Source Pollution especially in areas that have scarce data.

Using the concept of the Hybrid Cells in Series model in this study, a hydrodynamic riverine Non-point source pollution model is conceptualized to simulate conservative pollutants in natural

rivers. The Hybrid Cells in Series model was conceptualized to address the limitations identified in the classical advection dispersion model which is the foundation for all water quality modelling. The proposed model is a three-parameter model made up of three zones, which describes pure advection through time delay in a plug zone, and advection and dispersion occurring in two other thoroughly mixed zones linked in sequence. The model considers lateral inflow and pollutant loading along the river reach in addition to the point source pollutant entry and flow from upstream stations. The model equation for water quality along with hydrodynamic equation has been solved analytically using Laplace Transform. The derived mathematical formulation is appropriately coded, using FORTRAN programming language.

Other components such as hyporheic exchange process and first order kinetic reaction simulations are incorporated to the proposed model. The response of these models matches the numerical solution of the classical Advection Dispersion Equation model satisfactorily when compared. The potential of the proposed model is tested using field data obtained from verifiable existing literature. A performance evaluation at 95 percent confidence is carried out. The correlation results of the observed and simulated data are seen to be in good agreement.

The breakthrough curves obtained from the proposed model shows its capability to simulate Non-point source pollution transport in natural rivers effectively. The simplicity of the Hybrid Cells in Series model makes it a viable model for simulating contaminant transport from non-point sources. As the model has been validated using recorded data collected from the field for a specific tracer injection event, it is imperative to carry out investigation on changes in model parameters before, during and after storm events. However, this study adequately addressed and attempted to develop, validate new model components for simulating non-point source pollutant transport processes in stream.

TABLE OF CONTENTS

LIST OF FIGURES

LIST OF TABLES

ABBREVIATIONS

ADZ:	Aggregated Dead Zone Model
ADE:	Advection-Dispersion Equation
AGNPS	Agricultural non-point source model
AnnAGNPS	Annualised agricultural non-point source model
ANSWERS	Areal nonpoint source watershed environment response simulation model
ARS	Agriculture research service
BMP	Best management practice
BOD	Biological Oxygen Demand
BTC	Break through curve
CBOD	Carbonaceous biological oxygen demand
CEQUALRIV1	One-dimensional hydrodynamic and water quality model
CMBA	Chemical mass balance approach
CIS:	Cells in Series Model
CREAMS	Chemicals, runoff, and erosion from agricultural management systems model
C-t	Concentration-time
DMA	Distributed modelling approach
DO	Dissolved Oxygen
EPD-RIV1	One-dimensional riverine hydrodynamic and water quality model
GIS	Geographic information systems
HCIS:	Hybrid Cells in Series Model
HCIS-NPS	Hybrid Cells in Series Non- point source Model
HCIS-NPS*k*	Hybrid Cells in Series Non- point source Model with decay
HCIS-NPS*hez*	Hybrid Cells in Series Non- point source Model with hyporheic exchange
HRU	Hydrologic response units
HSPF	Hydrological simulation program FORTRAN model
HZ	Hyporheic zone
MA	Modified approach
N	Nitrogen
NO_3	Nitrate
NPS:	Non-Point Source
NSE	Nash-Sutcliffe efficiency coefficient

o-PO_4	Ortho-phosphate
P	Phosphorus
pH	Potential of Hydrogen
R^2	Coefficient of determination
SCS	Soil conservation service
SE	Standard error
SWAT	Soil and water assessment tool model
SWRRB	Simulator for water resources in rural basins model
TCOD	Total Chemical Oxygen Demand
TN	Total Nitrogen
TP	Total Phosphorus
TSM	Transient storage model
USLE	Universal soil loss equation
WQM	Water quality models

NOMENCLATURE

α	Residence time of plug flow cell
Δx	Size of Hybrid unit
$\emptyset$	Stream bed porosity
δ (.)	Dirac delta function
A	Cross-sectional area of flow
A*	Interface between the overflowing stream and Hyporheic zone
C	Pollutant concentration
C (x, t)	Pollutant concentration in space and time
C^*	Laplace transform of C
C_L	Concentration of runoff input into the channel from lateral flows
C_{Pf}	Concentration of pollutants in the plug flow cell
C_{M1}	Concentration of pollutants in the first mixing cell
C_{M2}	Concentration of pollutants in the second mixing cell
C_R	Boundary concentration
C_s	Concentration of trapped pollutants in hyporheic zone
d	Mean stream depth (m),
D	Depth of hyporheic zone
D_L	Longitudinal dispersion co-efficient
f	Proportionality constant
H	Depth of flow
K_a	Decay/ first order kinetic reaction
$K_{HCIS\text{-}NPS}$	Unit step response function of hybrid model with Non-point source inflows
$K_{HCIS\text{-}NPSk}$	Unit step response function of non-point source hybrid model with decay
$K_{HCIS\text{-}NPShez}$	Unit step response function of non-point source hybrid model with hyporheic exchange
n/m	Number of Hybrid cell
P_e	Peclet number
Q	Flow rate
q_L	Lateral in flow
R\R_f	Retardation factor
R_h	Hydraulic radius

RL	Reach length
t	Time
T_1	Residence time of first mixed cell
T_2	Residence time of second mixed cell
u	Flow velocity
U (t-α)	Step function
V	Volume of hybrid cells
V*	Volume of hyporheic zone
wp	Wetted parameter
x	Longitudinal distance along the channel

CHAPTER 1: INTRODUCTION

1.1 Background Information

Access to clean and potable water is a global requirement for healthy living. However, in coming years, chronic water stress is inevitable owing to the unavailability of fresh water caused by the discharge of pollutants into water bodies, resulting from rapid urbanisation, climate change, rising food demand, and production. Thus, Van Rooyen et al. (2009) stressed that water quality deterioration is a global threat that must be given due attention.

Rivers and or streams; as may be used intermittently; owe their existence to the nature of the catchment area it is situate, and the relationship of rainfall, soil properties and land use. Apart from effluents from municipal and industrial areas, the hydrological processes which occur within a catchment has a direct effect on rivers. A principal part of the hydrological process is the runoff generated within the catchment through rainfall. The runoff characterises soil erosion, transport of sediments, pollutants and chemicals otherwise called non-point source (NPS) pollutants. NPS pollutants are sourced through runoff from agricultural fields, informal settlements, mining fields, industrial areas, residential areas and roads and deposited into water bodies (Drechsel et al., 2006; Karikariay et al., 2007; Drechsel et al., 2008). These sources produce increased nutrient concentrates (sewage effluent from informal settlements and fertilisers from agricultural fields) and toxic substances, which affects the stream water quality in uncertain quantities (Ongley et al., 2010; Wu et al., 2012; Shen et al., 2014). Thus, affects aquatic biota and ultimately human health negatively. Rivers all over the world are threatened by increase in non-point source and point source pollution. Consequently, the pollutant loads of rivers are becoming increasing high and as such has stretched their natural self-cleansing and purifying mechanisms to its limits. This situation has a far-reaching effect on fresh water availability.

Of all surface water pollution sources, NPS pollution is considered a leading source of water quality degradation and an uncontrollable issue globally (Han et al., 2011; Ma et al., 2011; Amaya et al., 2012; Collins et al., 2016). Hence, the increasing rate of water scarcity associated with water pollution problems, makes water quality management an issue of great concern.

Most developed countries, like the United States of America, Canada, Australia, the community of European nations and in recent time China, have set up management plans on catchment basis towards improved water quality. The approach is centred largely on implementing best

management practices in agricultural fields to mitigate the release of fertilizers believed to be the main source of nutrients into water channels. Countries like China have made heavy investment in curbing NPS pollution through this process, but have achieved little success (Xia et al., 2011). Findings have proven that the management initiative of best management practices despite achieving some level of success, has failed systematically to wholly curb the release of this pollutant type in rivers. One of the many reasons is that it is difficult to select a suitable practice for all climatic and site-specific conditions. This is critical to finding the extent of pollution and resolving it. Lee et al. (2010) states that exact land-use data is needed to achieve a proper management process. Thus, release of Non-point source pollutants into the water body is inevitable.

To estimate the level of NPS pollution in catchments, various NPS models have been developed and used widely at different scales for pollutant transport simulations in catchment systems. The models are predominantly watershed based and focus on delineating run-off generating catchments and sub-catchments for NPS detection. However, resolving vital calibration parameters within the catchment is a major limitation of these models due to differing complexities in catchment physiognomies and data scarcity (Zhai et al., 2014). Moreover, in instances where these models are modified to simulate in-stream processes, they are complex, have numerous parameters with great uncertainties and require extensive data sets. Hence, they need parameter sensitivity analysis to be performed (Lee et al., 2010; Sexton et al., 2011). Consequently, there is a need for improvement in the development of non-point source pollutant models to cater for these deficiencies.

1.2 Motivation for the Research

Rivers globally are susceptible to effects of NPS pollution and degradation of surface water quality. African countries such as South Africa, have been affected in recent years by high pollution rates of their water resources. The pollution burden in most South African rivers are very high, threatening the bio-diversity and socio-economic development of the country (Lin et al., 2012; Hedden and Chillers, 2014). Presently the water quality models in use in South Africa are over-parametrized, complex, data intensive and expensive (Chinyama et al., 2014.) Unfortunately, like most developing countries, South Africa lacks enough hydrological and high-quality historical observatory data as Water Authorities database in South Africa consists of fortnightly data collected from selected monitoring stations which can't be used to verify non-point source

pollution and its in-stream pollutant transport processes (Moolman et al., 1999; Oberholster, 2010; Kollongei, 2015; DWS, 2016). However, this is not an indictment on monitoring and regulatory bodies. Rather, collection of such intensive data is expensive, while hydrological events could be far spaced and infrequent.

Nevertheless, mathematical modelling is still the required tool to address this situation. A growing consensus amongst researchers, is that to effectively monitor and simulate NPS pollution, the model should be simple and cost effective. Also, it must be flexible enough to simulate surface water quality with limited data sets without compromising the output. The challenge therefore, lies in the development of such a model which has all the generic inputs to represent the physical processes of the classical advection dispersion equation (ADE) model, represented as equation (1.1), but overcomes its limitations through the correct representation of concentration profiles achieved from field tracer tests (Kumarasamy et. al 2011; 2013).

$$\frac{\partial(AC)}{\partial t} = -\frac{\partial(AuC)}{\partial x} + \frac{\partial}{\partial x}\left(AD_L \frac{\partial C}{\partial x}\right) \tag{1.1}$$

Where, C is solute concentration (mgl^{-1}), D_L is coefficient longitudinal dispersion, u denotes flow velocity (ms^{-1}) and A is channel cross-sectional area (m^2). Several models have been developed towards overcoming these limitations. Amongst which is the hybrid cells in series (HCIS) model (Ghosh, 2001). Conceptually, a single hybrid unit of the HCIS model is made up of three cells, specifically a plug flow cell and two well mixed unequal cells, sequentially connected. The HCIS model was developed as an improvement to both the Cells in Series (CIS) and Aggregated Dead Zone (ADZ) models, to accurately simulate the skewness of break through curve profiles, as seen from field tracer test for conservative pollutants (Ghosh, 2001; Ghosh et al., 2004). Other advantages of the HCIS model has been shown through progressive research. The Model has the capacity to incorporate varying stream geometries, dead zones and hyporheic processes (Kumarasamy et al, 2011), it reproduces the skewness of C-t profiles for non-conservative pollutants as seen from tracer tests (Kumarsamy et al., 2013), its ease in parameter estimation and sensitivity certainty is demonstrated by Naidoo and Kumarasamy (2016) while Olowe and Kumarasamy (2017) successfully simulated the fate of nutrients from point source in rivers. Therefore, this forms the basis for its further development in this present work.

1.3 Research Questions Aim and Objectives

The aim of this research is to develop a riverine hydrodynamic model for simulation of Non-point source pollutants by introducing NPS components to the Hybrid Cells in Series (HCIS) Model. The HCIS model has been successfully used to overcome the limitations of the classical advection-dispersion equation (ADE), cell-in-series (CIS), and aggregated dead zone (ADZ) models. Movement of contaminants within a river occurs through a process of mixing, primarily due to mass transfer and kinetic interactions. Thus, several models have been developed over time to address NPS pollution and pollutants. Available models however, are found to be inadequate due to their limitations in operation, extensive and expensive data requirements and computational difficulties. Consequently, this work looks to develop a non-point source pollutant model that would not only adequately and effectively simulate non-point source pollutants in water bodies, but would also be easy to assess, user-friendly, less data intensive and time-efficient.

The research would attempt to answer the following questions.

1. Can the HCIS model be effectively modified to adequately simulate NPS pollution in streams and rivers?
2. Is the HCIS-NPS model a useful tool for simulation of NPS pollutants in streams and rivers, irrespective the nature of pollutant?

The research objectives can be summarised as follows:

1. Develop a HCIS model to simulate conservative non-point source pollutants in water channels.
2. Enhance the developed HCIS-NPS model for simulation of hyporheic exchange for conservative pollutants.
3. Develop a hydrodynamic model using the HCIS concept to simulate Non-conservative non-point source pollutants in water channels.
4. Establish the performance of the HCIS-NPS Model using field data.
5. Establish the performance of the HCIS-NPS model compared with the Numerical solution of the classical ADE model to validate the potentials of the proposed model as an alternative to the ADE model.

1.4 Expected Contribution to Knowledge

Hitherto, research work on NPS simulations has mainly been carried out through the modifications of existing Watershed based models. However, due to their intensive processes and data requirements, it still falls short of being a practical option for simulation of NPS pollutants in areas with limited data sets. More so, most modelling attempts do not simulate the joint processes of point source and NPS pollutant inflows in water channels. This research is unique as it takes its bearing from the classical ADE model and while improving on its limitations captures the inclusion of NPS inflows. Therefore, rather than treat the NPS pollution inflows in isolation to point source pollution, the total in-stream pollutant loading is simulated in a holistic manner from the near to the far reach. The HCIS model coupled with the NPS component is a new concept which would be used for the sustainable management of NPS pollution in rivers both in South Africa and in general. At the end an easy to use software, with less intensive data requirements will be developed through FORTRAN programming.

1.5 Organisation of Thesis

The thesis is made up of five chapters, references, and appendices. Chapter one outlines the general introduction and background of the present study. The motivation and objectives of this research are presented in the chapter.

Chapter two contains the review of literature of selected existing NPS models. The choice of models reviewed is due to their wider use and acceptance in the field of NPS research. The focal point of review of the models is their components, nature, area of use, strengths, and limitations.

Chapter three presents the methods used in the development of the mathematical formulation of a NPS model based on the HCIS concept for simulation of conservative pollutants, the analytical formulation of the HCIS-NPS model with enhanced capability to simulate hyporheic exchange occurring in water bodies and the derivation of reactive pollutant transport in natural rivers with non-point source hybrid cells in series model. The methods are presented in three sections.

In chapter four the results and discussions are presented. The models developed in chapter three are tested using synthetic data and field data obtained from literature. The breakthrough curves obtained from the conceptualised models adequately describe the behaviour and patterns of pollutant fate in rivers similar to that obtainable from field tracer tests.

Chapter five concludes and summarises the findings and contributions in the present work and presents a scope for further study.

CHAPTER 2: LITERATURE REVIEW

2.1 Preview

Clean water is essential in adequate quantity for the sustainability of aquatic ecosystems and for human health. However, constant release of non-point source pollutants into water bodies has resulted in water quality degradation. Water quality models are used to evaluate the level of pollution and support decision makers to control the pollution. This chapter presents a, review of ten non-point source models, namely: AGNPS, ANSWERS, CREAMS, SWRRB, HSPF, SWAT, EPD RIV1, DMA, CMBA, and MA. Consideration is given to their nature, components, area of use, strengths, and limitations. The review indicates that hydrological processes and mechanisms involved in the movement of non- point source pollutants have not been completely developed in these models. However, HSPF and EPD RIV1 models which have in-stream process components are limited due to limitations in their operations, and computational difficulties. The review provides insight to the drawbacks and limitations in existing models and provides a leverage for the present research to develop a non- point source pollutant model that would be adequate and effective in simulation of non-point source pollutants in water bodies.

2.2. Introduction

Water is necessary for meeting with agricultural, industrial and domestic needs. Unfortunately, population growth, urbanization, and industrialization have resulted in increased pollutant loadings into water bodies that cause distortions to its ecosystem and is detrimental to human health (Kumarasamy, 2015). Pollutants which enter streams from identifiable sources are easily recognized and given due attention. However, a greater challenge comes from pollutants generated from unidentifiable sources considered as non-point sources (NPS). NPS pollutants originate through runoff from agricultural areas, informal settlements, and contaminated lands (Dressing, 2003; Li and Li, 2010; Fu and Kang, 2012). Due to their ubiquitous nature, they degrade the natural environment and constitute a health risk. Thus, NPS pollution is considered a leading threat to water quality and an unmanageable water pollution problem globally (Ongley et al., 2010; Collick et al., 2015; Poudel, 2016).

2.3 Non-Point Source Pollution

NPS pollutants discharge into water bodies through several outlets and in uncertain quantities (Loague and Corwin, 2006). They are not easily traced to a source but are linked to weather and geographic conditions within a catchment and maintain an active presence within the ecosystem due to the storage characteristics within the receiving basin (Loague and Corwin, 2006; Jha et al., 2007; Dong et al., 2014). NPS are characterised by varying spatial and temporal pollutant loading, complex processes and mechanisms, with arbitrary and irregular occurrence (Wang et al., 2016). It is presumed more complicated to point source pollution, due to its complexities in monitoring and control especially during the monsoon periods (Zhang and Huang, 2011; Shen et al., 2012; Gao et al., 2015). Runoff from various watersheds at monsoon seasons pick up pollutants which contaminate and alter the biological, physical and in some cases chemical property of a water body (Li, 2009; Ongley et al., 2010; Wu et al., 2012; Shen et al., 2014). Discharge of non-point source pollutants into a water channel significantly affects the water quality (Han et al., 2011). Water quality deterioration resulting from NPS pollution is being studied globally (Ma et al., 2011; Amaya et al., 2012). Recent studies have established the impact of NPS pollutants in water environments. Lee et al. (2015) observed that NPS contaminants constituted 69.3% of the total pollution loads discharged from four major watersheds in Korea in 2010. Hu and Huang (2014), monitored NPS from an agricultural watershed in South China. The results put the percentage of NPS pollution against total pollutant loads at more than 80% between 2008 and 2010. An investigation into eutrophication of Dianchi lake by Chen (2009) revealed that the total phosphorus (TP) and nitrogen (TN) from NPS pollution in the Dianchi lake made up 26.7% and 4.5% of the total pollution load. In another study, Chen et al. (2013) observed a similar trend of major contributions of TP and TN from NPS to the overall pollution loading in Jinjiang River, China. In the USA NPS pollutants made up 83% of bacteria, 73% of the total chemical oxygen demand (TCOD), and 89% of TN in rivers (Zhai et al., 2014). While in South Africa according to Pegram and Bath (1995), 85% of total contaminants in the Mgeni River basin are from NPS. Further studies carried out on the effect of NPS pollutants on the Water Quality in Water bodies include, (Xia et al., 2012; Xu et al., 2013; Qiu, 2013; Wu and Chen, 2013; Gao et al., 2015; Wu et al., 2016). A major challenge faced by most researchers in assessing NPS pollutants is in predicting the occurrence of storm events, identifying safe and representative sampling locations and catchments, and the delineation of runoff quality parameters. Because, the mechanisms and hydrological processes required in pollutant migration are not adequately catered for in currently available models (Shen et al., 2012). However, these challenges were overcome by the use of GIS

techniques and remote sensing in estimating the NPS inflow percentages within the water bodies. The use of GIS and remote sensing is considered effective in delineating catchments which contribute NPS pollutants in water columns. However, despite the use of this technique, most researchers recorded some margin of error. Considering that approximately 30–50% of the world's land surface is affected by NPS pollutants (Pimental, 1993), accurate simulation and estimation of NPS are necessary to critically address NPS pollution.

2.4. Non-Point Source Pollution Modelling

Water quality models (WQM) were developed to determine the rate at which receiving bodies disperse pollutants and ascertain the occurrence of recovery through temporal responses. They were also developed to establish required flow augmentation for improved water quality (Benedini and Tsakaris, 2013; Sharma and Kansal, 2013; Wang et al., 2013a). However, the ever-increasing pollution loading in water systems has led to continuous improvement and development of WQM (Wang et al., 2013a). These upgrading are necessary when considering NPS pollution due to the challenge in identifying its source and quantifying its loading (Mamun and Salleh, 2014). Further, according to Li et al. (2014) and Liu et al. (2011) continuous research on NPS pollution modelling is required as there is no model presently able to simulate NPS pollution globally. Due to varying climatic conditions and anthropogenic and geographic backgrounds. In studying NPS pollution, modelling has been widely used in attempts to better understand the natural but complex processes of generation and transformation of NPS pollutants (Yanhua et al., 2012). Watershed models which simulate hydraulic responses, and receiving water models which simulate water quality and hydrodynamic transport are required to estimate NPS pollutants (Shoemaker et al., 2005). The most frequently used watershed models are continuous simulation and storm event models. Continuous simulation models analyze long-term effects of hydrological changes while storm event models examine severe single storm events. Only a few models have both storm event and long-term continuous simulation capabilities. Most models use simple empirical relations with robust algorithms, while others are physical based with rigorous numerical solutions (Borah and Bera, 2003; 2004). The simple models are sometimes unable to give the desired result, while the intensive models are considered prohibitive in large watersheds. Hence, it is a challenging task to find an appropriate model for all watersheds (Borah and Bera, 2003). The use of any model is assessed through the determination of its capability to handle accurately its set out criteria (Kliment et al., 2008). Over time, extensive work has dealt on the contributing factors of NPS

discharges from a watershed into the water body. However, the ultimate effect of the pollutant on the water body and its behavior within the water body is hardly considered.

2.5 Review of Non- Point Source Pollution Models

The complex processes that govern NPS pollutants makes it difficult to assess and quantify its spatial and temporal extent. Physical and chemical cycles which control the amount of pollutant loading in water bodies are represented using physically based computer modelling. There are numerous models in the public domain which have been used successfully in assessing and simulating NPS in watersheds. This review would, however, focus on Agricultural non-point source model (AGNPS), Areal nonpoint source watershed environment response simulation model (ANSWERS) and Soil and water assessment tool model (SWAT). Others include Chemicals, runoff, and erosion from agricultural management systems model (CREAMS), Simulator for water resources in rural basins model (SWRRB) and Hydrological simulation program FORTRAN model (HSPF). The One-dimensional riverine hydrodynamic and water quality model (EPD-RIV1) will also be considered. The choice of the models under review is due to their wider use and availability. The reviewed models are summarised in Table 2.1, which highlights the type, major components and key strengths and limitations of each model.

2.5.1 Agricultural Nonpoint Source Pollution Model (AGNPS)

AGNPS is an event driven and distributed parameter model developed by United States Department of Agriculture (USDA) Agricultural Research Service. It simulates runoff and estimates nutrient and sediment loads from agricultural watersheds for single storm events (Young et al., 1989). The water quality components of AGNPS are obtained by correlating nutrients and pesticides in runoff. The model calculates and estimates runoff and subsequent soil erosion, using universal soil loss equation (USLE). Further, it uses the unit hydrograph for uniform rainfall and soil conservation service (SCS) runoff curve approach. AGNPS consists of three principal components (Young et al., 1989). These are hydrology component for calculating peak flow rate and runoff volume, chemical transport component for estimating chemicals as phosphorus (P) and nitrogen (N), and erosion and sediment transport component. AGNPS is considered a very practical tool used in various watersheds for evaluting the impacts of diverse land cover scenarios (De Aussen et al., 1998). Land use parameters for specifying field processes and weather data required in AGNPS include; cropland, pasture, rangeland, forest, urban areas, precipitation, temperature, and sky cover. AGNPS is suitable when interfaced with GIS to accelerate data

capture and interpretation of model results (Bhuyan et al., 2003). The model is useful to understand erosion processes and locate areas that have high possibilty to lose nutrients within a watershed (Shen et al., 2012). It simulates the spatial distribution of catchment properties using a square grid cells system and evaluates the surface runoff for individual grid cells. The estimated runoff is routed through individual grids within the catchment towards the drain outlet. Different scenarios for minimizing nutrient and sediment discharge may be simulated, giving the user an advantage of immediate response compared with real life experiments (Mamun and Salleh, 2014). The model is a useful tool for management decisions on watersheds (Shen et al., 2012), and is predominantly used in the United States. Its effective use in other climes has been tested (Mohammed et al., 2004; Leon et al., 2004; Shen et al., 2012). AGNPS is however, not without its limitations. Catchment scale models like AGNPS require exclusive and extensive data, as simulation is done through unit grids which requires extensive input parameters. Technical documentation only exists for the input editor of AGNPS, where all the parameters are entered and edited. Moreso, adaptation of the model requires much work and programming competence (Finn et al., 2006). The model is also incapable of assessing nutrient transformation and in-stream processes and is only capable of simulating single events (Shoemaker et al, 2005). As a result of the limitations observed in AGNPS as an event based model, an annualized version AnnaAGNPS was developed as an improvement to the simulation capacity of AGNPS to evaluate long-term effects of NPS pollutants in large watersheds (Bingner and Theurer, 2001).

2.5.2 Areal Nonpoint Source Watershed Environment Response Simulation Model (ANSWERS)

ANSWERS is a distributed parameter and event-oriented model developed by the agricultural engineering department of Purdue University (Beasley and Huggins, 1981). The primary use of ANSWERS is in planning and evaluation of strategies to monitor NPS pollution from agricultural areas. The model predicts runoff, sediment transport, evapotranspiration and infiltration in agricultural watersheds. In this model, the hydrologic response to a storm event is the mechanism for movement of pollutants in the watershed. The model requires the subdivision of watersheds into square grids and simulates the processes within the watersheds following rainfall events. The processes which include runoff, sedimentation, and erosion are evaluated and routed for individual cells (Shen et al., 2012). Further, ANSWERS produces a number of output data which include; sediment yield hydrographs, runoff hydrographs, chemical movement masses, sediment loss and deposition masses for the individual cells. Program codes are easy to modify using ANSWERS

due to its modular program structure. However, its modelling capability of water quality is limited to phosphorous and nitrogen although the degradation of in-stream phosphorus and nitrogen is not considered. ANSWERS is unable to simulate many subprocesses including snowmelt processes or pesticides. The model like all distributed parameter models require elaborate and detailed input data preparations and is computationally intensive. Its output is sensitive to slight changes in input variables and this makes its validation challenging (De Roo et al., 1989). The erosion module of ANSWERS is empirical to a great extent.

2.5.3 Soil and Water Assessment Tool Model (SWAT)

SWAT is a continuous, semi-distributed and basin scale model developed for the agricultural research service (ARS) USDA (Neitsch et al., 2011). It is a physical based model which runs on a daily time step. SWAT combines and expands the features of models like CREAMS (Leonard and Knisel, 1986), and SWRRB (Williams et al.,1985). The model enables users to consider impacts of rural and agricultural management practices on the long-term. It develops soil and water conservation modules and processes of conflux and sediment confluence when used with GIS. The major processes of SWAT include; agriculture management, climate, pesticides, sediment, nutrients, vegetation growth, soil type, and surface and underground runoff. Additionally, its primary consideration is water, sediments, and chemical yields from agricultural lands in complex watersheds under differing soil types and management conditions. SWAT is used for more specialised processes such as bacteria transport, and estimating streamflow and nutrient loading in various watersheds (Abbaspour et al., 2007). The model works by dividing catchments into subunits known as hydrologic response units (HRUs) of similar land uses, soil types, and slopes (Maringanti et al., 2011). SWAT has a high calculative efficiency and is effective for simulating big basins without much time and high investment involved. It is sensitive to changes in climate, plant cover, and management processes (Ullrich and Volk, 2009). Though easy to use, an ArcGIS interface is required to facilitate simulation setup and modification due to large numbers of input files required to run the model. SWAT is only able to simulate a pesticide at a time through the stream network. It is unable to simulate daily change of dissolved oxygen within the water body (Shoemaker et al., 2005; Benaman et al., 2005). SWAT cannot accurately evaluate processes such as extreme daily flow occurrences, the complex dynamic evolution of soil nitrogen and carbon, and simulation of runoff yield (Borah and Bera, 2004; Abbaspour et al., 2007). It is incapable of simulating single flood events, while its database must be modified when used in different study areas. Amongst several studies, Lee et al (2010), by applying best management processes (BMPs)

in a select watershed, used SWAT and QuickBird high-resolution satellite imagery to evaluate the reduction effect of NPS pollution. Poudel et al (2013), monitored the quality of surface water in Louisiana, using SWAT. Xu et al (2013) applied SWAT model for estimation of NPS pollution loads in Zhangweinan river basin. SWAT was adopted with the small-scale watershed extended method (SWEM) for the simulation of NPS in Three Gorges Reservoir Region (Hong et al., 2012; Shen et al., 2013a; Shen et al., 2013b; Shen et al., 2014). Findings from these studies highlighted the strengths and flaws of the model. SWAT is the most widely used model when considering NPS pollution and best management processes (Li et al., 2014).

2.5.4 Chemicals, Runoff, and Erosion from Agricultural Management Systems Model (CREAMS)

CREAMS is a field scale lumped approach model developed by the USDA, for assessing agricultural management practices and pollution control (Leonard and Knisel, 1986). The model calculates peak flow, runoff volume, soil water content, percolation infiltration, and evapotranspiration daily. It determines storm load, average sediment concentrations and dissolved chemicals in the runoff. The analysis is executed through interconnecting sub-models of hydrology, erosion, and chemistry (Leonard and Knisel, 1986). The application of CREAMS varies from simple to complex systems, especially in extreme cases of climate and management approaches (Crowder and Young, 1985). In developing the model, some assumptions are made to simplify the complex systems and processes so that they are represented by simple mathematical terms. CREAMS employ SCS and USLE for continuous series and erosion simulation processes (Leonard and Knisel, 1986). Furthermore, it forecasts single rainfall events which provides average values for long-term rainfall. The simulated area in CREAMS is limited to a small field with the assumptions that the field has homogeneous soil, land use, and precipitation occurrences. The model inadequately simulates snow buildup, snowmelt, and subsequent runoff, and is limited in data management. CREAMS cannot provide process information or be used for large-scale river basins. It is also incapable of simulating in-stream processes (Kauppi, 1982). Users face certain restrictions if the model is run as three separate components. Because files generated by a component must first be recorded in order to pass the correct file to the next component. The user must, therefore, be attentive to the numerous files that would be generated for specific situations and understand the assumptions and intrinsic limitations of the model to prevent misapplication or interpretation of the model outputs (Leonard and Knisel, 1986).

2.5.5 Simulator for Water Resources in Rural Basins Model (SWRRB)

SWRRB was developed through the modification of subroutines in CREAMS to simulate rural basin processes (Williams et al., 1985). It is a long-term water and sediment yield simulator, capable of predicting the effect of management decisions and assessing water quality in ungauged rural basins. The model entails three components; climate, hydrology, and sedimentation. It considers both sediments attached and soluble pollutants from surface runoff, sedimentation, percolation, evapotranspiration, return flow, transmission losses, reservoir storage, and crop growth (Arnold et al., 1995). Total phosphorus and nitrogen are evaluated using relationships of runoff volume, sediment yield, and chemical concentration. Surface runoff is measured using the SCS curve number, while return flow is evaluated in relation to soil water content and travel time of return flow. SWRRB effectively models Large and complex watersheds which are subdivided based on soil, land use, or management. It is, however, incapable of simulating in-stream processes (Arnold et al., 1995). And its input and output files are massive.

2.5.6 Hydrologic Simulation Program FORTRAN (HSPF)

HSPF a model developed by US environmental protection agency (USEPA), is a comprehensive model which simulates water quality and watershed hydrology; over-land, in-stream, and in impoundments (Barnwell and Johanson, 1981). It is a broad water quality and watershed hydrology model that simulates both land and soil contaminant runoff processes. It simulates in-stream hydraulics, nutrients, and sediment exchanges for several organic pollutants (Shoemaker et al., 2005; Ribarova et al., 2008). HSPF effectively evaluates runoff flow rates, sediment transport and pesticide and nutrients concentrations. It generates time series results for water quality and quantity within a watershed (Tzoraki and Nikolaidis, 2007). Further, the model effectively assesses land-use change and flow diversions for point source and NPS pollutant management processes (Cho et al., 2009). Runoff capabilities in HSPF include simple relationships as empirical buildup, wash off and concentrations, and detailed soil process options. The in-stream nutrient processes include phosphorus and nitrogen reactions, BOD, DO, pH, benthic algae, phyto and zooplankton (Tzoraki and Nikolaidis, 2007). HSPF divides watersheds into homogeneous segments using the HRU concept. The model ignores the spatial variations within sub-watersheds, assumes overland flow to be one directional and considers the receiving water system as completely mixed. Any time-step may be simulated from as little as a minute to upwards of several years. However, HSPF represents physical processes through empirical relationships, and requires extensive calibrations and high level of expertise. HSPF does not

consider the spatial distribution of watersheds, therefore, resulting in increased model complexity. The model also does not consider simulation time as it becomes a distributed model when smaller sub-watersheds are used. HSPF is basically applied to well-mixed reservoirs, rivers and 1-Dimensional flows (Shoemaker et al; 2005).

2.5.7 The One Dimensional Riverine Hydrodynamic and Water Quality Model (EPD-RIV1)

EPD-RIV1 is a one-dimensional model, developed by Ohio State University as a modification of CE-QUAL-RIV1 model (Sharma and Kansal, 2013). The model employs the two points, 4th-order Holly-Preissman scheme to solve mathematical formulations. EPD-RIV1 consists of two components, the hydrodynamic (RIV1H) and water quality (RIV1Q) components. RIV1H simulates the dynamics in water bodies to analyze prevailing dynamic conditions and waste load allocations within the water column. RIV1Q has the capacity to simulate water temperature, phosphorus species, nitrogen species, carbonaceous biological oxygen demand (CBOD), dissolved oxygen (DO), algae, manganese, iron, and coliform bacteria. Further, it has the capacity to simulate the impact of NPS pollutants on water quality and in-stream processes over time. However, the two components are not run simultaneously. RIV1H is applied first, the output is written in a file which is transferred and used for simulation in RIV1Q. EPD-RIV1 evaluates longitudinal variants in water quality characteristics were lateral and vertical differences are small. Additionally, it predicts flows, depths, velocities, water surface elevations, and other hydraulic characteristics. The model uses differential equations to interpret changes in values of variables, with 1-day time step (Martin et al., 2002; Sharma and Kansal, 2013). In the application of EPD-RIV1, the assumption that the waterbody is one-dimensional is made. This assumption considers that velocities are suitably represented as average values over the cross-section. Further, it assumes that mixing in the lateral and vertical cross sections are adequate, thereby allows for cross-sectional homogeneity. This assumption may not be true since contaminants discharged into a waterway may not mix completely for some distance downstream. It is, therefore, inappropriate in areas where complete mixing has not taken place (Martin et al., 2002). The hydrodynamic model solves the St. Venants equations as the governing flow equations and includes both point and NPS inflows and outflows. The software consists; computer system shell, deliberator, preprocessor, post-processor and pre-run. The required input data consists of initial conditions, geometric data, control and hydraulic parameters, and calibration data. However, data requirements of this model is high (Martin et al., 2002; Sharma and Kansal, 2013). The Governing equation of EPD-RIV1 is as shown in equation 2.1.

$$\frac{\partial \alpha}{\partial t} + \bar{u}\frac{\partial \alpha}{\partial x} = D\frac{\partial^2 \alpha}{\partial x^2} + \frac{q}{A}(\gamma - \alpha) - K_s\alpha + Sinks \quad (2.1)$$

Where; α is mass concentration (mgl^{-1}), t represents time (s), $\bar{u}$ is flow velocity (ms^{-1}), x is the longitudinal distance (m), D represents dispersion coefficient (m^2s^{-1}), A is cross sectional area (m^2), q is the lateral inflow rate ($m^3s^{-1}m^{-1}$), γ is concentration of the runoff from distributed flow K_s represents biochemical decay rates (+) and growth rates (-) (s^{-1}) and Sinks is the biochemical sources(+) and sinks(-).

2.6 Other Attempts at Modelling Non-Point Source pollution

In recent time, however, attempts at modelling NPS have seen the emergence of mathematical models using several approaches.

2.6.1 Distributed Modelling Approach (DMA)

This approach is used in the estimation of NPS outflow from agricultural watersheds to a water column. It involves the collection of data from each field within a watershed by dividing it into small regular units. However, a major challenge is delineating hydrological uniform areas, when subdividing the watershed (Leon et al., 2001). The equation used for agricultural watersheds is expressed in equation 2.2.

$$C_{out} = \frac{1}{100R_{off}}(1-k)\left(C_{in} + C_{np}\right) \quad (2.2)$$

Where C_{out} is concentration of the water quality constituent leaving the reach (mgl^{-1}), C_{in} is concentration of the water quality constituent entering the reach (mgl^{-1}). C_{np} is the concentration of the NPS pollutants generated within the river reach (mgl^{-1}), R_{off} is the total runoff (mm) and k is the decay coefficient (s^{-1}). In the distributed modelling approach, the dissolvable concentration of NPS pollutants is combined with the reduction occurrences of the soluble concentration of water quality constituents at the inlet of the river. This situation, however, according to Jha et al (2007) and Leon et al (2001), is not consistent with actual field conditions. Rather, NPS pollutants enter the water column through overland flow adjacent to it (Jha et al., 2007).

2.6.2 Chemical Mass Balance Approach (CMBA)

CMBA is presented in equation 2.3 (Jain, 2000; Jha et al., 2007). The equation estimates the magnitude of NPS as the variance in the sum of watershed discharge and point source discharges.

(Novotny, 1994). It has been previously used in indirect estimations of point and non-point loadings through upstream and downstream measurements in receiving water bodies.

$$Q_d C_d = Q_u C_u + \sum_{i=1}^{n} L_i \tag{2.3}$$

Where Q_d and Q_u are downstream and upstream discharge (m^3s^{-1}), C_d and C_u are downstream and upstream concentrations (mgl^{-1}) and $\sum_{i=1}^{n} L_i$ is the net outcome of individual loadings plus any losses or gain within the river. If significant changes in contaminants occur upstream, the chemical mass balance equation might not be considered reliable in accounting for all pollutants, especially those which undergo significant changes except in conditions where the travel time of pollutants between downstream and upstream is small (Jain, 2000).

2.6.3 Modified Approach (MA)

MA is based on reaction kinetics and conservation of mass. The model estimates the inflow of NPS pollutants into a river reach during rainy and off- rainy seasons (Jha et al., 2007). The approach assumes NPSs as uniformly distributed adjacent to the river reach. The limitations observed in the Distributed and Chemical mass balance approach, where tackled using the modified approach indicated as equation (2.4).

$$Q_d C_d = Q_u C_u e^{-kt} + Q_{np} C_{np} \tag{2.4}$$

Q_{np} is NPS discharge (m^3s^{-1}), while k is the rate of attenuation (s^{-1}), and t is travel time (s). This approach was successfully used in estimating nitrate (NO_3) and ortho-phosphate ($o\text{-}PO_4$) loads due to NPS in River Kali (Jha et al., 2007). MA is found to be effective in loading and simulating NPS pollutants in-stream. However, a major flaw in this model could be in its development process where the inclusion of point source pollutants in-stream is neglected. This does not give a holistic in-stream scenario. Considering, that simultaneous existence of multiple sources of pollutants leads to a significant variation in its concentration within the water column. Negating any one source could result in errors. Further, its use may be restricted to rivers similar in geographic, climatic and hydraulic conditions to that for which it was developed (Jha et al., 2005).

Table 2.1: Summary of NPS Water quality models under review

Model	Type	Major components	Strength	Limitations
AGNPS	Event driven distributed model	Hydrology, chemical and erosion/sediment transport	Simulates spatial distribution of catchment properties. Gives immediate response compared with experiments. Useful in understanding erosion processes.	Requires exclusive and extensive data. It requires much work and programming competence. It is unable to assess nutrient transformation and in-stream processes.
ANSWERS	Distributed parameter, Event oriented model	Hydrology, evapotranspiration, infiltration and overland sediment transport	Program codes are easy to modify and predicted results are comparable with observed data.	Unable to simulate in-stream processes. It is unable to simulate sub-processes like snowmelt or pesticides. It requires elaborate and detailed input data preparations and is computationally intensive. Its output is sensitive to slight changes in input variables and this makes its validation challenging
SWAT	Continuous, semi-distributed, basin scale model	Hydrology, climate, nutrients, sediment transport.	Considers long term impacts of agricultural and rural management practices, and conflux and sediment confluence. Can be used for specialized processes such as bacteria transport.	Requires large numbers of input files to run the model. It is unable to simulate daily changes of dissolved oxygen in water bodies. It cannot accurately evaluate extreme daily flow occurrences, complex dynamic evolution of soil nitrogen and carbon, and simulation of runoff yield. Its database must be modified when used in different study areas.
CREAMS	Field scale lumped approach model.	Hydrology, chemical and erosion/sediment transport.	Forecasts single rainfall events, calculates runoff volume and storm loads. Can be represented with simple mathematical terms.	Limited simulation capability, incapable of simulating in-stream processes. High level of competence is required by user. It is easy to misapply and interpret model outputs.
SWRRB	Long term water and sediment yield model.	Hydrology, climate and sediment transport.	Capable of modelling large and complex watersheds.	It is incapable of simulating in-stream processes. Its input and output files are massive.
HSPF	Long-term continuous simulation model	Hydrology, climate and sediment transport.	Effectively evaluates runoff flow rates, nutrient and sediment transport and pesticide concentrations. It predicts results satisfactorily, and is capable of simulating in-stream processes	It relies on several empirical relationships to represent physical processes. It requires extensive calibrations and high level of expertise. High data sets are required. It cannot simulate the spatial distribution

				occurring in watersheds. The model is complex.
EPD-RIV 1	One dimensional hydrodynamic model.	Hydrodynamic and water quality	Simulates the impact of non-point source pollutants on the water quality and in-stream processes due to time variance.	Data requirement is high. High level of expertise is required.
DMA	Mathematical model.	hydrology	Estimates NPS outflows in Watersheds.	Cannot delineate hydrological uniform areas, when subdividing the watershed. Does not consider NPS input as overland flow.
CMBA	Mathematical model.	Chemical mass balance.	It estimates non-point loadings through upstream and downstream measurements in receiving water bodies.	Is not reliable in accounting for all pollutants for long distances between downstream and upstream.
MA	Mathematical model.	Conservation of mass and reaction kinetics.	It estimates the inflow of NPS pollutants into a river reach during both rainy and off- rainy seasons. The approach assumes NPS input as overland flow	Is not reliable in accounting for all pollutants when the river reach is long..

2.7 Summary

Ten non-point source pollution models were reviewed: AGNPS, ANSWERS, CREAMS, SWRRB, HSPF, SWAT, EPD RIV1, DMA, CMBA, and MA. The basic operation of each model was carefully highlighted with consideration given to their nature, components, area of use, strengths, and limitations. ANSWERS and AGNPS are in operation single-event, distributed parameter models while SWAT, HSPF, and CREAMS are long-term continuous simulation models. SWRRB a modification of CREAMS simulates basin scale processes. AGNPS, HSPF, CREAMS, and SWAT have three major components comprising chemical, hydrology and sedimentation components. AGNPS lacks the capacity to predict sediment, water, and chemical discharges due to variance in time which is critical for analyses, due to its computationally intensive numerical structures. ANSWERS and SWRRB have hydrology and overland sediment as their main components but exclude in stream sediment simulation and chemical transport. SWRRB however, has a weather component. ANSWERS and HSPF, use storage-based equations for flow routing while AGNPS, CREAMS, SWRRB, and SWAT use SCS runoff curve number to estimate peak flows and runoff volumes. Additionally, HSPF and CREAMS require continuous precipitation data. It is however observed that hydrological processes and mechanisms involved in the movement of pollutants in-stream have not been completely developed in these models. The limitations observed in DMA, CMBA models were addressed by the MA model. However, MA model would require further modification in terms of the reach length to be considered which is vital for Non-point source modelling. Also, the model neglects point source pollutant inflows in its operation. In view of all models reviewed, both HSPF and EPD RIV1 have the capability of simulating in-stream processes. However, both HSPF and EPD-RIV1 have limitations which preclude their overall capability to effectively and easily evaluate non-point source pollutants in water bodies. HSPF delineate physical processes through several empirical relationships. It lumps simulation processes for different land use types at catchment levels and transits to a distributed type model when the watershed is small resulting in an increase in simulation time and model complexity. HSPF requires extensive calibrations and high level of expertise with high data requirement. EPD-RIV1 is a one-dimensional model, comprising of two codes; hydrodynamic code, RIV1H, and water quality code, RIV1Q which do not run concurrently. RIV1H is applied first and stored before RIV1Q uses its output file to drive the transport of the water quality parameters. The assumption made in EPD-RIV1 on the homogeneity in the cross-section of a water column may not stand true, which makes the model inappropriate in areas where complete mixing has not occurred. This necessitates the need for further research to develop a non- point

source pollution model that would adequately and effectively simulate non-point source pollutants in water bodies. Such a model should be easy to assess, user- friendly, flexible to adopt different water quality parameters and scenarios, less data intensive and time-efficient.

CHAPTER 3: METHODOLOGY

3.1 Preamble

This chapter presents the development of the mathematical formulations of NPS model components based on the HCIS concept in three sections. Section 3.2 shows the model component development for simulation of conservative pollutants considering non-point source pollutant transport along with advection and dispersion only. Section 3.3 describes the enhancement of the HCIS model to simulate hyporheic exchange processes in stream channel for conservative pollutants along with lateral loading of pollutants. Section 3.4 presents the derivation of the model component to simulate reactive or decaying pollutant transport in natural rivers with non-point source based on the HCIS model

3.2 Model Component 1: Development of a Hybrid Cells In Series Based Non-Point Source Model

3.2.1 Theoretical Framework for Model Development

The release of pollutants in water environments through overland flows is on an alarming increase (Wang et al., 2013b; Hu and Huang, 2014; Bi et al., 2015; Strokal et al., 2016). Pollutants originate from agricultural runoff, informal settlements, and urban areas, henceforth, Non-Point Sources (NPS). Storm water transports pollutants from these sources and discharges into receiving waters, as a result it impacts the eco-environment and human health negatively. (Hu and Cheng, 2013; Zhao et al., 2012; Hofstra and Vermeulen, 2016; Wen et al., 2017). The pollution process is complex involving diverse pollutant types. Hence, NPS pollution is a significant environmental and water quality problem globally (Shen et al., 2011; Voß et al., 2012; Fu et al., 2013; Li et al., 2017). Studies on NPS pollution control focus primarily on best management practices (BMP). Though BMP limits NPS pollution, it does not prevent its entry into Rivers. NPS pollutants are distributed along the water channel from diffuse sources. Consequently, though the amounts deposited at any specific point of a river may be small due to BMP, the cumulative mass loading is substantial while its impact extends downstream (Runkel and Bencala, 1995). For this reason, a good understanding of the spatio-temporal variations of NPS pollution is required (Huang and Hong, 2010; Chen et al., 2013; Dechmi and Skhiri, 2013; Zhang, 2015).

Modelling is considered an effective mechanism for quantifying the characteristics of NPS pollution. It simplifies the intricate processes of generation and transformation associated with this pollutant type (Yanhua et al., 2012; Wang et al., 2013b). Attempts at addressing NPS pollution led to several models being developed at different scales (Ongley et al., 2010; Lam et al., 2010; Olsen et al., 2012; Yanhua et al., 2012; Zhang et al., 2012). Models such as AnnAGNPS, an annualized version of AGNPS, SWAT and HSPF are some of the widely used NPS models. A significant drawback with these models is the intricacy in operation, which require high levels of expertise, large data sets, exhaustive parameter estimation processes, extensive calibration and validation processes (Huang and Hong, 2010; Zhang and Huang, 2011; Shen et al., 2011, Chen et al., 2013; Ouyang et al., 2016). Extensive reviews on NPS models are found in (Borah and Bera, 2004; Shen et al., 2012; Adu and Kumarasamy, 2018). Several researchers have evaluated NPS pollution in watersheds using these models. Diaz-Ramirez et al (2011) used HSPF, to simulate the hydrological processes in watersheds in Puerto Rico, Alabama and Mississippi. Yan et al (2014) simulated the hydrological processes of Jiaoyi watershed in China by use of HSPF. Chahor et al (2014) assessed the suitability of AnnAGNPS to predict sediment yield and runoff in a small Mediterranean agricultural watershed in Spain. Likewise, Zema et al (2016) used AnnAGNPS to evaluate runoff in a large Mediterranean catchment. Lam et al (2010) applied SWAT to model point and non-point source nitrate pollution in Kielstau catchment, North Germany. Kim et al (2015) employed SWAT to assess impacts of climate change on snowmelt and possible NPS pollution discharges in elevated catchments in South Korea. Also, Piniewski et al (2015) used SWAT to quantify the spatial distribution of NPS pollution of a Meso-scale catchment in Poland. Evidently, these models are predominantly used for evaluation of NPS pollution in relation to rainfall-runoff processes, sediment transport, soil erosion, pollutant source identification and migration within catchments (Chen et al., 2013; Ouyang et al., 2016). Further, they are difficult to use in developing countries and in terrains not native to their conceptualisation. Thus, limiting their wider use in other regions (Ongley et al., 2010; Li et al., 2014). The investigation into behavior patterns of NPS pollutant clouds within water bodies is uncommon. However, study on the hydrodynamic processes which occur within a water body due to NPS loading, and the rate NPS pollutant concentration patterns distribute in-stream, cannot be ignored due to its far-reaching effects. The difficulties associated with effectively predicting in-stream flux of pollutants from NPSs requires a simplified and easy to interpret model, which must be able to balance the model complexity with available data. Hence, it is necessary to build a flexible model capable of

simulating water quality in rivers inclusive of in-stream NPS pollution for use in areas with limited data.

Mathematical models are generally founded on the fundamentals of conservation of mass which combined with Fickian law of diffusion represents the temporal and spatial effects of advection and dispersion of contaminants in water bodies (Benedini and Tsakiris, 2013). Research over time, identified limitations in the foremost Advection-Dispersion Equation (ADE) model (Rutherford, 1994: Lees et al., 2000; Neuman and Tartakovsky, 2009). Thus, leading to the development of models like the Cells in Series (CIS) and Aggregated Dead Zone (ADZ) models. The practical application of ADE is flawed due to its inadequacy to interpret observed tracer profiles where uniform mixing due to turbulence occurs (Lees et al., 2000). Accuracy in simulating tracer profiles which are dependent on the dispersion coefficient within the stream has also been observed as a flaw of the ADE model (Bencala and Walters, 1983; Lees et al., 2000; Ghosh et al., 2001, 2004, 2008; Neuman and Tartakovsky, 2009; Muthukrishnavellaisamy et al., 2009). The CIS model was considered as an alternative to ADE. It successfully reduced ADE to a first order differential equation from the conventional second-order differential equation. However, the CIS model considers its individual cells as thoroughly mixed, therefore, it fails to simulate in-stream advection processes adequately. This limitation of the CIS model limits its use in natural streams (Rutherford 1994; Ghosh et al., 2008; Kumarasamy, 2015). Conversely, the ADZ model recognizes storage zones in stream beds and banks, which is considered a significant factor for dispersion within water bodies. It decouples advection and dispersion which allows pure time delay for advection to occur. Thus, it adequately describes observed concentration profiles in natural streams. However, parameter estimation and determination of the model orders is the primary challenge with ADZ (Rutherford, 1994; Lees et al., 2000; Ghosh et al., 2008). Other models which have been considered as suitable alternatives to ADE model, includes, the Transient storage model (TSM) (Bencala and Walters, 1983) modeled in line with ADZ, and the Hybrid Cells in Series (HCIS) model (Ghosh, 2001).

3.2.2 Derivation of the Hybrid Cells in Series Non-Point Source Model Equations

The HCIS model as developed by Ghosh (2001), is a conceptual model whose process is based on the physiognomies of the mixing cells concept. The model describes pure advection through time delay within each cell while dispersion occurs only when the cell is presumed as thoroughly mixed. It is a three-parameter model and presents the Gaussian distribution of continuous time.

The HCIS considers a stream network as a series of hybrid units. Each unit is made of three cells namely a plug flow and two unequal thoroughly mixed cells presented in figure 3.1. The plug flow cell is characterized by pure advection, suggesting no change in solute concentration, while advection and dispersion processes occur in the two distinct mixing cells. Each cell has an independent residence time in which fluids flowing through is replaced. In other words, effluent from one cell after moving through the cell over a specific residence time becomes the influent of the next cell. α equated as V_0/Q represents the residence time of the plug flow cell, while T_1 and T_2; V_1/Q and V_2/Q are the residence time of the first and second mixed cells respectively. Q is the rate of flow of solutes in each cell, while V_0, V_1, and V_2 are the respective volumes of the plug flow cell, the first and the second mixed cells. These time parameters (α, T_1 and T_2) are determined empirically using the longitudinal dispersion coefficient (D_L) and mean flow velocity (u) in relation with the Peclet number (Pe) as given in equations (3.1 to 3.3). The size of each hybrid unit Δx must satisfy Peclet number conditions where $Pe = \Delta x u / D_L \geq 4$.

$$\alpha = \frac{0.04\Delta x^2}{D_L} \tag{3.1}$$

$$T_1 = \frac{0.05\Delta x^2}{D_L} \tag{3.2}$$

$$T_2 = \frac{\Delta x}{u} - \frac{0.04\Delta x^2}{D_L} \tag{3.3}$$

Alternatively, the model parameters can be obtained through the least square optimization method. This method is flexible in parameter estimation using the Marquardt algorithm (Marquardt, 1963; Ghosh et al., 2008). And considered preferable to both the method of moments and method of partial first moments (Ghosh et al., 2008).

The HCIS model was initially conceptualized to simulate conservative pollutants in streams and rivers (Ghosh, 2001). However, Kumarasamy et al (2011, 2013) implemented the inclusion of pollutant sorption and decay processes to the model. Additionally, Kumarasamy (2015) simulated DO concentration in streams by adding up De-oxygenation and Re-aeration component to HCIS model, while Olowe and Kumarasamy (2017) demonstrated its suitability for simulating Ammonia in rivers by incorporating the first-order kinetic equation for Ammonia nutrients. The flexibility

and adaptability demonstrated by the HCIS model, forms the basis for its use in developing a model capable of simulating in-stream NPS pollution. This section therefore, presents the process of deriving a model based on the HCIS concept for simulation of NPS pollutants in streams and rivers.

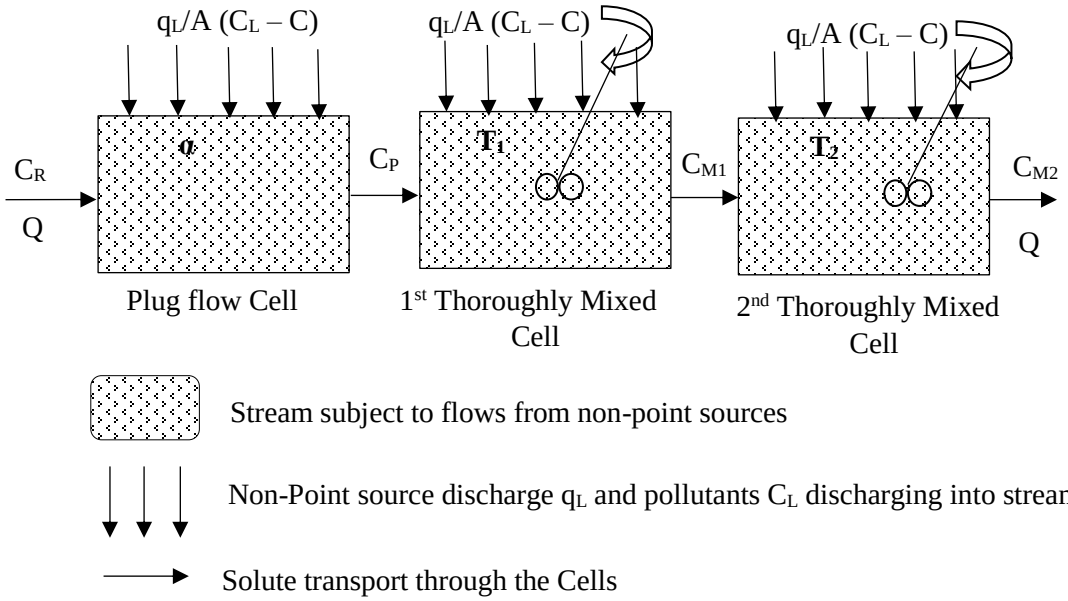

Figure 3. 1: HCIS Unit inclusive of uniformly distributed lateral flow

3.2.2.1 Pollutant Concentration in Plug Flow Component of First Hybrid Unit with Non-Point Source Pollution

Differential equations for most water quality models, are obtained by use of the fundamental concept of conservation of mass. In deriving the governing equations, a mass balance is carried out on a stream segment. Consider a stream of control volume ΔV, length Δx, and cross-sectional area A. The stream has a mass flow entering upstream the channel and a uniformly distributed lateral surface inflow along the channel reach as expressed in O'Conner (1976). Neglecting longitudinal dispersion, and assuming the pollutant to be conservative, the mass balance at Δt yields.

$$\Delta VC = QC\Delta t + C_L \Delta Q_L \Delta t - \left(C + \frac{\partial C}{\partial x}\Delta x \right)\left(Q + \frac{\partial Q}{\partial x}\Delta x \right)\Delta t \qquad (3.4)$$

Expanding equation (3.4) gives

$$V\Delta C = QC\Delta t + C_L \Delta Q_L \Delta t - CQ\Delta t - C\frac{\partial Q}{\partial x}\Delta x\Delta t - Q\frac{\partial C}{\partial x}\Delta x\Delta t - \frac{\partial^2 QC}{\partial x^2}\Delta x\Delta t \tag{3.5}$$

By substituting $V = A\Delta x$ and dividing both sides of the equation by $\Delta x\Delta t$, while neglecting all higher derivatives, equation (3.5) becomes;

$$\frac{\partial}{\partial t}(AC) = -C\frac{\partial Q}{\partial x} - Q\frac{\partial C}{\partial x} + C_L\frac{\partial Q_L}{\partial x} \tag{3.6}$$

Simplifying equation (3.6) and applying St Venant's continuity equation (3.7),

$$\frac{\partial A}{\partial t} + \frac{\partial Q}{\partial x} - q_L = 0 \tag{3.7}$$

Yields equation (3.8)

$$\frac{\partial C(x,t)}{\partial t} = -u\frac{\partial C(x,t)}{\partial x} + \frac{q_L}{A}\left(C_L - C(x,t)\right) \tag{3.8}$$

Where, $C(x, t)$ (mgl^{-1}) is pollutant concentration in the water body, u (ms^{-1}) is flow velocity, t (s) is time interval of pollutant displacement, x (m) is distance from source, q_L ($m^3s^{-1}m^{-1}$) is lateral inflow, C_L (mgl^{-1}) is pollutant concentration in lateral inflow, and A (m^2) is the water channel cross-sectional area.

Equation (3.8) is a first-order differential equation consistent with Bencala and Walter (1983) for conservative pollutants in water bodies, excluding dispersion and transient storage component. It is also valid for plug flow component of HCIS (Ghosh, 2001). This equation is therefore proposed for application as the background for simulation of NPS pollution in water channels. Hence it forms the governing equation for the Hybrid Cells in Series Non-Point Source (HCIS-NPS) model. The capability of the proposed model to simulate pollutant transport under both unsteady and steady flow conditions is enhanced, by incorporating the St. Venant's equation of continuity for unsteady flow in the derivation of the equation.

By means of the developed first order differential equation (3.8), simulation of a conservative pollutant will be executed. A conservative pollutant of no certain type is considered as transported

downstream a river comprising of hybrid units made up of a plug flow cell and two thoroughly mixed cells. Inflows from both non-point and point sources are taken into consideration. The inflows from NPS is assumed as being uniformly distributed along the river reach as shown in figure. 3.1. Let qL/A be denoted as ψ and initial and boundary conditions be;

$$C(x, 0) = 0;\ x > 0 \tag{3.9a}$$

$$C(0, t) = C_R;\ t \geq 0 \text{ and} \tag{3.9b}$$

$$C(\alpha u, t) = 0;\ 0 < t < \alpha \tag{3.9c}$$

where the initial boundary concentration of point source pollutants in each cell changes from C to C_R. Applying Laplace transform for all terms in equation (3.8) becomes;

$$\mathrm{L}\left(\frac{\partial C}{\partial t}\right) = SC^* \tag{3.10a}$$

$$\mathrm{L}\left(\frac{\partial C}{\partial x}\right) = \frac{dC^*}{dx} \tag{3.10b}$$

$$\mathrm{L}\left(C\right) = C^* \tag{3.10c}$$

Substituting equations. 3.10(a-c) in (3.8) and rearranging all terms, yields

$$\frac{\partial C^*}{\partial x} + \left(\frac{S}{u} + \frac{\psi}{u}\right)C^* = \frac{\psi}{u}C_L \tag{3.11}$$

Simplifying equation (3.11) and taking the integrals of the equation gives

$$C^* \exp^{+\left[\frac{S+\psi}{u}\right]x} = \frac{\psi C_L \exp^{+\left[\frac{S+\psi}{u}\right]x}}{S+\psi} + W \tag{3.12}$$

Where *W* is the integration constant. If boundary conditions 3.9 (a and b) are fulfilled. *W* can be computed by considering $C^* = C_R/S + C_L/S$ to give;

$$W = \frac{C_R}{S} + \frac{C_L}{S} - \frac{\psi C_L}{S + \psi S} \tag{3.13}$$

Substituting equation (3.13) into (3.12), simplifying and taking the inverse Laplace transform of the resultant equation yields

$$C_{Pf}\left(\alpha u, t\right) = C_R U\left(t-\alpha\right)\exp^{-\psi\alpha} + C_L U\left(t-\alpha\right)\exp^{-\psi\alpha} - \psi C_L U\left(t-\alpha\right)\exp^{-\psi t} + \psi C_L \exp^{-\psi t} \tag{3.14}$$

Where, C_{Pf} is the concentration of pollutants exiting the plug flow cell with NPS contribution. Valid when $t \geq \alpha$, and where U (t - α) is the step function of the equation.

3.2.2.2 Operating Process in First Thoroughly Mixed Cell

The HCIS model operates in series. Therefore, the first thoroughly mixed cell becomes the receptor of effluents leaving the plug flow after occupying the plug flow cell over a residence time α and is replaced with new inflow. Thus, outflow concentrations from the plug flow becomes in-stream influent concentrations for first mixed cell. NPS pollutant inflows are also introduced into the system. The first mixed cell has a fill time of T_1 as defined earlier. The Mass balance equation for the cell becomes;

$$V_1 \Delta C_{M\,C1} = C_{Pf} Q\Delta t - C_{M\,C1} Q\Delta t + \frac{q_L}{A}\left(C_L - C_{M\,C1}\right)V_1\Delta t \tag{3.15}$$

Where the first term of the equation, is the change in mass of the first mixed cell. The first term on the right is mass leaving the plug flow cell into the first mixed cell. The middle term represents effluent moving through and exiting the first mixed cell, while the last term is mass inflow from uniformly distributed non-point sources along the river. Substituting equation (3.14) into (3.15), dividing the equation through by $V_1\Delta t$ and simplifying in differentials yields;

$$\begin{aligned}\frac{dC_{M\,C1}}{dt} = {} & \frac{C_R U\left(t-\alpha\right)\exp^{-\psi\alpha}}{T_1} + \frac{C_L U\left(t-\alpha\right)\exp^{-\psi\alpha}}{T_1} - \frac{\psi C_L U\left(t-\alpha\right)\exp^{-\psi t}}{T_1} + \frac{\psi C_L \exp^{-\psi t}}{T_1} \\ & + \psi C_L - \left[\frac{1+\psi T_1}{T_1}\right] C_{M\,C1}\end{aligned} \tag{3.16}$$

Combining like terms and by multiplying equation (3.16) through by $\exp^{+\left[\frac{1+\psi T_1}{T_1}\right]t}$ becomes;

$$\frac{dC_{M\,C1}}{dt}(\aleph)+\left[\frac{1+\psi T_1}{T_1}\right]C_{M\,C1}(\aleph)=\frac{C_R U(t-\alpha)\{\mathsf{A}\}}{T_1}+\frac{C_L U(t-\alpha)\{\mathsf{A}\}}{T_1}-\frac{\psi C_L U(t-\alpha)\{\Im\}}{T_1}$$
$$+\frac{\psi C_L\{\Im\}}{T_1}+\psi C_L\{\aleph\} \tag{3.17}$$

Where;

$$\mathsf{A}=\left[\exp^{-\psi\alpha}\exp^{+\left[\frac{1+\psi T_1}{T_1}\right]t}\right]$$

$$\Im=\left[\exp^{-\psi t}\exp^{+\left[\frac{1+\psi T_1}{T_1}\right]t}\right]$$

$$\aleph=\left[\exp^{+\left[\frac{1+\psi T_1}{T_1}\right]t}\right]$$

Integrating equation (3.17) with respect to "t" yields;

$$C_{M\,C1}(\aleph)=\frac{C_R U(t-\alpha)\{\mathsf{A}\}}{1+\psi T_1}+\frac{C_L U(t-\alpha)\{\mathsf{A}\}}{1+\psi T_1}-\psi C_L U(t-\alpha)\{\Im\}+\psi C_L\{\Im\}+\frac{\psi C_L T_1\{\aleph\}}{1+\psi T_1}+P \tag{3.18}$$

Where P is the constant of integration. Solving when $C_{M1} = 0$ and $t = \alpha$, P becomes

$$P=-\frac{C_R U(t-\alpha)\{\mathsf{A}\}}{1+\psi T_1}-\frac{C_L U(t-\alpha)\{\mathsf{A}\}}{1+\psi T_1}+\psi C_L U(t-\alpha)\{\Im\}-\psi C_L\{\Im\}-\frac{\psi C_L T_1\{\aleph\}}{1+\psi T_1} \tag{3.19}$$

Substituting equation (3.19) into (3.18) and simplifying the resultant equation yields;

$$C_{M\,C1}=\frac{C_R U(t-\alpha)\exp^{-\psi\alpha}}{1+\psi T_1}\{\Re\}+\frac{C_L U(t-\alpha)\exp^{-\psi\alpha}}{1+\psi T_1}\{\Re\}-\psi C_L U(t-\alpha)\{\mathsf{M}\}+\psi C_L\{\mathsf{M}\}$$
$$+\frac{\psi C_L T_1}{1+\psi T_1}\{\Re\} \tag{3.20}$$

Where:

$$\Re=\left[1-\exp^{-\left[\frac{1+\psi T_1}{T_1}\right](t-\alpha)}\right];\qquad \mathsf{M}=\left[\exp^{-\psi t}-\exp^{-\psi\alpha}\exp^{-\left[\frac{1+\psi T_1}{T_1}\right](t-\alpha)}\right]$$

Equation (3.20) is the pollutant concentration exiting the first thoroughly mixed cell. Thus, C_{MC1} is total pollutant concentration from both point and NPS exiting the cell.

3.2.2.3 Operating Process in Second Thoroughly Mixed Cell

Effluent from the first mixed cell becomes influent to the second thoroughly mixed cell with inclusion of uniformly distributed lateral inflow. The residence time within this cell is T_2. Hence, performing mass balance for the second mixed cell at time intervals of t to t + Δt, where all terms of change in pollutant concentration within the cell, effluent mass entering and moving through the second mixed cell and lateral inflow are all accounted for, and hence yields,

$$V_2 \Delta C_{M\,C2} = C_{M\,C1} Q \Delta t - C_{M\,C2} Q \Delta t + \frac{q_L}{A}\left(C_L - C_{M\,C2}\right) V_2 \Delta t \tag{3.21}$$

Substituting C_{MC1} into equation (3.21), dividing the equation through by $V_2\Delta t$ and rearranging reduces the equation to the differential form

$$\begin{aligned}\frac{dC_{M\,C2}}{dt} &= \frac{C_R U\left(t-\alpha\right)\exp^{-\psi\alpha}}{T_2\left(1+\psi T_1\right)} + \frac{C_L U\left(t-\alpha\right)\exp^{-\psi\alpha}}{T_2\left(1+\psi T_1\right)} - \frac{\psi C_L U\left(t-\alpha\right)\exp^{-\psi t}}{T_2} + \frac{\psi C_L \exp^{-\psi t}}{T_2} \\ &- \frac{C_R U\left(t-\alpha\right)\exp^{-\psi\alpha}\exp^{-\left[\frac{1+\psi T_1}{T_1}\right](t-\alpha)}}{T_2\left(1+\psi T_1\right)} - \frac{C_L U\left(t-\alpha\right)\exp^{-\psi\alpha}\exp^{-\left[\frac{1+\psi T_1}{T_1}\right](t-\alpha)}}{T_2\left(1+\psi T_1\right)} \\ &+ \frac{\psi C_L U\left(t-\alpha\right)\exp^{-\psi\alpha}\exp^{-\left[\frac{1+\psi T_1}{T_1}\right](t-\alpha)}}{T_2} - \frac{\psi C_L \exp^{-\psi\alpha}\exp^{-\left[\frac{1+\psi T_1}{T_1}\right](t-\alpha)}}{T_2} + \frac{\psi C_L T_1}{T_2\left(1+\psi T_1\right)} \\ &- \frac{\psi C_L T_1 \exp^{-\left[\frac{1+\psi T_1}{T_1}\right](t-\alpha)}}{T_2\left(1+\psi T_1\right)} - \left[\frac{1+\psi T_2}{T_2}\right] C_{M\,C2} + \psi C_L\end{aligned} \tag{3.22}$$

By combining like terms and multiplying the equation through by $\exp^{+\left[\frac{1+\psi T_2}{T_2}\right]t}$ equation (3.22) becomes;

$$\frac{dC_{MC2}}{dt}\{B_3\}+\left[\frac{1+\psi T_2}{T_2}\right]C_{MC2}\{B_3\}=\frac{C_R U(t-\alpha)\{B_1\}}{T_2(1+\psi T_1)}+\frac{C_L U(t-\alpha)\{B_1\}}{T_2(1+\psi T_1)}-\frac{\psi C_L U(t-\alpha)\{B_2\}}{T_2}+\frac{\psi C_L\{B_2\}}{T_2}$$

$$+\frac{\psi C_L T_1\{B_3\}}{T_2(1+\psi T_1)}-\frac{C_R U(t-\alpha)\{B_4\}}{T_2(1+\psi T_1)}-\frac{C_L U(t-\alpha)\{B_4\}}{T_2(1+\psi T_1)}+\frac{\psi C_L U(t-\alpha)\{B_4\}}{T_2} \quad (3.23)$$

$$-\frac{\psi C_L\{B_4\}}{T_2}-\frac{\psi C_L T_1\{B_5\}}{T_2(1+\psi T_1)}+\psi C_L\{B_3\}$$

Where;

$$B_1=\left[\exp^{-\psi\alpha}\exp^{+\left[\frac{1+\psi T_2}{T_2}\right]t}\right];\qquad B_2=\left[\exp^{-\psi t}\exp^{+\left[\frac{1+\psi T_2}{T_2}\right]t}\right];\qquad B_3=\left[\exp^{+\left[\frac{1+\psi T_2}{T_2}\right]t}\right]$$

$$B_4=\left[\exp^{-\psi\alpha}\exp^{-\left[\frac{1+\psi T_1}{T_1}\right](t-\alpha)}\exp^{+\left[\frac{1+\psi T_2}{T_2}\right]t}\right];\qquad B_5=\left[\exp^{-\left[\frac{1+\psi T_1}{T_1}\right](t-\alpha)}\exp^{+\left[\frac{1+\psi T_2}{T_2}\right]t}\right]$$

By integrating equation (3.23), it becomes

$$C_{MC2}\{B_3\}=\frac{C_R U(t-\alpha)\{B_1\}}{(1+\psi T_2)(1+\psi T_1)}+\frac{C_L U(t-\alpha)\{B_1\}}{(1+\psi T_2)(1+\psi T_1)}-\psi C_L U(t-\alpha)\{B_2\}+\psi C_L\{B_2\}$$

$$+\frac{\psi C_L T_1\{B_3\}}{(1+\psi T_2)(1+\psi T_1)}-\frac{C_R T_1 U(t-\alpha)\{B_4\}}{(T_1-T_2)(1+\psi T_1)}-\frac{C_L T_1 U(t-\alpha)\{B_4\}}{(T_1-T_2)(1+\psi T_1)}-\frac{\psi C_L T_1\{B_4\}}{(T_1-T_2)} \quad (3.24)$$

$$+\frac{\psi C_L T_1 U(t-\alpha)\{B_4\}}{(T_1-T_2)}-\frac{\psi C_L T_1 T_1\{B_5\}}{(T_1-T_2)(1+\psi T_1)}+\frac{\psi C_L T_2\{B_3\}}{(1+\psi T_2)}+H$$

Where H is the constant of integration. Solving H when $C_{MC2} = 0$ and $t = \alpha$, gives

$$H = -\frac{C_R U(t-\alpha)\{\mathrm{k}\}}{(1+\psi T_2)(1+\psi T_1)} - \frac{C_L U(t-\alpha)\{\mathrm{k}\}}{(1+\psi T_2)(1+\psi T_1)} + \psi C_L U(t-\alpha)\{\mathrm{k}\} - \psi C_L \{\mathrm{k}\}$$

$$- \frac{\psi C_L T_1 \exp^{+\left[\frac{1+\psi T_2}{T_2}\right]\alpha}}{(1+\psi T_2)(1+\psi T_1)} + \frac{C_R T_1 U(t-\alpha)\{\mathrm{k}\}}{(T_1-T_2)(1+\psi T_1)} + \frac{C_L T_1 U(t-\alpha)\{\mathrm{k}\}}{(T_1-T_2)(1+\psi T_1)} + \frac{\psi C_L T_1 \{\mathrm{k}\}}{(T_1-T_2)} \qquad (3.25)$$

$$- \frac{\psi C_L T_1 U(t-\alpha)\{\mathrm{k}\}}{(T_1-T_2)} + \frac{\psi C_L T_1 T_1 \exp^{+\left[\frac{1+\psi T_2}{T_2}\right]\alpha}}{(T_1-T_2)(1+\psi T_1)} - \frac{\psi C_L T_2 \exp^{+\left[\frac{1+\psi T_2}{T_2}\right]\alpha}}{(1+\psi T_2)}$$

Where;

$$\mathrm{k} = \left[\exp^{-\psi\alpha} \exp^{+\left[\frac{1+\psi T_2}{T_2}\right]\alpha} \right]$$

Combining equation (3.24) and (3.25) and multiply through by $\exp^{-\left[\frac{1+\psi T_2}{T_2}\right]t}$ yields

$$C_{M\ C2} = \frac{C_R U(t-\alpha)\exp^{-\psi\alpha}}{(1+\psi T_2)(1+\psi T_1)} + \frac{C_L U(t-\alpha)\exp^{-\psi\alpha}}{(1+\psi T_2)(1+\psi T_1)} - \psi C_L U(t-\alpha)\exp^{-\psi t} + \psi C_L \exp^{-\psi t} + \frac{\psi C_L T_1}{(1+\psi T_2)(1+\psi T_1)} - \frac{C_R T_1 U(t-\alpha)\exp^{-\psi\alpha}\exp^{-\left[\frac{1+\psi T_1}{T_1}\right](t-\alpha)}}{(T_1-T_2)(1+\psi T_1)}$$

$$- \frac{C_L T_1 U(t-\alpha)\exp^{-\psi\alpha}\exp^{-\left[\frac{1+\psi T_1}{T_1}\right](t-\alpha)}}{(T_1-T_2)(1+\psi T_1)} + \frac{\psi C_L T_1 U(t-\alpha)\exp^{-\psi\alpha}\exp^{-\left[\frac{1+\psi T_1}{T_1}\right](t-\alpha)}}{(T_1-T_2)} - \frac{\psi C_L T_1 \exp^{-\psi\alpha}\exp^{-\left[\frac{1+\psi T_1}{T_1}\right](t-\alpha)}}{(T_1-T_2)} - \frac{\psi C_L T_1 T_1 \exp^{-\left[\frac{1+\psi T_1}{T_1}\right](t-\alpha)}}{(T_1-T_2)(1+\psi T_1)} + \frac{\psi C_L T_2}{(1+\psi T_1)}$$

$$- \frac{C_R U(t-\alpha)\exp^{-\psi\alpha}\exp^{-\left[\frac{1+\psi T_2}{T_2}\right](t-\alpha)}}{(1+\psi T_2)(1+\psi T_1)} - \frac{C_L U(t-\alpha)\exp^{-\psi\alpha}\exp^{-\left[\frac{1+\psi T_2}{T_2}\right](t-\alpha)}}{(1+\psi T_2)(1+\psi T_1)} + \psi C_L U(t-\alpha)\exp^{-\psi\alpha}\exp^{-\left[\frac{1+\psi T_2}{T_2}\right](t-\alpha)} - \psi C_L \exp^{-\psi\alpha}\exp^{-\left[\frac{1+\psi T_2}{T_2}\right](t-\alpha)}$$

$$- \frac{\psi C_L T_1 \exp^{-\left[\frac{1+\psi T_2}{T_2}\right](t-\alpha)}}{(1+\psi T_2)(1+\psi T_1)} + \frac{C_R T_1 U(t-\alpha)\exp^{-\psi\alpha}\exp^{-\left[\frac{1+\psi T_2}{T_2}\right](t-\alpha)}}{(T_1-T_2)(1+\psi T_1)} + \frac{C_L T_1 U(t-\alpha)\exp^{-\psi\alpha}\exp^{-\left[\frac{1+\psi T_2}{T_2}\right](t-\alpha)}}{(T_1-T_2)(1+\psi T_1)} - \frac{\psi C_L T_1 U(t-\alpha)\exp^{-\psi\alpha}\exp^{-\left[\frac{1+\psi T_2}{T_2}\right](t-\alpha)}}{(T_1-T_2)}$$

$$+ \frac{\psi C_L T_1 \exp^{-\psi\alpha}\exp^{-\left[\frac{1+\psi T_2}{T_2}\right](t-\alpha)}}{(T_1-T_2)} - \frac{\psi C_L T_1 T_1 \exp^{-\left[\frac{1+\psi T_2}{T_2}\right](t-\alpha)}}{(T_1-T_2)(1+\psi T_1)} + \frac{\psi C_L T_2 \exp^{-\left[\frac{1+\psi T_2}{T_2}\right](t-\alpha)}}{(1+\psi T_1)} \qquad (3.26)$$

The step response of the HCIS-NPS unit valid when $t \geq \alpha$. is;

$$K_{HCIS-NPS} = \frac{C_R \exp^{-\psi\alpha} U(t-\alpha)}{1+\psi T_1}[\varepsilon] + \frac{C_L \exp^{-\psi\alpha} U(t-\alpha)}{1+\psi T_1}[\varepsilon] - \psi C_L U(t-\alpha)[\chi - \varpi] + \frac{\psi C_L T_1}{1+\psi T_1}[\varepsilon] + \psi C_L [\chi - \xi] + \psi C_L T_2 [\Gamma] \tag{3.27}$$

Where:

$$\varepsilon = \left[\frac{1-\exp^{-\left[\frac{1+\psi T_1}{T_1}\right](t-\alpha)}}{1+\psi T_2} - \frac{T_1\left(\exp^{-\left[\frac{1+\psi T_1}{T_1}\right](t-\alpha)} \exp^{-\left[\frac{1+\psi T_2}{T_2}\right](t-\alpha)}\right)}{T_1 - T_2} \right]$$

$$\chi = \left[\exp^{-\psi t} - \exp^{-\psi\alpha} \exp^{-\left[\frac{1+\psi T_2}{T_2}\right](t-\alpha)} \right]; \qquad \varpi = \left[\frac{T_1 \exp^{-\psi\alpha}\left(\exp^{-\left[\frac{1+\psi T_1}{T_1}\right](t-\alpha)} + \exp^{-\left[\frac{1+\psi T_2}{T_2}\right](t-\alpha)}\right)}{T_1 - T_2} \right]$$

$$\xi = \left[\frac{T_1 \exp^{-\psi\alpha}\left(\exp^{-\left[\frac{1+\psi T_1}{T_1}\right](t-\alpha)} - \exp^{-\left[\frac{1+\psi T_2}{T_2}\right](t-\alpha)}\right)}{T_1 - T_2} \right]; \quad \Gamma = \left[\frac{1-\exp^{-\left[\frac{1+\psi T_1}{T_1}\right](t-\alpha)}}{1+\psi T_2} \right]$$

Equation (3.27) is the pollutant concentration leaving the second thoroughly mixed cell. It represents the step response of pollutant concentration in the first hybrid unit for a unit step input valid for $t \geq \alpha$. When $U(t-\alpha) = 1$ for $t \geq \alpha$ and $U(t-\alpha) = 0$ for $t < \alpha$.

$K_{HCIS-NPS}$ denotes the step response function of the initial hybrid unit. Differentiating equation (3.27) with respect to 't' produces the impulse response function for the same hybrid unit equation (3.28). Where $k_{HCIS-NPS}$ is the impulse response function.

$$k_{HCIS-NPS}(n, \Delta t) = \frac{K_{HCIS-NPS}(n\Delta t) - K_{HCIS-NPS}((n-1)\Delta t)}{\Delta t} \tag{3.28}$$

To estimate the concentration of pollutants at the end of 'n^{th}' hybrid unit, for 'n' number of hybrid units in a river reach, the convolution method is implemented.

3.2.3 Estimation of Downstream Concentrations by Method of Convolution

By use of the convolution technique presented in equation (3.29), the response of the pollutants further downstream from point of pollutant first entry can be estimated. The river reach is assumed to be delineated into n number of hybrid units. The effluent concentration from the first hybrid unit is transferred, by convolution and is the influent for the next hybrid unit. This process continues through for n ≥ 2 hybrid units.

$$C(i\Delta x, n\Delta t) = \sum_{\gamma=1}^{n} C[(i-1)\Delta x, \gamma]\, \delta_{HCIS-NPS}\, [n-\gamma+1, \Delta t] \tag{3.29}$$

3.3 Model Component 2: Development of Hyporheic Exchange Simulation Model in Natural Rivers with Non-Point Source Pollution Loads

3.3.1 Theory of Hyporheic Zones, Exchange and In-stream Time Delays

Pollutant concentration profiles differ from reach to reach in natural rivers. This difference is attributed to several processes which occur within the water body and is controlled largely by channel geometry, hydrology and basin geology (winter, 1998). Natural rivers are characterized by irregular cross-sections, with vegetated pockets which act as dead zones, where moving water either becomes stagnant or flows at reduced velocities (Kumarasamy, 2011). The presence of dead zones otherwise referred as hyporheic zones and in some cases transient storage; results to a temporary trapping of a part of in-stream pollutants within its sediments. This occurrence impedes the movement of pollutants in the water body. However, as the concentration gradients of the main channel and the storage zone changes due to continuous stream flows, trapped pollutants are gradually released back into the mainstream (Kumar and Dalal, 2014). This trapping and release process increase the travel time of pollutants within the waterbody and is referred to as hyporheic exchange (Gooseff et al., 2003). Hyporheic exchange occurs due to different hydraulic mechanisms which retard the transport of the pollutants in water bodies. The dynamics of hyporheic exchange, include the spatio-temporal scales of the flux, especially if the retention timescale in the storage zone is far greater than the travel time in the main water channel. Long retention periods are caused by temporary storage in the porous medium or hyporheic zones (Tonina and Buffington, 2009; Cardenas, 2009).

The hyporheic zone (HZ) is integral to river ecosystems (Hester and Gooseff, 2010; Harvey and Gooseff, 2015). It refers to the bed and sediments porous banks in and around the river as seen in figure 3.2. Solute passing through HZ stays there longer and flows at a slower rate than in the overflowing channel. The interactions between the river, inflows from non-point and point sources, and HZ is essential to figure out the sustainability of the eco environment and the river quality (Krause et al., 2011; Bardini et al., 2012; Boano et al., 2014). These factors all contribute to the health of the River, and influences the metabolic activity and nutrient cycles of both the river and HZ (Krause et al., 2011; Harvey et al., 2012; Bardini et al., 2012)

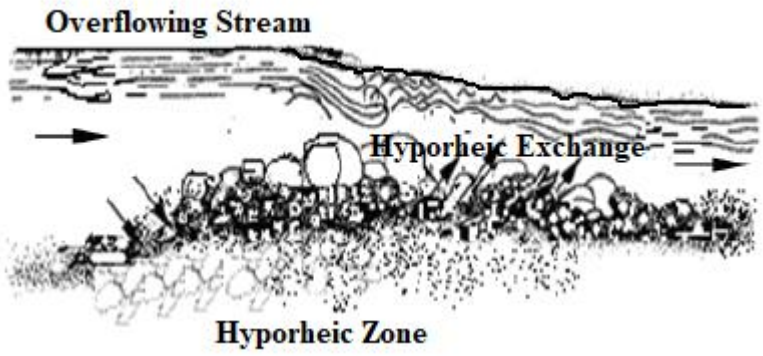

Figure 3. 1: Stream Section showing Hyporheic Zone and Exchange process (Kumarasamy, 2011).

The fate of pollutants in natural rivers depends on the hydrodynamic exchange within storage zones. Two significant parameters determine the effect of the hyporheic zone. The first is the cross-sectional area or volume of the zone while the second is the coefficient of mass exchange rate. Thus, the flux of mass exchange is comparable to a change in solute concentrations between the dead storage zone and the river. This is demonstrated by the reduction in pollutant concentration gradients within the river as the solute in the near field gets entrapped in the dead zone but increases due to its gradual release back into the main stream with increase in over flow. The delay of entrapped pollutants in the hyporheic zone is responsible for the long tails in breakthrough curves produced from field measurements (Ge and Boufadel, 2006).

The one-dimensional ADE model with a combined first-order mass exchange between the dead zone and river body, in its simplest form, is the most common approach in explaining pollutant transport in rivers where mass exchange with the hyporheic or transient zones occur (Runkel et

al., 2003; Briggs et al., 2009). However, to quantify the retention of pollutants in the hyporheic zone the ratio of the solute velocity to the velocity of water contaminant otherwise called the retardation factor (R_f), is measured (Hansen and Vesselino, 2018). Early researchers considered R_f in the vadose zone as constant. However, recent studies show that R_f changes under varying conditions (Huo et al., 2013). If local equilibrium for reactive substances is assumed, the classical ADE model may be expressed as equation. (3.30) (Rutherford, 1994) for a homogeneous porous medium.

$$R_f \frac{\partial C}{\partial t} = D \frac{\partial^2 C}{\partial x^2} - U \frac{\partial C}{\partial x} \tag{3.30}$$

Where R_f is retardation factor, C (mgl^{-1}) is pollutant concentration, t (min) is time, D (m^2/min) is coefficient of longitudinal dispersion, x (m) is distance and U (ms^{-1}) is flow rate. The inability of the classical ADE model to replicate the elongated tail in C-t profiles for pollutant transport is a significant shortcoming of the model (Cardenas, 2015). This is confirmed by Rutherford, (1994) who states that the ADE model sufficiently predicts the behaviour of tracer centroid and variance but is incapable to adequately predict its skewness. Amongst the many models proposed to adequately describe the natural processes due to these delays, TSM (Bencala and Walters, 1983; Bencala, 1983) is prominent.

TSM is a modification of the ADZ model inclusive of a transient storage component (Lees et al., 2000). The transient storage component accounts for the elevated tails and skewness in the representation of its simulated C-t profiles. TSM considers shear flow in uniform channels to simulate dispersion within a stream. It goes on to divide flows in rivers into two interacting zones linked by a first order mass exchange. The zones comprise of the stream channel, where transport mechanisms of advection and dispersion occur, and a transient storage zone (Bencala and Walter, 1983). The model suggests that advection and dispersion processes occur only in the overflow. While the flow in the storage zone or dead zone area consisting of vegetative pockets, bank irregularities and or permeable sub-surfaces; is presumed stagnant in variance to that of the overflow, (Bencala and Walters, 1983; Bencala, 1983; Runkel and Chapra, 1993; Kumar and Dalal, 2014).

The model is conceptualized on the basis that as the pulse of solute moves along a water channel, the concentration of the solute within the channel is attenuated while some solute mass remains within the storage zones. As the pulse passes through the channel, the retained solute in the storage

zone, is released back into the main stream resulting to the gradual tailing of the C-t profile (Runkel and Bencala, 1995). The governing equations of TSM which describes a one-dimensional transport of solutes under uniform and steady flow conditions are (Bencala and Walters, 1983; Runkel and Chapra, 1993).

$$\frac{\partial C}{\partial t} = \frac{Q}{A}\frac{\partial C}{\partial x} + E\frac{\partial C^2}{\partial x^2} + \frac{q_L}{A}\left(C_L - C\right) + \alpha\left(C_S - C\right) \tag{3.31}$$

$$\frac{\partial C_S}{\partial t} = \alpha\frac{A}{A_S}\left(C_S - C\right) \tag{3.32}$$

Where C and C_s (mgl^{-1}) are the concentration of solute in the stream and storage zone respectively, A and A_s (m^2) represents the cross-sectional area of the stream and storage zone. The volumetric flow rate of the reach is denoted by Q (m^3s^{-1}), E (m^2s^{-1}) is the longitudinal dispersion coefficient while α (s^{-1}) is the storage exchange coefficient of the stream. t (s) represents time while x (m) denotes distance. q_L is lateral inflow ($m^3s^{-1}m^{-1}$) and C_L is pollutant concentration in lateral inflow (mgl^{-1}).

Although the coupling term α (c_s - c) in equations (3.31 and 3.32) appear simple, the numerical solutions of both equations require as many as three parameters for calibration. Estimating these parameters is difficult and complicated (Rutherford, 1994; Lee et al., 2000). Thus, the parameter uncertainties in TSM restricts its wider use (Harvey et al., 1996; Wagner and Harvey, 1997; Fuller and Harvey, 2000; Zaramella et al., 2003; Bottacin Busolin, 2010). Though, much work has been carried out in modelling hyporheic zone processes, Bencala, (2000) and Runkel et al. (2003) suggest that a lot more needs to be done.

Kazezyılmaz-Alhan and Medina (2006) developed an enhanced TSM. The enhanced model introduced the process of advection and dispersion within the hyporheic zone. They presented a numerical solution using implicit finite difference method. The partial differential equations so derived for both the overflow channel and hyporheic zone are solved simultaneously to obtain solute concentrations in both zones. This is nevertheless cumbersome and numerical oscillations which occur in numerical solutions makes it difficult to derive satisfactory results (Rutherford, 1994). Multi rate mass transfer Model (MRMT) was proposed by Haggerty et al. (2000). MRMT expresses transient storage by integral convolution of pollutant concentration, residence time and

distribution. Bourke (2014) characterised hyporheic exchange parameters based on radon activities of longitudinal streams. Kumar and Dalal, (2014) developed a diffusive transfer zone model (DTSM) by analytically solving the diffusive exchange model, developed by Jonsson et al. (2003). These attempts have however not been without their complications in approach and applications. Trends in HZ processes and model development are well described in Boano et al. (2014).

Relevant physical processes towards describing mathematically the interactions that occur between the stream overflow and solute stored and released from the porous medium in the hyporheic zone is necessary. Sorption and or desorption processes retard the transport of the plume due to interactions with the porous medium. (Maghrebi et al., 2013; Kim et al., 2014). Moreover, transport of solute in the porous media is complex and subject to delays. The mobility of the pollutant depends on the relationship of the retardation factor R_f and sorption distribution coefficient K_d equation (3.33) (Krupka et al., 1999).

$$R_f = 1 + \alpha K_d \tag{3.33}$$

And

$$\alpha = \frac{\rho_b}{n} \tag{3.34}$$

Where n (-) is porosity of the porous medium and ρ_b (-) is the bulk density. Equation (3.33) assumes that sorption is linear and instantaneous. To adequately predict retardation effects, sorption processes must be quantitatively described and estimated. This is a prime function of K_d. However, in most cases K_d for most reactive solutes is considered as heterogeneous. A limiting factor to this relationship is that most modellers assume the porous medium does not affect the migration of pollutants and set K_d as default (Krupka et al., 1999; Deng et al., 2013). In addition, including K_d as a term in R_f, infers that reactions which occur in the channel are reversible and in equilibrium, and do not vary in time or space (Muller et al., 1982). This often is not the case in natural environments (Krupka et al., 1999). Coles (2007) stipulates that pollutant migration may be underestimated if K_d is employed when pollutant concentrations are not within linear range. However, due to a lack of adequate data in most sites this concept has been largely accepted bearing that, K_d measurements can be deduced from small scale laboratory experiments (Deng et al., 2013).

Different attempts have been made to adequately and practically define retardation factor. Maghrebi et al. (2013) derived effective retardation for varied porous formations using numerical simulations and approximate analytical solution to predict average plume delays. Deng et al. (2013) Studied retardation factor for graded porous media with multimodal mineral facies. While most researchers define retardation factor consistent with equation (3.33), other researchers such as Dentz and Castro (2009), Kumarasamy (2011), and Bolster and Dentz (2012) have defined differently. Kumarasamy (2011) formulated a hybrid model for pollutant mass exchange between the overflowing stream and underlying soil, defining retardation factor as

$$R = \left(1 + \frac{\phi w_P D.f}{A}\right) \tag{3.35}$$

R is the retardation factor (-), ϕ is stream bed porosity (-), w_p is wetted perimeter of stream overflow interface and hyporheic zone (m), D is depth of HZ (m), A is cross-sectional area of stream (m^2) while f is a proportionality constant (-). This section also extends the work of Kumarasamy (2011) by incorporating a non-point source component to the HCIS model for pollutant transport simulation in streams with hyporheic exchange and aims to provide validation for equation (3.35). The ability of the proposed HCIS-NPS model to adequately simulate hyporheic exchange processes in natural rivers with non-point source inflows when compared to the modified ADE model is also tested.

3.3.2 Conceptualisation and derivation of the Hybrid Cells in Series Non-Point Source Hyporheic Zone (HCIS-NPShez) Model

The process of the conceptual model starts from the plug flow zone, where the injected pollutants undergo a pure advective translation with minimal variation in concentration due to exchange occurring between the overflow and HZ and dilution from non-point source inflows rather than dispersive processes. To study the fate of pollutants at varying locations in a natural river with interactions occurring between the stream flow, the hyporheic zone and NPS inflows, a HCIS model henceforth denoted as HCIS-NPS*hez* model is conceptualised. The stream network is conceptually split into several hybrid units as shown in Figure 3.3 which consist of three zones each of disparate retention times. The effluents from the plug zone flows into the first well mixed zone. In this zone the solute is subject to advective propagation. As the effluent travels through the first well mixed zone, it is subjected to thorough mixing due to advection and dispersion processes occurring. At the exit of the first well mixed zone the solutes flow into the second well

mixed zone and forms the influent for this zone. The same process as the first mixed zone takes place in the second mixed zone. The retention time within each zone is a function of its volume (V) and the rate of stream flow (Q) (m^3s^{-1}). If the volume in each zone be denoted as V_1, V_2 and V_3 respectively. Then, retention time of the plug flow and two mixed zones are $\alpha = V_1/Q$, $T_1=V_2/Q$ and $T_2=V_3/Q$. Interactions with the hyporheic zone and inflows from non-point sources occur in all three zones.

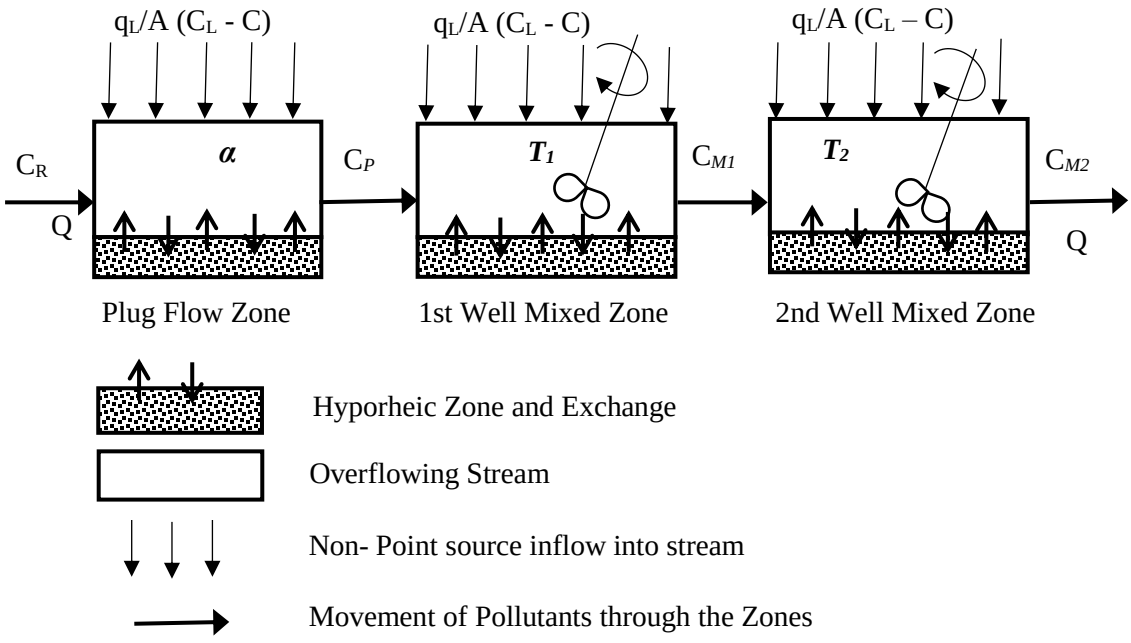

Figure 3. 2: Conceptualised HCIS-NPS model with hyporheic Zone and Exchange

3.3.2.1 Derivation of the Plug Flow Component

The governing first order kinetic equation for a control volume of a natural river/stream with non-point source pollutant inputs, subject to hyporheic exchange is described by a partial differential equation as:

$$\frac{\partial C(x,t)}{\partial t} = -u\frac{\partial C(x,t)}{\partial x} + \frac{q_L}{A}\left(C_L - C(x,t)\right) - \frac{\phi D}{R_h}\frac{\partial C_S(x,t)}{\partial t} \tag{3.36}$$

Where C (x, t) (mgl^{-1}) is pollutant concentration in the stream flow, t (min) is time interval of pollutant displacement, x (m) is longitudinal distance and u (ms^{-1}) is flow rate. q_L($m^3s^{-1}m^{-1}$) is lateral inflow, C_L (mgl^{-1}) represents non-point source pollutant concentration in lateral inflow, ϕ

is porosity of the stream bed, D (m) is depth of the underlying zone, R_h (m) is the hydraulic radius of the stream = A/W_P. A (m^2) and W_P (m) stands for the cross-section area and wetted perimeter of the stream and $C_S(x, t)$ (mgl^{-1}) is concentration of trapped pollutants in HZ. If HZ is well mixed, the flux between the zone and the overlying water depends on the concentration of the solute between both zones given as equation (3.37) (Rutherford, 1994).

$$C_S(x,t) = f\,C(x,t) \tag{3.37}$$

Where f is the proportion of the HZ to the stream bed. $f = V^*/V$. when V^* (m^3) is HZ volume and V (m^3) is volume of the cell. The volume of the hyporheic zone could be found through the relationship $\phi A^* D$ where A^* is the interface that links the stream and the hyporheic zone. If in a given situation, the hyporheic zone extends beyond the wetted perimeter of the stream, then A^* becomes the sum of the wetted perimeter and the residence time of pollutants within the control volume. According to Rutherford (1994) if the hyporheic zone occupies 50% of the length of the entire bed, extending across the entire channel then $f \approx 0.50$.

To analytically derive the plug flow component of the first hybrid unit equation (3.37) is substituted in (3.36) and solved by implementing Laplace transforms and integral processes. For a control volume governed by hyporheic exchange and inflow of uniformly flowing non-point source pollutants as seen in figure 3.3. Let Initial and boundary conditions be $C(x, 0) = 0$; $x > 0$, $C(0, t) = C_R$; $t \geq 0$ and $C(\alpha u, t) = 0$; $0 < t < \alpha$ also let q_L/A is denoted as ξ.

Therefore, simplifying equations (3.36) and (3.37) and using Laplace transform for each term, the equation reduces to,

$$SC^* = -u\frac{dC^*}{dx} + \xi C_L - \xi C^* - f\,SC^* \tag{3.38}$$

Rearranging equation (3.38), yields an ordinary differential equation given as,

$$\frac{dC^*}{dx} + \left(\frac{SR}{u} + \frac{\xi}{u}\right)C^* = \frac{\xi}{u}C_L \tag{3.39}$$

Multiply both sides by $\exp^{+\left[\frac{SR+\xi}{u}\right]x}$ equation (3.39) becomes

$$\frac{dC^*}{dx}\exp^{+\left[\frac{SR+\xi}{u}\right]x}+\left(\frac{SR}{u}+\frac{\xi}{u}\right)C^*\exp^{+\left[\frac{SR+\xi}{u}\right]x}=\frac{\xi}{u}C_L\exp^{+\left[\frac{SR+\xi}{u}\right]x} \tag{3.40}$$

Integrating equation (3.40) gives

$$C^*\exp^{+\left[\frac{SR+\xi}{u}\right]x}=\frac{\xi C_L\exp^{+\left[\frac{SR+\xi}{u}\right]x}}{S+\xi}+N \tag{3.41}$$

where N is the integration constant. Resolving when $x = 0$, $C = C_R + C_L$ and $C^* = C_R/S + C_L/S$, N becomes

$$N=\frac{C_R}{S}+\frac{C_L}{S}-\frac{\xi C_L}{SR+\xi} \tag{3.42}$$

Combining equation (3.41) and (3.42) and solving by inverse Laplace transform, the resultant equation gives the pollutant concentration exiting the plug flow zone given as equation (3.43).

$$C_P\left(\alpha u,t\right)=C_R U\left(t-\alpha R\right)\exp^{-\xi\alpha}+C_L U\left(t-\alpha R\right)\exp^{-\xi\alpha}-\psi C_L U\left(t-\alpha R\right)\exp^{-\xi t}+\psi C_L\exp^{-\xi t} \tag{3.43}$$

Equation (3.43) is the step response of pollutants leaving the plug flow zone. The step response describes a travel distance of αu at time t from injection through the plug zone. $U\ (t - \alpha R)$ is the step function of the equation when $t < \alpha R$, $U\ (t - \alpha R) = 0$ and for $t \geq \alpha R$, $U\ (t - \alpha R) = 1$. Subsequently, $C_P\ (\alpha u, t)$ is the point source and in stream influent for the first well mixed zone.

3.3.2.2 Pollutant Concentration in the First and Second Well Mixed Zone

To obtain the pollutant concentration profiles within and leaving the first well mixed zone, a mass balance equation is written as;

$$V_2\Delta C_{M1}=C_P Q\Delta t-C_{M1}Q\Delta t+\frac{q_L}{A}\left(C_L-C_{M1}\right)V_2\Delta t-\frac{\phi D}{R_h}\frac{\partial C_S\left(x,t\right)}{\partial t} \tag{3.44}$$

The mass balance equation accounts for the inflow from the plug flow zone, inflow from non-point sources as well as effects of hyporheic exchange. The volume of the first well mixed zone is denoted as $V_2 = QT_1$ as earlier defined. All other parameters are as previously defined. Substituting C_P which is the effluent from the plug flow zone into equation (3.44) yields;

$$V_2\Delta C_{M1} = \begin{bmatrix} C_R U\left(t-\alpha R\right)\exp^{-(\xi\alpha)} + C_L U\left(t-\alpha R\right)\exp^{-(\xi\alpha)} - \xi C_L U\left(t-\alpha R\right)\exp^{-(\xi t)} \\ +\xi C_L \exp^{-(\xi t)} \end{bmatrix} Q\Delta t \qquad (3.45)$$

$$- C_{M1} Q\Delta t + \xi\left(C_L - C_{M1}\right)V_2\Delta t - \frac{\phi D}{R_h}\frac{\partial C_s}{\partial t}$$

Simplifying equation (3.45) by dividing both sides by $V_2\Delta t$ and substituting the reduced proportionality constant"*f"* yields the following differential equation

$$\frac{dC_{M1}}{dt} = \frac{C_R U\left(t-\alpha R\right)\exp^{-\xi\alpha}}{T_1} + \frac{C_L U\left(t-\alpha R\right)\exp^{-\xi\alpha}}{T_1} - \frac{\xi C_L U\left(t-\alpha R\right)\exp^{-\xi t}}{T_1}$$

$$+ \frac{\xi C_L \exp^{-\xi t}}{T_1} + \xi C_L - \left[\frac{1+\xi T_1}{T_1}\right]C_{M1} - f\frac{dC_{M1}}{dt} \qquad (3.46)$$

Combine like terms, multiply both sides of equation (3.46) by $\exp^{+\left[\frac{1+\xi T_1}{RT_1}\right]t}$ when (1+ *f*) is Retardation Coefficient (*R*). and Integrate with respect to "t" produces

$$C_{M1}\exp^{+\left[\frac{1+\xi T_1}{RT_1}\right]t} = \frac{C_R U\left(t-\alpha R\right)\exp^{-\xi\alpha}\exp^{+\left[\frac{1+\xi T_1}{RT_1}\right]t}}{1+\xi T_1} + \frac{C_L U\left(t-\alpha R\right)\exp^{-\xi\alpha}\exp^{+\left[\frac{1+\xi T_1}{RT_1}\right]t}}{1+\xi T_1}$$

$$- \frac{\xi C_L U\left(t-\alpha R\right)\exp^{-\xi t}\exp^{+\left[\frac{1+\xi T_1}{RT_1}\right]t}}{\left[\xi(R-1)T_1 - 1\right]} + \frac{\xi C_L \exp^{-\xi t}\exp^{+\left[\frac{1+\xi T_1}{RT_1}\right]t}}{\left[\xi(R-1)T_1 - 1\right]} \qquad (3.47)$$

$$+ \frac{\xi C_L T_1 \exp^{+\left[\frac{1+\xi T_1}{RT_1}\right]t}}{1+\xi T_1} + A$$

Further, substitution where *A* is the integration constant. And solving *A* when $C_{M1} = 0$ and $t = \alpha R$, equation (3.47) becomes,

$$C_{M1} = \frac{C_R U(t-\alpha R)\exp^{-\xi\alpha}}{1+\xi T_1} + \frac{C_L U(t-\alpha R)\exp^{-\xi\alpha}}{1+\xi T_1} - \frac{\xi C_L U(t-\alpha R)\exp^{-\xi t}}{\left[\xi(R-1)T_1 - 1\right]} + \frac{\xi C_L \exp^{-\xi t}}{\left[\xi(R-1)T_1 - 1\right]}$$
$$+ \frac{\xi C_L T_1}{1+\xi T_1} - \frac{C_R U(t-\alpha R)\exp^{-\xi\alpha}\exp^{-\left[\frac{1+\xi T_1}{RT_1}\right](t-\alpha R)}}{1+\xi T_1} - \frac{C_L U(t-\alpha R)\exp^{-\xi\alpha}\exp^{-\left[\frac{1+\xi T_1}{RT_1}\right](t-\alpha R)}}{1+\xi T_1}$$
$$+ \frac{\xi C_L U(t-\alpha R)\exp^{-(\xi\alpha R)}\exp^{-\left[\frac{1+\xi T_1}{RT_1}\right](t-\alpha R)}}{\left[\xi(R-1)T_1 - 1\right]} - \frac{\xi C_L \exp^{-(\xi\alpha R)}\exp^{-\left[\frac{1+\xi T_1}{RT_1}\right](t-\alpha R)}}{\left[\xi(R-1)T_1 - 1\right]}$$
$$- \frac{\xi C_L T_1 \exp^{-\left[\frac{1+\xi T_1}{RT_1}\right](t-\alpha R)}}{1+\xi T_1} \qquad (3.48)$$

Hence, C_{M1} is the Concentration of the effluent at the end of the first well mixed zone. Subsequently, C_{M1} flows into the second well mixed zone and therefore becomes the point source influent to the zone. Thus, the mass balance equation for the second mixed zone with the inclusion of non-point source inflows and assuming hyporheic exchange is

$$V_3 \Delta C_{M2} = C_{M1} Q\Delta t - C_{M2} Q\Delta t + \frac{q_L}{A}(C_L - C_{M2})V_2\Delta t - \frac{\phi D}{R_h}\frac{\partial C_S(x,t)}{\partial t} \qquad (3.49)$$

Combining equation (3.48) and (3.49) yields

$$V_3\Delta C_{M2} = \left[\begin{array}{l} \dfrac{C_R U(t-\alpha R)\exp^{-\xi\alpha}}{1+\xi T_1} + \dfrac{C_L U(t-\alpha R)\exp^{-\xi\alpha}}{1+\xi T_1} - \dfrac{\xi C_L U(t-\alpha R)\exp^{-\xi t}}{\left[\xi(R-1)T_1-1\right]} + \dfrac{\xi C_L \exp^{-\xi t}}{\left[\xi(R-1)T_1-1\right]} \\ + \dfrac{\xi C_L T_1}{1+\xi T_1} - \dfrac{C_R U(t-\alpha R)\exp^{-\xi\alpha}\exp^{-\left[\frac{1+\xi T_1}{RT_1}\right](t-\alpha R)}}{1+\xi T_1} - \dfrac{C_L U(t-\alpha R)\exp^{-\xi\alpha}\exp^{-\left[\frac{1+\xi T_1}{RT_1}\right](t-\alpha R)}}{1+\xi T_1} \\ + \dfrac{\xi C_L U(t-\alpha R)\exp^{-(\xi\alpha R)}\exp^{-\left[\frac{1+\xi T_1}{RT_1}\right](t-\alpha R)}}{\left[\xi(R-1)T_1-1\right]} - \dfrac{\xi C_L \exp^{-(\xi\alpha R)}\exp^{-\left[\frac{1+\xi T_1}{RT_1}\right](t-\alpha R)}}{\left[\xi(R-1)T_1-1\right]} \\ - \dfrac{\xi C_L T_1 \exp^{-\left[\frac{1+\xi T_1}{RT_1}\right](t-\alpha R)}}{1+\xi T_1} \end{array}\right] Q\Delta t$$

$$- C_{M2} Q\Delta t + \xi\left(C_L - C_{M2}\right)V_3\Delta t - \frac{\phi D}{R_h}\frac{\partial C_s}{\partial t} \qquad (3.50)$$

Divide the equation through by $V_3\Delta t$ and rewriting in differentials yields

$$\begin{aligned} \frac{dC_{M2}}{dt} &= \frac{C_R U(t-\alpha R)\exp^{-(\xi\alpha)}}{T_2(1+\xi T_1)} + \frac{C_L U(t-\alpha R)\exp^{-(\xi\alpha)}}{T_2(1+\xi T_1)} - \frac{\xi C_L U(t-\alpha R)\exp^{-(\xi t)}}{T_2\left[\xi(R-1)T_1-1\right]} - \frac{\xi C_L \exp^{-(\xi t)}}{T_2\left[\xi(R-1)T_1-1\right]} \\ &+ \frac{\xi C_L \mathrm{T}_1}{T_2(1+\xi T_1)} - \frac{C_R U(t-\alpha R)\exp^{-(\xi\alpha)}\exp^{-\left[\frac{1+\xi T_1}{RT_1}\right](t-\alpha R)}}{T_2(1+\xi T_1)} - \frac{C_L U(t-\alpha R)\exp^{-(\xi\alpha)}\exp^{-\left[\frac{1+\xi T_1}{RT_1}\right](t-\alpha R)}}{T_2(1+\xi T_1)} \\ &+ \frac{\xi C_L U(t-\alpha R)\exp^{-(\xi\alpha R)}\exp^{-\left[\frac{1+\xi T_1}{RT_1}\right](t-\alpha R)}}{T_2\left[\xi(R-1)T_1-1\right]} - \frac{\xi C_L \exp^{-(\xi\alpha R)}\exp^{-\left[\frac{1+\xi T_1}{RT_1}\right](t-\alpha R)}}{T_2\left[\xi(R-1)T_1-1\right]} - \frac{\xi C_L \mathrm{T}_1 \exp^{-\left[\frac{1+\xi T_1}{RT_1}\right](t-\alpha R)}}{T_2(1+\xi T_1)} \\ &+ \xi C_L - \frac{1+\xi T_2}{T_2} C_{M2} - f\frac{dC_{M2}}{dt} \end{aligned} \qquad (3.51)$$

Solution of equation (3.51) produces the step response of the pollutant concentration leaving the second well mixed zone as,

$$C_{M2}=\frac{C_R U\left(t-\alpha R\right)\exp^{-(\xi\alpha)}}{\left(1+\xi T_2\right)\left(1+\xi T_1\right)}+\frac{C_L U\left(t-\alpha R\right)\exp^{-(\xi\alpha)}}{\left(1+\xi T_2\right)\left(1+\xi T_1\right)}-\frac{\xi C_L U\left(t-\alpha R\right)\exp^{-(\xi t)}}{\left[\xi\left(R-1\right)T_2-1\right]\left[\xi\left(R-1\right)T_1-1\right]}+\frac{\xi C_L\exp^{-(\xi t)}}{\left[\xi\left(R-1\right)T_2-1\right]\left[\xi\left(R-1\right)T_1-1\right]}$$

$$+\frac{\xi C_L T_1}{\left(1+\xi T_2\right)\left(1+\xi T_1\right)}-\frac{C_R T_1 U\left(t-\alpha R\right)\exp^{-(\xi\alpha)}\exp^{-\left[\frac{1+\xi T_1}{RT_1}\right](t-\alpha R)}}{\left(T_1-T_2\right)\left(1+\xi T_1\right)}-\frac{C_L T_1 U\left(t-\alpha R\right)\exp^{-(\xi\alpha)}\exp^{-\left[\frac{1+\xi T_1}{RT_1}\right](t-\alpha R)}}{\left(T_1-T_2\right)\left(1+\xi T_1\right)}$$

$$+\frac{\xi C_L T_1 U\left(t-\alpha R\right)\exp^{-(\xi\alpha R)}\exp^{-\left[\frac{1+\xi T_1}{RT_1}\right](t-\alpha R)}}{\left(T_1-T_2\right)\left[\xi\left(R-1\right)T_1-1\right]}-\frac{\xi C_L T_1\exp^{-(\xi\alpha R)}\exp^{-\left[\frac{1+\xi T_1}{RT_1}\right](t-\alpha R)}}{\left(T_1-T_2\right)\left[\xi\left(R-1\right)T_1-1\right]}-\frac{\xi C_L T_1 T_1\exp^{-\left[\frac{1+\xi T_1}{RT_1}\right](t-\alpha R)}}{\left(T_1-T_2\right)\left(1+\xi T_1\right)}$$

$$+\frac{C_L T_2\xi}{\left(1+\xi T_2\right)}-\frac{C_R U\left(t-\alpha R\right)\exp^{-(\xi\alpha)}\exp^{-\left[\frac{1+\xi T_2}{RT_2}\right](t-\alpha R)}}{\left(1+\xi T_2\right)\left(1+\xi T_1\right)}-\frac{C_L U\left(t-\alpha R\right)\exp^{-(\xi\alpha)}\exp^{-\left[\frac{1+\xi T_2}{RT_2}\right](t-\alpha R)}}{\left(1+\xi T_2\right)\left(1+\xi T_1\right)}$$

$$+\frac{\xi C_L U\left(t-\alpha R\right)\exp^{-(\xi\alpha R)}\exp^{-\left[\frac{1+\xi T_2}{RT_2}\right](t-\alpha R)}}{\left[\xi\left(R-1\right)T_2-1\right]\left[\xi\left(R-1\right)T_1-1\right]}-\frac{\xi C_L\exp^{-(\xi\alpha R)}\exp^{-\left[\frac{1+\xi T_2}{RT_2}\right](t-\alpha R)}}{\left[\xi\left(R-1\right)T_2-1\right]\left[\xi\left(R-1\right)T_1-1\right]}-\frac{\xi C_L T_1\exp^{-\left[\frac{1+\xi T_2}{RT_2}\right](t-\alpha R)}}{\left(1+\xi T_2\right)\left(1+\xi T_1\right)}$$

$$+\frac{C_R T_1 U\left(t-\alpha R\right)\exp^{-(\xi\alpha)}\exp^{-\left[\frac{1+\xi T_2}{RT_2}\right](t-\alpha R)}}{\left(T_1-T_2\right)\left(1+\xi T_1\right)}+\frac{C_L T_1 U\left(t-\alpha R\right)\exp^{-(\xi\alpha)}\exp^{-\left[\frac{1+\xi T_2}{RT_2}\right](t-\alpha R)}}{\left(T_1-T_2\right)\left(1+\xi T_1\right)}-\frac{\xi C_L T_1 U\left(t-\alpha R\right)\exp^{-(\xi\alpha R)}\exp^{-\left[\frac{1+\xi T_2}{RT_2}\right](t-\alpha R)}}{\left(T_1-T_2\right)\left[\xi\left(R-1\right)T_1-1\right]} \tag{3.52}$$

$$+\frac{\xi C_L T_1\exp^{-(\xi\alpha R)}\exp^{-\left[\frac{1+\xi T_2}{RT_2}\right](t-\alpha R)}}{\left(T_1-T_2\right)\left[\xi\left(R-1\right)T_1-1\right]}-\frac{\xi C_L T_1 T_1\exp^{-\left[\frac{1+\xi T_2}{RT_2}\right](t-\alpha R)}}{\left(T_1-T_2\right)\left(1+\xi T_1\right)}+\frac{C_L T_2\xi\exp^{-\left[\frac{1+\xi T_2}{RT_2}\right](t-\alpha R)}}{\left(1+\xi T_2\right)}$$

$C_{M2} = K_{HCIS-NPShez}$ is the pollutant concentration leaving the second well mixed zone. Hence it is the step response of the first hybrid unit. The equation is valid when $t \geq \alpha R$. The derivative of equation (3.52) with respect to" t" yields equation (3.53) which is the unit impulse response function $\delta_{HCIS\text{-}NPShez}(n, \Delta t)$ at the end of the first hybrid unit and describes the variations in solute concentrations at the boundaries valid for $t \geq \alpha$.

$$\delta_{HCIS-NPShez}(n,\Delta t) = \frac{K_{HCIS-NPShez}(n\Delta t) - K_{HCIS-NPShez}\left((n-1)\Delta t\right)}{\Delta t} \tag{3.53}$$

Equations (3.52) and (3.53) are the step and impulse responses at the end of the first hybrid unit for the river channel. Hence, with the help of convolution technique, subsequent pollutant concentrations at downstream locations along the river is obtained. Where the effluent concentration at the end of the *nth* hybrid unit at $i\Delta t$ is,

$$C(n\Delta x, i\Delta t) = \sum_{\gamma=1}^{i} C\left[(n-1)\Delta x, \gamma\Delta t\right] \delta_{HCIS-NPShez}\left[(i-\gamma+1), \Delta t\right] \tag{3.54}$$

3.3.3 Performance of Proposed HCIS-NPShez in Comparison with ADE-NPShez

As previously mentioned the classical ADE model has long been the basis for simulation of solutes in rivers. However, due to its inability to adequately represent the behaviour of solutes in natural streams and rivers, various modifications have been attempted. In showing the potential of the proposed model as an alternate to the ADE model, both models are tested with the inclusion of Non-point source and Hyporheic exchange components to the classical ADE.

$$\frac{\partial C(x,t)}{\partial t} = -u\frac{\partial C(x,t)}{\partial x} + D_L\frac{\partial^2 C(x,t)}{\partial x^2} + \frac{q_L}{A}\left(C_L - C(x,t)\right) - \frac{\phi D}{R_h}\frac{\partial C_S(x,t)}{\partial t} \tag{3.55}$$

The step response function of the ADE-NPS*hez* model obtained when equation (3.55) is numerically solved with the explicit finite difference method is,

$$C(x,t+\Delta t)=C(x,t)\left[1-\frac{2D_L\Delta t}{R\Delta x^2}-\frac{q_L}{AR}\Delta t\right]-C(x+\Delta x,t)\left[\frac{u\Delta t}{2R\Delta x}-\frac{D_L\Delta t}{R\Delta x^2}\right] \quad (3.56)$$
$$+C(x-\Delta x,t)\left[\frac{u\Delta t}{2R\Delta x}+\frac{D_L\Delta t}{R\Delta x^2}\right]+C_L\left[\frac{q_L}{AR}\Delta t\right]$$

To prevent oscillations in the numerical solution, conditions to satisfy the courant number through the relationship $u\Delta t/\Delta x \leq 1$ is adhered to (Chapra, 2008). Equation (3.56) is further numerically differentiated with respect to "t" to produce the unit impulse response of ADE-NPS*hez* model. Through application of numerical convolution, the pollutant concentration from the near to the far field of the stream at distances of 200, 600, 1400 and 2000m is simulated. The numerical solution of the ADE-NPS*hez* model derived through the explicit finite difference method is compared to the analytical solution of the HCIS-NPS*hez* model for the same reach lengths. The same parameters used previously are maintained except for Δx which is set at 100m to satisfy the conditions for the courant number. Also, for ADE-NPS*hez* the unique parameters of α, T_1, and T_2 are not used. The impulse response of the ADE-NPS*hez* and HCIS-NPS*hez* models are simulated when R=1.2 and is presented as figure 4.9.

3.3.4 Validation of Retardation Equation

Equation 3.35 derived by Kumarasamy (2011) is used to obtain the retardation coefficient for the proposed model. To ensure the validity of the equation, data from Knapp et al. (2017) is utilised. Knapp et al. (2017) presented a retardation factor of resazurin to be within the range of 1.45 when the medium porosity is 0.39. Using equation (3.35) and inputting data as presented in Knapp et al. (2017) the retardation factor is calculated. Validation and discussion of results are presented in chapter four.

3.4 Derivation of Reactive Pollutant Transport in Natural Rivers with Non-Point Source Hybrid Cells in Series Model

3.4.1 Reactive pollutant and processes

Studies in recent years have shown that most reactive pollutants in natural rivers originate from Non-point sources through storm water runoff. This section expands the development of a non-point source model towards simulating non-conservative pollutants in rivers.

Pollutants from point and/or NPS when released into water bodies follow a scheme of occurrences (Lopez et al., 2013; Gao et al., 2015). Generally, the presence of pollutants classified either as conservative or non-conservative/reactive in water bodies, degrades it and makes it unfit for any kind of use. Rivers, naturally, have a self-purifying mechanism which restores its balance. However, when pollutant loads exceed the self-cleansing capacity of the river, the entire eco-system becomes distorted (Wen et al., 2017; Kumarasamy et al., 2015). Reactive pollutants which are subject to decay constitute most of freshwater pollutants (Nyenje et al., 2010; Varol and Sen, 2012; Kiedrzyńska et al., 2014; McDowell et al., 2017). A large proportion of reactive pollutants have been found as being sourced from NPS through runoff mainly from agricultural lands and informal settlements (Nyenje et al., 2010; Gavrilescu et al., 2015; Yuceer et al., 2016, Wen et al, 2017; McDowell et al., 2017). The pollutant contributions from non-point sources influence in-stream water quality of usable water considerably with its impact felt downstream the river network. (Jiake et al., 2011; Mueller-Warrant et al., 2012; Poudel et al., 2013). The processes that occur within the water body over time, determines the fate of the pollutants, as they undergo chemical and or biological changes within the water channel due to decay.

These processes influence the pollutant concentration as it moves downstream from the source of entry. Depletion of oxygen, excessive toxic algae growth from the enrichment of the water body due to excess nutrient loading and loss of biodiversity in the eco-system, are a direct fall out from these occurrences. Quantifying, therefore, these processes and its effects have become necessary. This is even of more importance when such pollutants are generated from non-point sources (Abon et al., 2009; Loucks and Beek, 2017). In this regard, water quality management requires deep understanding on the distribution and behaviour of the pollutants in water systems to restore its quality to acceptable levels. The difficulties linked with the behaviour of reactive contaminants in waterways, inform the need for simplified interpretive models. It is essential that the model does not need extensive data input for calibration, and that the necessary data can be obtained with reasonable resource allocation.

Vast research involving modelling of the transport of reactive substances have been carried out. Initial attempts focused on predictions of in-stream pollutant concentration, the fate of in-stream fluxes and the threat of nutrient pollution in rivers generated from point sources (Voβ et al., 2012). However, not much has been done when it concerns contributions from non-point sources since it

is cumbersome to predict when compared to point source pollution (Abon et al., 2009). This forms the motivation for this work, bearing in mind as earlier stated, that significant quantities of nutrients and reactive pollutants generated from agricultural lands and informal settlements find their way into surface water through rainfall run-off, otherwise classified as non-point sources (Corriveau et al., 2010; Oliveira et al., 2012; Gavrilescu et al., 2015; Yuceer et al., 2016, Nuruzzaman et al., 2017). Consequently, the development of a simulation tool for water quality management for streams and rivers susceptible to reactive pollutant build-up from non-point sources is necessary. Such a tool is necessary to understand the movement of such pollutants along natural watercourses for effective pollution management.

3.4.2 Scope for development of the new model component to simulate decaying pollutant

Decay is generally presented by a first order kinetic equation, where concentration with respect to time and distance is expressed as equation (3.57) (Bear, 1972)

$$C(x,t) = \frac{x}{2t\sqrt{\pi D_L t}} \exp\left[\frac{-(x-ut)^2}{4D_L t} - kt\right] \tag{3.57}$$

Equation 3.56 is the analytical solution of the classical ADE model for impulse injection of reactive pollutants for steady and uniform flow conditions in rivers (Bear, 1972; Abon et al., 2009; Cherubini et al., 2014). A major challenge, however, lies in estimating the dispersion coefficient. Fischer (1968) used the routing method in estimating dispersion coefficients, by matching predicted concentration-time profiles with measured concentration-time profiles for assumed values of the dispersion coefficient. This is done until a minimal difference between both patterns as measured by the sum of squared differences is achieved. This method however is cumbersome and in practice difficult to measure (Benedini and Tsakiris, 2013). Also, according to Benedini and Tsakiris, (2013), the ADE does not entirely represent the on-site observations of the behaviour of pollutants in natural rivers accurately. The shortcomings of the traditional fickian based models, led to several modelling attempts including the HCIS model (Ghosh, 2001). Since a significant proportion of pollutants from non-point sources have been found to be susceptible to decay, the HCIS-NPS model will be further extended to include a decay component. Therefore, without targeting any specific type of pollutant, this section looks to incorporate a first-order kinetic component to the current HCIS-NPS model, henceforth referred as HCIS-NPS*k* model, for the simulation of non-conservative contaminants in rivers. This will contribute to understanding the in-stream processes of non-conservative pollutants in water bodies with non-point source inflows.

3.4.3 Hybrid Cells in Series (HCIS) Model

The HCIS model developed by Ghosh (2001) as an alternative model to the Fickian based ADE and other associated models for pollutant transport in natural rivers and streams has been further developed over the years with the inclusion of other components. Kumarasamy et al. (2013) developed a HCIS model to simulate pollutant transport with first-order decay kinetics to predict the concentration of non-conservative point source pollutants in a natural river. In the model, Kumarasamy et al. (2013) considers that the decay process of pollutants in a water body is governed by the Streeter-Phelps first-order reaction kinetics equation (3.58) (Fischer et al., 1979).

$$\frac{dC(x,t)}{dt} = -k_a C(x,t) \tag{3.58}$$

ka (per min) is the first order decay constant, and *C(x,t)* (mgl^{-1}) is the concentration of the pollutant in the water (Kumarasamy et al., 2013; Kahil, 2016). The negative sign in the equation indicates pollutant abatement or decay (Fischer et al., 1979; Ki et al., 2009: Kahil, 2016). The conceptualised HCIS-NPS*k* model, which incorporates decay processes of first-order reaction kinetics is presented in figure 3.4. The proposed HCIS-NPS*k* model consists of a plug flow cell and two mixing cells connected in series and with unequal residence time, decided by the volume (*V*) and the flow rate (*Q*) within each cell. As the non-conservative pollutant moves through the plug cell, the moving plume is replaced in α time by pure advection with minimal drop in pollutant concentration due to decay. The effluent flows into the first mixing cell with residence time T_1 where thorough mixing takes place; through the joint process of advection and dispersion. Within this cell decomposition of the pollutant takes place. After T_1 time, the effluent flows into the second mixing cell with residence time T_2, where continuous mixing and decay also occur.

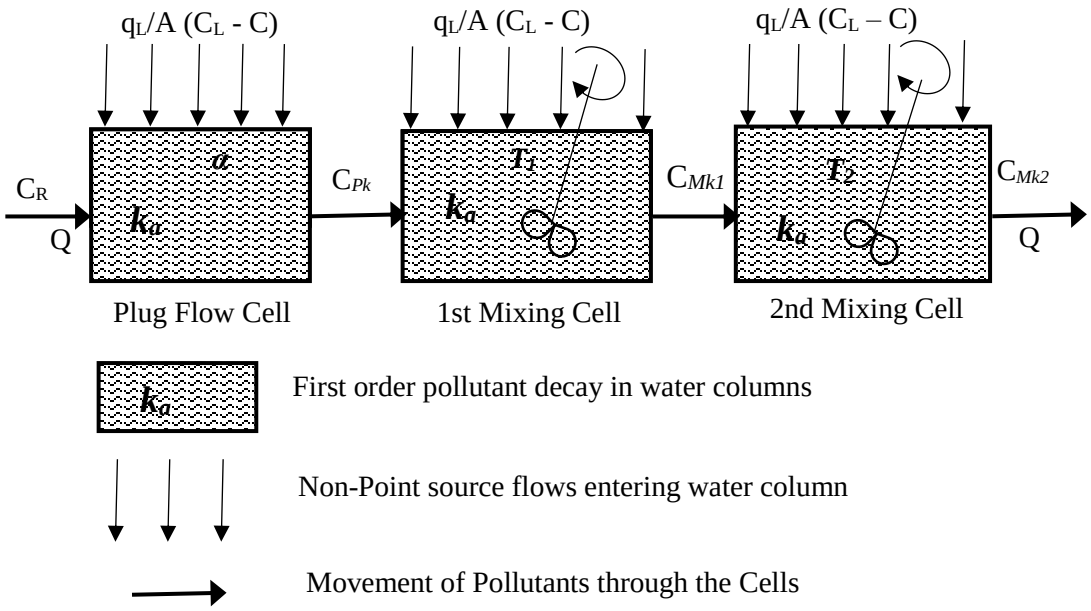

Figure 3. 3: HCIS-NPS unit with in-stream first order kinetic reactions

3.4.3.1 Derivation of Pollutant Concentration through the Plug Flow Zone

The Initial and boundary conditions which expresses the initial state of pollution and concentration at the boundary of the river are set as $C\,(x, 0) = 0$; $x > 0$, $C\,(0, t) = C_R$; $t \geq 0$ and $C\,(\alpha u, t) = 0$; $0 < t < \alpha$. The initial boundary concentration of pollutants in each cell changes from zero to C_R with time.

The plug flow cell of the HCIS-NPS*k* model which has a conceptualised control volume V and length Δx, subject to advection processes, first-order decay and lateral inflow of pollutant is expressed as shown in the mass balance equation.

$$\frac{\partial C(x,t)}{\partial t} = -u\frac{\partial C(x,t)}{\partial x} + \frac{q_L}{A}\left(C_L - C(x,t)\right) - k_a C(x,t) \tag{3.59}$$

$C\,(x, t)$ is the pollutant concentration in the water body (mgl^{-1}), u is flow velocity of the water body (ms^{-1}), t is time interval of solute displacement (s), x is distance from source (m), q_L is lateral inflow ($m^3s^{-1}m^{-1}$), C_L is pollutant concentration in lateral inflow (mgl^{-1}), k_a is the first order decay

constant (s^{-1}) while A is the cross-sectional area of water channel (m^2). Henceforth, q_L/A is denoted as ψ while $\epsilon = \psi + k_a$.

Taking the Laplace transform of all terms in equation (3.59) reduces to

$$u\frac{dC^*}{dx} = -SC^* - \epsilon C^* + \psi C_L \tag{3.60}$$

Simplifying equation (3.60) yields

$$\frac{dC^*}{dx}\exp^{+\left[\frac{S+\epsilon}{u}\right]x} + \left[\frac{S+\epsilon}{u}\right]C^*\exp^{+\left[\frac{S+\epsilon}{u}\right]x} = \frac{\psi}{u}C_L\exp^{+\left[\frac{S+\epsilon}{u}\right]x} \tag{3.61}$$

Equation (3.61) is solved by integration, when $x = 0$, $C = C_R + C_L$ and $C^* = C_R/S + C_L/S$. Then, solving by inverse Laplace transforms equation (3.61) yields

$$C_{Pk}(\alpha u, t) = C_R U(t-\alpha)\exp^{-\epsilon\alpha} + C_L U(t-\alpha)\exp^{-\epsilon\alpha} - \psi C_L U(t-\alpha)\exp^{-\epsilon t} + \psi C_L \exp^{-\epsilon t} \tag{3.62}$$

Equation (3.62) stands for the concentration of the pollutant leaving the plug flow cell, for pollutants subject to decay at conditions when $t \geq \alpha$. While U $(t - \alpha)$ is the step function which ranges from 0 when $t < \alpha$ to 1 when $t \geq \alpha$.

3.4.3.2 Derivation of Pollutant Concentration through the First Mixing Cell

Outflow from the plug flow cell, equation (3.62), having travelled through the cell over α time, forms the influent to the first mixing cell. In the mass balance equation, the change in solute concentration within the cell and the effluent mass leaving the plug flow cell into the first mixing cell are accounted for. Also considered are the effluent moving through the first mixing cell, the uniformly distributed lateral inflow into the cell and the mass decayed within the cell. All terms mentioned follow the same sequence in the presentation of the equation. The mass balance equation for the first mixing cell is presented as equation (3.63).

$$V_1\Delta C_{Mk1} = C_{Pk}Q\Delta t - C_{Mk1}Q\Delta t + \frac{q_L}{A}(C_L - C_{Mk1})V_1\Delta t - k_a C_{Mk1}V_1\Delta t \tag{3.63}$$

where V_1 is the volume of the mixing cell, and Q is the flow rate within the cell. The fill time of the cell is $T_1 = V_1/Q$. Thus, rewritten in differentials, equation (3.63) becomes;

$$\frac{dC_{M\,k1}}{dt} = \frac{C_R U\left(t-\alpha\right)\exp^{-\epsilon\alpha}}{T_1} + \frac{C_L U\left(t-\alpha\right)\exp^{-\epsilon\alpha}}{T_1} - \frac{\psi C_L U\left(t-\alpha\right)\exp^{-\epsilon t}}{T_1} + \frac{\psi C_L \exp^{-\epsilon t}}{T_1} - \left[\frac{1+\epsilon T_1}{T_1}\right] C_{M\,k1} + \psi C_L \tag{3.64}$$

The solution of equation (3.64) gives the concentration of pollutants exiting the first mixing cell with decay occurring as expressed in equation (3.65). And is valid when $t \geq \alpha$.

$$C_{M\,k1} = \frac{C_R U\left(t-\alpha\right)\exp^{-\epsilon\alpha}}{1+\epsilon T_1} + \frac{C_L U\left(t-\alpha\right)\exp^{-\epsilon\alpha}}{1+\epsilon T_1} - \psi C_L U\left(t-\alpha\right)\exp^{-\epsilon t} + \psi C_L \exp^{-\epsilon t} + \frac{\psi C_L T_1}{1+\epsilon T_1} - \frac{C_R U\left(t-\alpha\right)\exp^{-\epsilon\alpha}\exp^{-\left[\frac{1+\epsilon T_1}{T_1}\right](t-\alpha)}}{1+\epsilon T_1} - \frac{C_L U\left(t-\alpha\right)\exp^{-\epsilon\alpha}\exp^{-\left[\frac{1+\epsilon T_1}{T_1}\right](t-\alpha)}}{1+\epsilon T_1} + \psi C_L U\left(t-\alpha\right)\exp^{-\epsilon\alpha}\exp^{-\left[\frac{1+\epsilon T_1}{T_1}\right](t-\alpha)} - \psi C_L \exp^{-\epsilon\alpha}\exp^{-\left[\frac{1+\epsilon T_1}{T_1}\right](t-\alpha)} - \frac{\psi C_L T_1 \exp^{-\left[\frac{1+\epsilon T_1}{T_1}\right](t-\alpha)}}{1+\epsilon T_1} \tag{3.65}$$

3.4.3.3 Derivation of Pollutant Concentration through the Second Mixing Cell

Similarly, effluent from the first mixing cell, C_{MK1}, becomes infeed to the second mixing cell, with a fill time of $T_2 = V_2/Q$, where V_2 is volume of the second mixing cell. Subsequently, the mass balance for the cell is;

$$V_2 \Delta C_{M\,k2} = C_{M\,k1} Q\Delta t - C_{M\,k2} Q\Delta t + \frac{q_L}{A}\left(C_L - C_{M\,k2}\right)V_2 \Delta t - k_1 C_{M\,k2} V_2 \Delta t \tag{3.66}$$

Divide equation (3.66) through by $V_2 \Delta t$ and written in differential form yields

$$\frac{dC_{Mk2}}{dt}=\frac{C_R U\left(t-\alpha\right)\exp^{-\epsilon\alpha}}{T_2\left(1+\epsilon T_1\right)}+\frac{C_L U\left(t-\alpha\right)\exp^{-\epsilon\alpha}}{T_2\left(1+\epsilon T_1\right)}-\frac{\psi C_L U\left(t-\alpha\right)\exp^{-\epsilon t}}{T_2}+\frac{\psi C_L\exp^{-\epsilon t}}{T_2}$$

$$-\frac{C_R U\left(t-\alpha\right)\exp^{-\epsilon\alpha}\exp^{-\left[\frac{1+\epsilon T_1}{T_1}\right](t-\alpha)}}{T_2\left(1+\epsilon T_1\right)}-\frac{C_L U\left(t-\alpha\right)\exp^{-\epsilon\alpha}\exp^{-\left[\frac{1+\epsilon T_1}{T_1}\right](t-\alpha)}}{T_2\left(1+\epsilon T_1\right)}$$

$$+\frac{\psi C_L U\left(t-\alpha\right)\exp^{-\epsilon\alpha}\exp^{-\left[\frac{1+\epsilon T_1}{T_1}\right](t-\alpha)}}{T_2}-\frac{\psi C_L\exp^{-\epsilon\alpha}\exp^{-\left[\frac{1+\epsilon T_1}{T_1}\right](t-\alpha)}}{T_2} \tag{3.67}$$

$$-\frac{\psi C_L T_1\exp^{-\left[\frac{1+\epsilon T_1}{T_1}\right](t-\alpha)}}{T_2\left(1+\epsilon T_1\right)}-\left[\frac{1+\psi T_2}{T_2}\right]C_{Mk2}+\psi C_L-k_a C_{Mk2}$$

Integrating equation (3.67) with respect to "t" yields

$$C_{Mk2}=K_{HCIS-NPSk}=\frac{C_R U\left(t-\alpha\right)\exp^{-\epsilon\alpha}}{\left(1+\epsilon T_1\right)}\left[\Re\right]+\frac{C_L U\left(t-\alpha\right)\exp^{-\epsilon\alpha}}{\left(1+\epsilon T_1\right)}\left[\Re\right]-\psi C_L U\left(t-\alpha\right)\left[\mathrm{E}-\Im\right]$$

$$+\psi C_L\left[\mathrm{E}-\Im\right]+\frac{\psi C_L T_1}{\left(1+\epsilon T_1\right)}\left[\Re\right]+\frac{\psi C_L T_2}{\left(1+\epsilon T_2\right)}\left[\aleph\right] \tag{3.68}$$

Where;

$$\Re=\left[\frac{1-\exp^{-\left[\frac{1+\epsilon T_2}{T_2}\right](t-\alpha)}}{\left(1+\epsilon T_2\right)}-\frac{T_1\left[\exp^{-\left[\frac{1+\epsilon T_1}{T_1}\right](t-\alpha)}-\exp^{-\left[\frac{1+\epsilon T_2}{T_2}\right](t-\alpha)}\right]}{\left(T_1-T_2\right)}\right];\quad \aleph=\left[1-\exp^{-\left[\frac{1+\epsilon T_2}{T_2}\right](t-\alpha)}\right]$$

$$\mathrm{E}=\left[\exp^{-\epsilon t}-\exp^{-\epsilon\alpha}\exp^{-\left[\frac{1+\epsilon T_2}{T_2}\right](t-\alpha)}\right];\qquad \Im=\left[\frac{T_1\exp^{-\epsilon\alpha}\left[\exp^{-\left[\frac{1+\epsilon T_1}{T_1}\right](t-\alpha)}-\exp^{-\left[\frac{1+\epsilon T_2}{T_2}\right](t-\alpha)}\right]}{\left(T_1-T_2\right)}\right]$$

Equation (3.68) is the effluent concentration and step response $K_{\text{HCIS-NPS}k}$, at the end of the first hybrid unit. Valid when $t \geq \alpha$. α is the residence time in the plug flow cell.

The response to unit impulse perturbation $k_{\text{HCIS-NPS}k}$ at the end of the first hybrid unit is derived when $K_{\text{HCIS-NPS}k}$ is differentiated with respect to "t" as given in equation (3.69) to yield equation (3.70).

$$k_{HCIS-NPSk} = \delta_{HCIS-NPSk}\left(n,\Delta t\right) = \frac{K_{HCIS-NPSk}\left(n\Delta t\right) - K_{HCIS-NPSk}\left(\left(n-1\right)\Delta t\right)}{\Delta t} \tag{3.69}$$

hence:

$$\begin{aligned} k_{HCIS-NPSk} = \frac{K_{HCIS-NPSk}}{dt} &= \frac{C_R U\left(t-\alpha\right)\exp^{-\in\alpha}}{\left(1+\in T_1\right)}\left[\lambda\right] + \frac{C_L U\left(t-\alpha\right)\exp^{-\in\alpha}}{\left(1+\in T_1\right)}\left[\lambda\right] + \frac{\psi C_L T_1}{\left(1+\in T_1\right)}\left[\lambda\right] \\ &- \psi C_L U\left(t-\alpha\right)\left[\wp+\hbar\right] + \psi C_L\left[\wp-\hbar\right] + \frac{\psi C_L T_2}{\left(1+\in T_2\right)}\left[\Omega\right] \end{aligned} \tag{3.70}$$

where:

$$\lambda = \left[\frac{\exp^{-\left[\frac{1+\in T_1}{T_1}\right](t-\alpha)}}{T_2} + \frac{\left(1+\in T_1\right)\exp^{-\left[\frac{1+\in T_1}{T_1}\right](t-\alpha)} - T_1\left(1+\in T_2\right)\exp^{-\left[\frac{1+\in T_2}{T_2}\right](t-\alpha)}}{T_2\left(T_1-T_2\right)}\right]$$

$$\wp = \left[-\in\exp^{-\in t} + \frac{\left(1+\in T_2\right)\exp^{-\in\alpha}\exp^{-\left[\frac{1+\in T_2}{T_2}\right](t-\alpha)}}{T_2}\right]; \qquad \Omega = \left[\frac{\left(1+\in T_2\right)\exp^{-\left[\frac{1+\in T_2}{T_2}\right](t-\alpha)}}{T_2}\right]$$

$$\hbar = \left[-\frac{\exp^{-\in\alpha}\left[\left(1+\in T_1\right)\exp^{-\left[\frac{1+\in T_1}{T_1}\right](t-\alpha)} + T_1\left(1+\in T_2\right)\exp^{-\left[\frac{1+\in T_2}{T_2}\right](t-\alpha)}\right]}{T_2\left(T_1-T_2\right)}\right]$$

Equation (3.70) describes the temporal variation in concentration which corresponds to the unit impulse input at the boundaries valid for $t \geq \alpha$.

To find the fate of the pollutants at downstream locations of the river channel in subsequent hybrid units, the method of convolution is applied by the discrete kernel method.

$$D\left(\mathrm{m},t\right) = \int_0^t c\left[\left(m-1\right),\tau\right]\psi\left(t-\tau\right)d\tau \tag{3.71}$$

And by numerical integrals equation (3.71) reduces to equation (3.72)

$$C(\mathrm{m}\,\Delta x, n\Delta t) = \sum_{\gamma=1}^{n} C\left[\left(m-1\right)\Delta x, \mathrm{n}\,\Delta t\right]\,\delta_{HCIS-NPSk}\left[\left(n-\gamma+1\right),\Delta t\right] \tag{3.72}$$

Equation (3.72) produces the response at the mth hybrid unit, when $m \geq 2$ for any number of hybrid units along the river reach.

3.4.4 Performance of proposed HCIS-NPSk model in comparison with ADE-NPSk Model

To further evaluate the adequacy of the proposed HCIS-NPS*k* model, the model is compared with the ADE model. Which is numerically solved with the Explicit Finite difference method, equation (3.73). The equation is inclusive of decay and non-point source components to the classical ADE and is denoted as ADE-NPS*k*. The numerical solution is compared with the results obtained from the HCIS-NPS*k* model when all boundary conditions are maintained and satisfied.

$$\frac{\partial C(x,t)}{\partial t} = -u\frac{\partial C(x,t)}{\partial x} + D_L\frac{\partial^2 C(x,t)}{\partial x^2} + \frac{q_L}{A}\left(C_L - C(x,t)\right) - k_a C(x,t) \tag{3.73}$$

$C(x,t)$ (mgl^{-1}) is the pollutant concentration in the water body, u (ms^{-1}) is flow velocity of the water body, t (s) is time interval of solute displacement, x (m) is distance from source, D_L (m^{2}s^{-1}) is the Longitudinal Dispersion coefficient, q_L (m^{3}s^{-1}m^{-1}) is lateral inflow, A (m^2) is the cross-sectional area of the stream, C_L (mgl^{-1}) is lateral inflow concentration, while k_a (s^{-1}) is the first order decay constant. Equations. (3.74, 3.75 and 3.76) which represent the forward difference in time, backward upwind for advection, and central difference in space for dispersion were used to solve equation (3.73).

$$\frac{\partial C(x,t)}{\partial t} = \frac{C(x,t+\Delta t) - C(x,t)}{\Delta t} \tag{3.74}$$

$$\frac{\partial C(x,t)}{\partial x} = \frac{C(x+\Delta x,t) - C(x-\Delta x,t)}{2\Delta x} \tag{3.75}$$

$$\frac{\partial^2 C(x,t)}{\partial x^2} = \frac{C(x+\Delta x,t) - 2C(x,t) + C(x-\Delta x,t)}{\Delta x^2} \tag{3.76}$$

The solution of equation (3.73) is the step response of the ADE-NPS*k* given as equation (3.77).

$$\begin{aligned} C(x,t+\Delta t) = {} & C(x,t)\left[1 - \frac{2D_L\Delta t}{\Delta x^2} - \frac{q_L}{A}\Delta t - k_a\Delta t\right] - C(x+\Delta x,t)\left[\frac{u\Delta t}{2\Delta x} - \frac{D_L\Delta t}{\Delta x^2}\right] \\ & + C(x-\Delta x,t)\left[\frac{u\Delta t}{2\Delta x} + \frac{D_L\Delta t}{\Delta x^2}\right] + C_L\left[\frac{q_L}{A}\Delta t\right] \end{aligned} \tag{3.77}$$

Equation (3.76) is numerically differentiated with respect to time, to obtain the impulse response of the ADE-NPS*k*. Synthetic data as previously mentioned, was used for the simulation of both models. While ensuring that in selecting a uniform space step and time step for the ADE-NPS*k* model, the Courant number did not exceed 1 to reduce oscillations and ensure numerical stability.

1.2 3.5 Summary and Conclusion

In this chapter, a HCIS-NPS model is proposed for simulating pollutant transport in water bodies affected by NPS pollution. A NPS component is incorporated to the general HCIS model which has been tested for its flexibility and adaptability for varying water quality processes and is found to overcome the flaws and complexities associated with the fickian based and other mixing cell models. In the second section of the chapter, the derivation of a HCIS-NPS*hez* model for simulation of pollutant fate and transport in natural streams and rivers subject to NPS inflows and in-stream retardation through hyporheic exchange is presented. The presence of hyporheic zones in streams has been observed to be accountable for the long tails in breakthrough curves produced from field measurements. A clear majority of non-conservative/reactive pollutants are known to be sourced from non-point sources especially from agricultural settlements and urban areas situated within close proximities to open water channels. In view of this, a Hybrid cells in series, Non-point source model with an added component for simulation of first-order reaction kinetics (HCIS-NPS*k*) is proposed and presented in the third section of the chapter.

Mass balance equations are developed for the three models representing the processes which occur within water bodies. The equations are solved through Laplace transforms to derive the mathematical solution of the models. FORTRAN program is used to compute the mathematical solution and simulate the river process.

CHAPTER 4: RESULTS AND DISCUSSION

4.1 Preamble

The performance of the three components of the HCIS model developed in section 3.3, 3.4 and 3.5 are analysed and discussed in sections 4.2, 4.3 and 4.4 of this chapter to establish the suitability of the proposed model as an effective tool in water quality management. The models in section 3.3 and 3.4 were tested with synthetic data and field data provided by Prof Ken Bencala and Rob Runkel on request. The model in section 3.5 is tested with synthetic data, this is due to the absence of data for reactive substances from Non-point source tracer tests. According to Mishra and Jain (1999), in the absence of relevant and appropriate data the efficacy of a model can be determined using synthetic data, as demonstrated by Ki et al (2009). Thus, synthetic data is used in testing the proposed model to validate its capability in accounting for NPS loading and in-stream simulations. Detailed data as extracted from Bencala et al (1990) and provided by Prof Kenneth Bencala and Robert Runkel of USGS, hydrological center, Colorado USA are presented in Appendix B.

4.2 Testing of Model Component 1 (the HCIS-NPS Model)

4.2.1 Testing with Synthetic Data

The developed model is tested under five scenarios to demonstrate its response to NPS loading. Data sets are generated based on real but random river geometries. The data is used to calibrate the size of each hybrid unit and to estimate the resident time α, T_1 and T_2 in each cell of the hybrid, using equations (3.1 - 3.3). Values for lateral flow (q_L) and pollutant concentrations (C_L) are assumed. In-stream background concentration and point source influent (C_R) is set at 1.0mgl^{-1}. The detailed parameters used for validation of the model is given in Table 4.1.

The simulated concentration profiles for both step and impulse response at end of the 1st through 5th hybrid units of the conceptualised river reach for all NPS input conditions are presented as figure 4.1 and 4.2 respectively. In all five scenarios, the C-t profiles demonstrate a drop in peak concentrations as the pollutant moved downstream from the near field, producing a long tail in the falling limb. The C-t profiles for scenario 1, is consistent with profiles produced for natural in-stream flows from point sources. In this situation instream conditions are constant and exclude

lateral inflow. Scenario 2 is simulated with inclusion of lateral inflow free of pollutants. The C-t profile presents immediate instream dilution with drop in background pollutant concentration.

Table 4.1: Synthetic data used for simulations of proposed HCIS-NPS Model

Scenarios	Q (m^3s^{-1})	U (m/min)	D_L (m^2/min)	A (m^2)	Δx (m)	α (min)	T_1 (min)	T_2 (min)	C_R (mgl^{-1})	C_L (mgl^{-1})	q_L ($m^3s^{-1}m^{-1}$)
1	6.67	20	1000	20	250	2.5	3.13	6.88	1.0	0.0	0.0
2	6.67	20	1000	20	250	2.5	3.13	6.88	1.0	0.0	0.16
3	6.67	20	1000	20	250	2.5	3.13	6.88	1.0	0.8	0.16
4	6.67	20	1000	20	250	2.5	3.13	6.88	1.0	0.8	1.6
5	6.67	20	1000	20	250	2.5	3.13	6.88	1.0	1.8	0.16

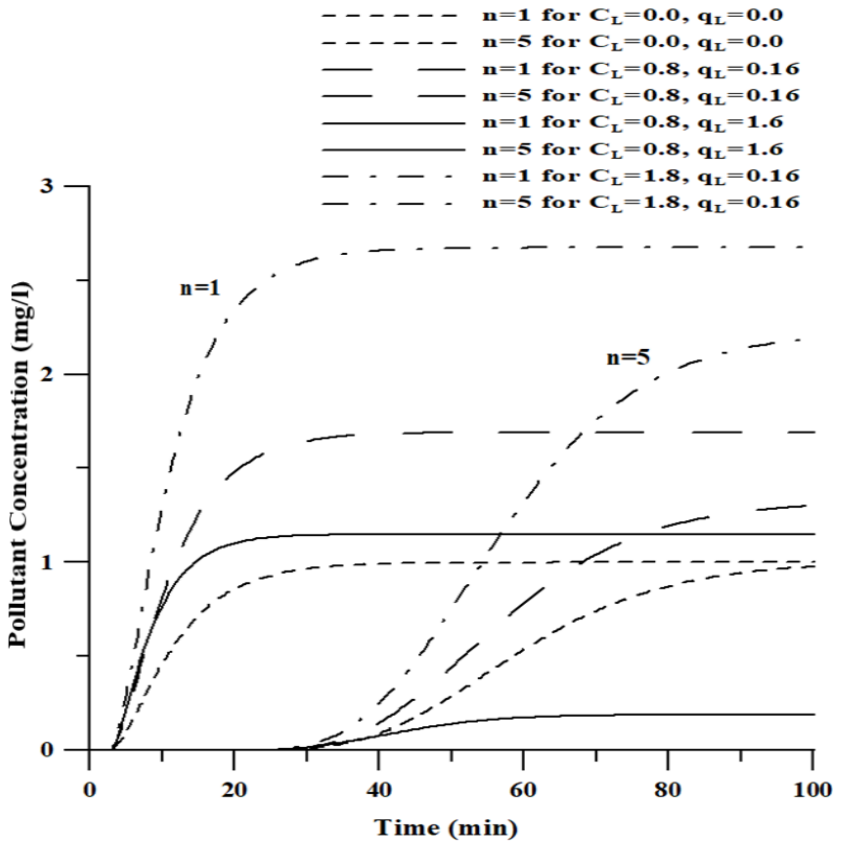

Figure 4. 1: Unit step response of HCIS-NPS model at end of 1st (n=1) and 5th (n=5) hybrid units when C_L= 0 mgl^{-1}, q_L= 0 $m^3s^{-1}m^{-1}$; C_L= 0.8 mgl^{-1}, q_L= 0.16 $m^3s^{-1}m^{-1}$; C_L=0.8 mgl^{-1}, q_L=1.6 $m^3s^{-1}m^{-1}$ and C_L=1.8 mgl^{-1}, q_L=0.16 $m^3s^{-1}m^{-1}$.

In Scenario 3, lateral inflow contains some amount of pollution and is used as a reference point for performance variation of both lateral inflow and concentration. For scenario 4, lateral inflow is increased while the pollutant concentration of scenario 3 is kept constant. In this case, the c-t profile first experiences a spike in pollutant concentration due to C_L after which dilution occurs. Increase in q_L raises instream flow rate, resulting to dilution within the water body. Attenuation in this instance is not associated with decay or reactions taking place in the water body considering the pollutant is conservative. Consequently, the concentration profile of pollutant downstream the river is not solely dependent on its characteristics, but on timescales and in-stream flows occurring in the waterbody. In Scenario 5, q_L.is held constant as in scenario 3, while C_L is increased beyond the boundary concentration C_R. This is adequately depicted in the C-t curve produced. The C-t curves produced by the model simulation proves that inclusion of NPS flows in a river, results to variations in pollutant concentration from the near to the far field of a river. The response of the proposed HCIS-NPS model to different lateral flow rates q_L alongside pollutant concentration of the flow C_L is consistent with expected patterns.

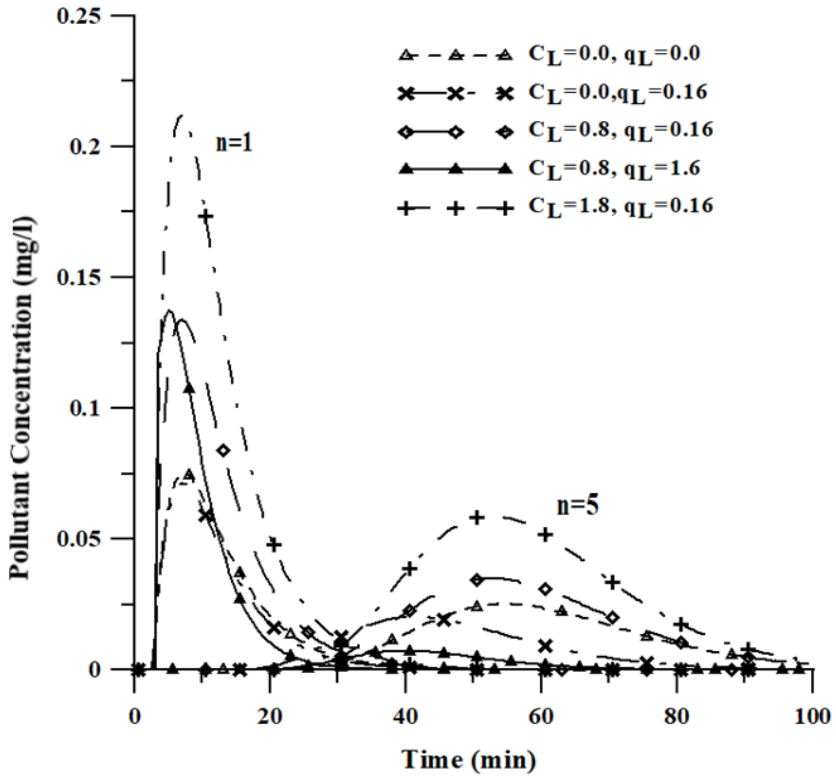

Figure 4. 2: Unit impulse response of HCIS-NPS model at end of 1st (n=1) and 5th (n=5) Hybrid units when C_L=0 mgl^{-1}, q_L=0 $m^3s^{-1}m^{-1}$; C_L=0 mgl^{-1}, q_L=0.16 $m^3s^{-1}m^{-1}$; C_L=0.8 mgl^{-1}, q_L= 0.16 $m^3s^{-1}m^{-1}$; C_L=0.8 mgl^{-1}, q_L=1.6 $m^3s^{-1}m^{-1}$ and C_L=1.8 mgl^{-1}, q_L=0.16 $m^3s^{-1}m^{-1}$.

4.2.2 Validation of the HCIS-NPS model using Field Data

The performance of the proposed HCIS-NPS model is tested using the well-documented field data

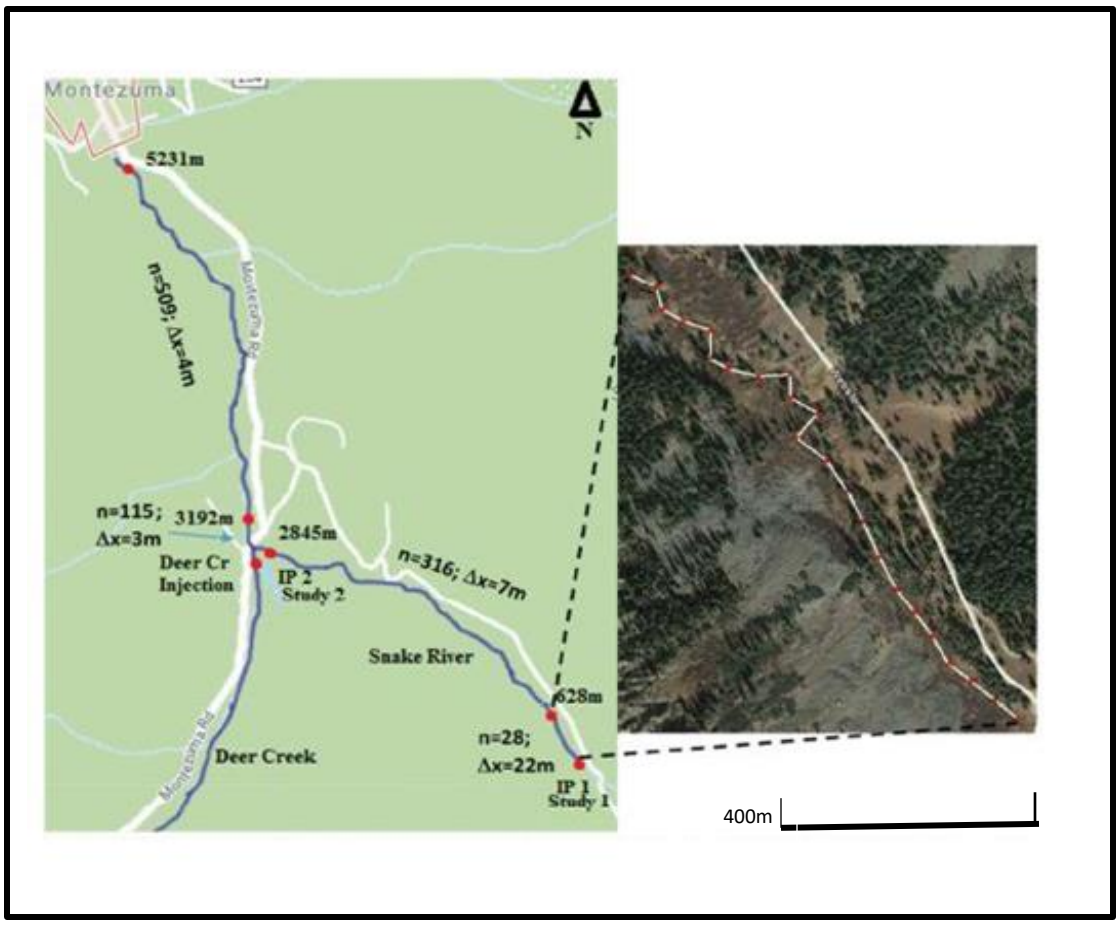

for the Snake River, Colorado, USA. Figure 4.3 (Bencala et al., 1990).

Figure 4. 3: Snake River (Colorado State, USA) study area map used in McKnight and Bencala (1989) showing Injection point, selected sampling and simulation points and delineation of hybrid units. Source: Google Map.

Table 4.2 presents selected data extracted from Bencala et al (1990) for the four sample points considered. The data as documented in Bencala et al (1990) and presented in table 4.2 includes; the selected reach lengths downstream of the injection point, stream cross-sectional area, dispersion coefficient D_L, lateral inflow q_L and lateral pollutant concentrations C_L. Table 4.3 presents data used in simulating the proposed HCIS-NPS model. The proposed model does not

include a transient storage component therefore, data for transient storage presented in Bencala et al (1990) is excluded. Detailed data as provided in Bencala et al (1990) is presented as Appendix B. The C-t profiles generated using the HCIS-NPS is compared with that reproduced with observed data from the Snake River (Bencala et al., 1990). The field data used in reproducing the C-t profile of the TS model presented in (Bencala et al., 1990) was provided by Prof Ken Bencala and Prof Rob Runkel of U.S. Geological Survey (USGS) department, Denver, Colorado, USA.

In the field experiment conducted by McKnight and Bencala (1989) 10.49 $moLl^{-1}$ of Lithium chloride, a conservative salt, is injected continuously over a 6-hour period into the Snake River at a rate of 86.6$mLmin^{-1}$ starting at 09:00hrs. The discharge rate at inception is 0.224m^3s^{-1}, with a Lithium background concentration of zero. Further downstream after the confluence with Deer creek as shown in figure 4.3 an increase in discharge rate of 0.81m^3s^{-1} occurs due to inflows from Deer Creek and consecutive distributed inflows. All field procedures and data are detailed in McKnight and Bencala (1989) and Bencala et al (1990). The HCIS-NPS model simulation is performed for sampling points 628m and 2845m from first point of tracer injection. Further downstream, after the Deer Creek confluence, sampling points 3192m and 5231m as shown in figure 4.3 are also simulated. Each reach length is divided into hybrid process units of size Δx, which is determined from the given D_L and computed $U = Q/A$ when the condition of $Pe=\Delta xu/D_L \geq 4$ is satisfied. The residence time parameters α, T_1 and T_2 of the hybrid unit are determined by use of equations (3.1 -3.3). All other parameters are as presented in Table 4.2. Since there are variations in flow along the river reach, the model parameters vary from reach to reach. Flexibility of the HCIS-NPS model lies in adopting flow variations through varying model parameters. This can be achieved by selecting hybrid unit sizes in each river reach as presented in Table 4.3.

Table 4. 2: Excerpts of field data of tracer tests for selected points of Snake River and Deer Creek

Sampling points (m)	Stream cross sectional area A (m^2)	Computed flow rate U (ms^{-1})	Dispersion coefficient D_L (m^2s^{-1})	Lateral Inflow $q_L x\ 10^{-3}$ ($m^3s^{-1}m^{-1}$)	Lateral solute inflow C_L (µM)
		Before Confluence			
628	0.61	0.37	0.75	0.062	5
2845	0.70	0.32	0.20	0.028	5
		After Confluence			
3192	1.08	0.75	0.20	0.176	4
5231	1.60	0.51	0.20	0.090	4

Source: Bencala et al (1990)

Table 4. 3: Parameters used for the HCIS-NPS simulations of Snake River and Deer Creek

Resident Time			Δx(m)	RL(m)	Δt(s)	U(ms^{-1})	$D_L(m^2s^{-1})$	Pe	No of Hybrid units
α(s)	T_1(s)	T_2(s)							
Before Confluence									
27	33.65	0.619	22	628	0.5	0.37	0.75	11	28
9.453	11.816	0.214	7	2845	0.5	0.32	0.20	11	316
After Confluence									
1.721	2.151	0.039	3	3192	0.5	0.75	0.20	11	115
3.772	4.652	0.086	4	5231	0.5	0.51	0.20	11	509

The simulations in Bencala et al (1990) were interpreted in square pulses of arrival time zero with a rapid increase in concentration. Figures 4.4 and 4.5 present the C-t curves of the observed data and simulated results from HCIS-NPS model downstream after the injection point and further downstream after the confluence. While figure 4.6 shows a comparison of peak concentrations as the pollutants travel to the far field from the near for all four sampling points. The simulated results of the proposed HCIS-NPS model compare well and are in good agreement with the measured field data as shown. Although the observed measurements had some irregular peaks more prominent in the first reach, the simulated and observed concentration curves for 628m match satisfactorily with the leading and trailing edges of the arrival time produced accurately. At 2845m the HCIS-NPS model presents a late arrival time which rapidly peaks consistent with the observed data. This lag could be due to the boundary conditions used and a difference in the time and space discretization in the HCIS-NPS model since each sampling site is split into several hybrid units. Figure 4.5 shows that irrespective of increased and varying discharge flows downstream the Snake River and after the confluence with Deer Creek, simulated to observed C-t curves for both 3192m and 5231m compared well. However, the falling limb of the simulated curve at 3192m arrived earlier than the observed curve, while at 5231m there was a minimal lag in arrival time. In all cases nevertheless, pollutant concentrations increased sharply to plateau levels at initial arrival to sampling sites, exhibiting characteristic trends. The peak levels of the pollutant decreased in consecutive sampling sites downstream the injection point. The performance of the observed to simulated data is tested at a confidence level of 95percent for all reaches. The Coefficient of determination (R^2) is 0.9842 and 0.9382 for 628m and 2845m, while for reaches 3192 and 5231, R^2 is 0.8352 and 0.9712. Further, the standard error (SE) for reaches 628m and 2845m are 2.279E-

2 and 2.697E-2 while 3192m and 5231m are 2.321E-2 and 9.35E-3 respectively. The results show a good correlation between the C-t profile of the observed data and the simulated data. The results indicate that the proposed model is capable to simulate pollutant transport in rivers from non-point sources with variation in flow rate as shown downstream. The output of the proposed HCIS-NPS model was not compared with the simulations of TSM undertaken in Bencala et al (1990). The purpose of using the field data in simulating the model is to establish its suitability and capability for NPS in-stream simulation with limited available data.

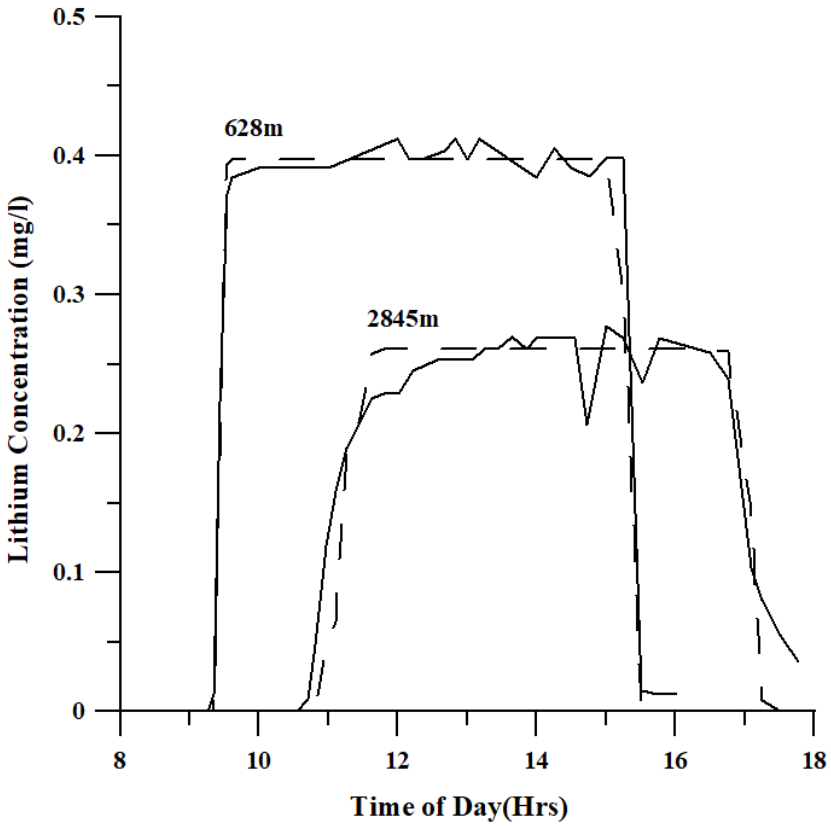

Figure 4. 4: Comparison of C-t profiles from Observed data (solid lines) Bencala et al (1990) with results simulated by proposed HCIS-NPS model (broken lines) at 628m and 2845m downstream from tracer injection point.

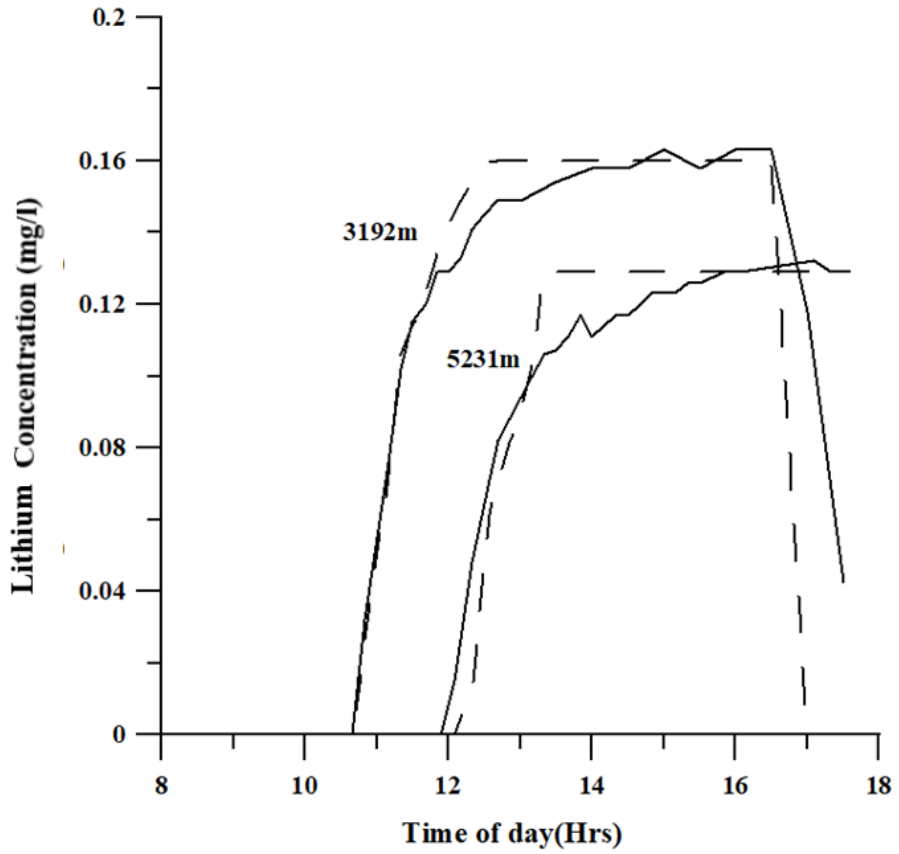

Figure 4. 5: Comparison of C-t profiles from Observed data (solid lines) Bencala et al (1990) with results simulated by proposed HCIS-NPS model (broken lines) at 3192m and 5231m from tracer injection point after Deer creek confluence.

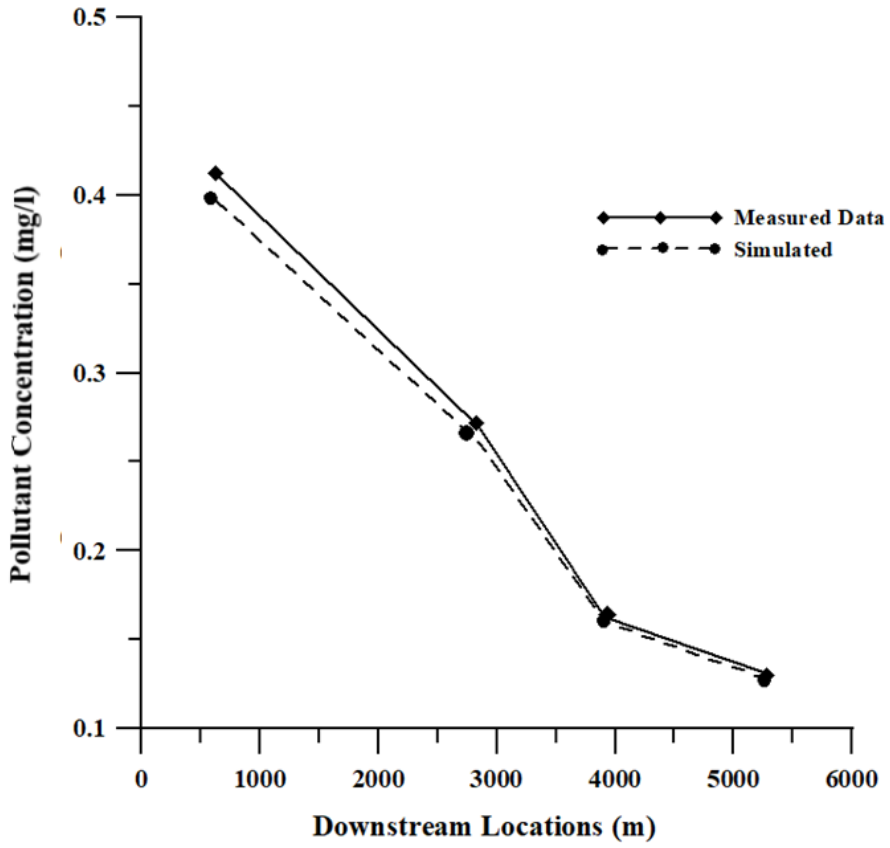

Figure 4. 6: Comparison of peak concentrations for measured data (solid lines) Bencala et al (1990) and simulated peak concentrations with proposed HCIS-NPS model (broken lines) at 628, 2845, 3192 and 5231m downstream.

4.3 Testing of Model Component 2 (the HCIS-NPS*hez* Model)

4.3.1 Verification of the Model Considering Hyporheic Exchange using Synthetic Data

Spatio-temporal variance of pollutant concentration in a hypothetical river is simulated using synthetic data sets to confirm the potentials of the proposed model. A 2 km River Channel with a $20m^2$ cross sectional area and flow rate of $400m^3$/min is conceptualised. The River is divided into several hybrid units with Δx size of 200m and is obtained when peclet number $Pe = \Delta xu / D_L \geq 4$. Values of Dispersion coefficient (D_L) of $1000m^2$/min and flow velocity (u) of 20m/min satisfies this condition. The retention time parameters α, T_1, and T_2 are derived from the relationships where $\alpha = 0.04\Delta x^2/D_L$, $T_1 = 0.05\Delta x^2/D_L$ and $T_2 = (\Delta x/u) - (0.09\Delta x^2/D_L)$ provided that the dimensionless relationship of $(\alpha + T_1 + T_2)\, u/\Delta x \approx 1$ (Ghosh 2001; Ghosh et al., 2004, 2008). NPS in-flow rate

and concentration q_L and C_L are set as 0.016m^3/min/m and 0.08 mgl^{-1} respectively. A hyporheic zone depth of 0.72m is estimated, while porosity (ϕ) values of 0.0 and 0.3 are considered for comparative purposes. The stream hydraulic radius is 0.53m, while the proportionality constant is set at 0.5 (Rutherford, 1994). Inputting the data into equation 3.35 gives a retardation factor (R) of 1.0 and 1.2 for the varying values of the HZ porosity. A conservative pollutant of no specific type is used; while, the initial and boundary pollutant concentration C_R is set as 1.0 mgl^{-1}. The simulated impulse response of the model at the end of the first, third, seventh and tenth hybrid units when R = 1.0 and 1.2 is presented in figure 4.7. The break through curve (BTC) presented in figure 4.7 clearly shows that with a retardation factor of 1.0 which represents a HZ medium porosity of 0.0 there is no exchange between the HZ and the stream overflow. This means that retardation does not occur when R = 1.0 (Coles, 2007; Buragohain et al., 2018) and is correctly described by equation 3.35.

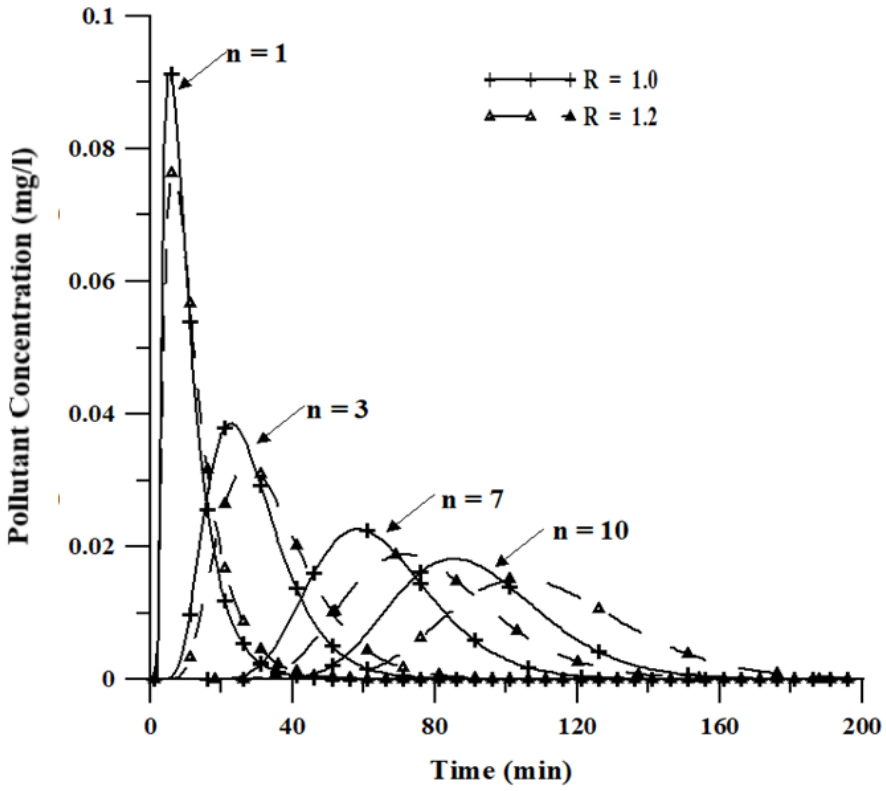

Figure 4. 7: Unit impulse responses of the HCIS–NPS*hez* model at the end of 200m (n = 1), 600m (n = 3), 1400m (n = 7) and 2000m (n = 10) hybrid units when R = 1.0 and 1.2.

When R = 1.0, the BTC produced presents steep concentration gradients and shorter tails as expected. However, with increased porosity when R = 1.2, the BTC accurately describes the skewness of the curve and elongated arrival and trailing tails as seen from stream tracer tests. In comparing both curves, there is a marked drop in pollutant concentration when R = 1.2, as the solute travels from the near to the far field. Considering that the pollutant is conservative in nature, the reduction in pollutant concentration can only be attributed to the retention of pollutants in the HZ and gradual release of the pollutants back into the main stream with increased flows. Since both simulations are performed under the same conditions of lateral inflow, this could be the only possible reason for the drop in solute concentrations and subsequent longer tails. Though it is observed that for the first hybrid unit both curves arrive at the same time, it however, presents a delay in the trailing tail at R=1.2. Subsequent curves however, show late arrival and trailing edges for R=1.2 compared to R=1.0.

4.3.2 Testing of the Model Considering Hyporheic Exchange using Field Data

To further validate the model, field data obtained from Bencala et al (1990) for the Snake River, Colorado, USA shown in figure 4.3 is utilised. In testing the HCIS-NPS*hez* model the conservative salt Chloride concentration data is considered. The data used for the simulation is as presented in Tables 4.2 and 4.3. However, the background concentration of the Chloride tracer is 5µM. The study area is a mountainous area, mostly underlain by Precambrian rocks, plume granite and Swandyke hornblende gneiss (Hornberger et al., 1994). The porosity of the underlying bed is estimated as 0.2 (Morin et al., 1993; Leeman et al., 2009). Therefore, the estimated retardation factor is 1.3 which is used to simulate C-t profiles for the entire study reach as there are no other information available for varying this parameter. The C-t profiles for both the measured and simulated values for reach lengths of 628m and 2845m before the Deer Creek confluence and 3192m and 5231m after the confluence are presented in figure 4.8.

The results show that the C-t profiles for the first reach 628m, is in good agreement with the measured data. However, for the other reaches, the model presented late arrivals. This could be as a result of the time and space discretization of the proposed model. Also, the HCIS-NPS*hez* model presently simulates equilibrium conditions only therefore interactions between the storage zone and overflowing stream is minimal. The performance of the model is evaluated at 95 percent confidence using regression analysis. The R^2 and SE for the four reaches is 0.9724 and 1.462E-1 for 628m, 0.8468 and 2.227E-1 for 2845m, 0.9341 and 7.616E-2 for 3192m while for 5231m is

0.7577 and 1.224E-1. The results show a good correlation between both measured and simulated results for the river. For all the reaches R^2 is relatively high with corresponding low SE.

Further, the performance of the proposed model component was also tested without retardation processes by taking R=1.0 and corresponding C-t profiles for 628m and 2845m were produced and presented in figure 4.8. An early arrival of pollutants was observed in case of no retardation as shown in figure 4.8 which is consistence in both reaches as expected and agree with McKnight and Bencala, 1989; Bencala et al., 1990; Runkel and Chapra, 1993; Runkel et al., 2003; Kumar and Dalal, 2014.

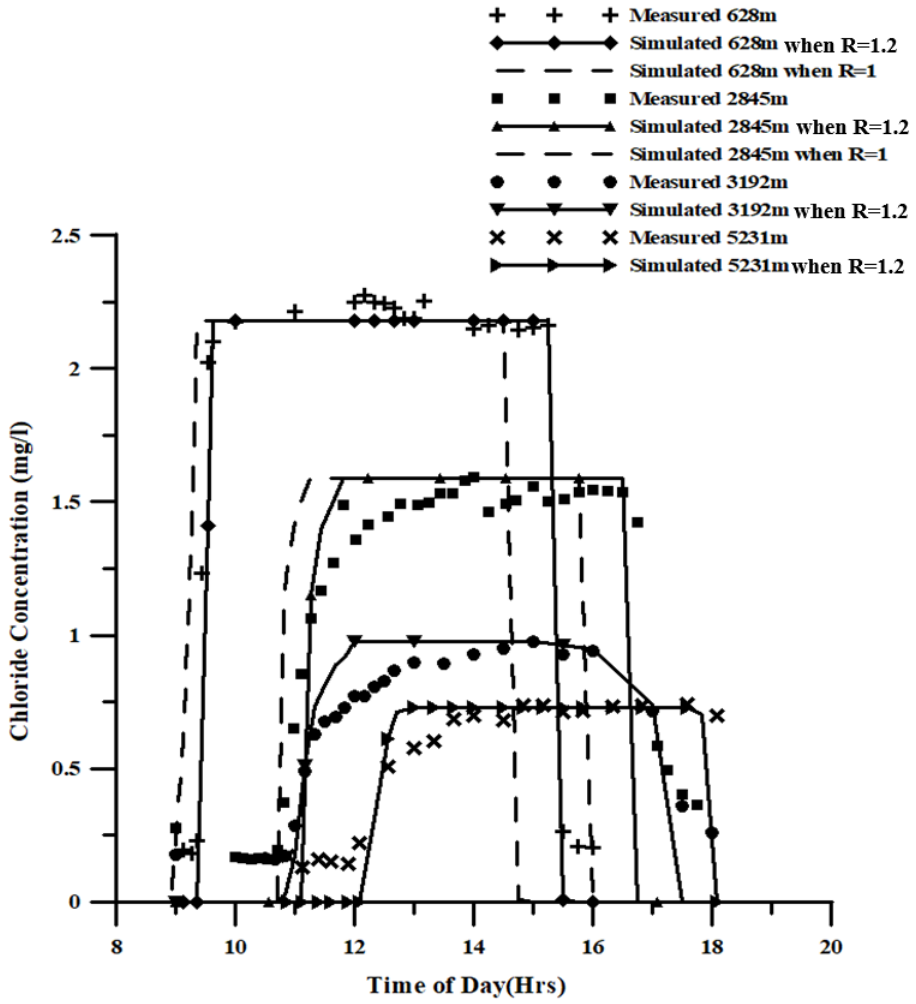

Figure 4. 8: Comparison of C-t profiles from Observed data (symbols only) Bencala et al (1990) with results simulated by proposed HCIS-NPS*hez* model (solid lines) at 628m and 2845m downstream from tracer injection point and 3192m and 5231m after the Deer Creek confluence when R=1.2. And simulated C-t profiles by HCIS-NPS*hez* model for reaches 628m and 2845m when R=1.0 (dashed lines).

4.3.3 Performance of Proposed HCIS-NPShez in Comparison with ADE-NPShez

From figure 4.9, the BTCs produced by both models show similar trends in time to peak. However, a difference in peak concentrations is observed. This could likely be due to truncations in grid sizes applied in the numerical solution of the ADE-NPS*hez* and the space discretization of the HCIS-NPS*hez*. Figure 4.9 also shows that the first hybrid unit presents a right skewed curve. However, further downstream, the curves tend towards normal distributed skewed curves. This is understandable as the first hybrid unit represents point of first injection to the control volume.

The HCIS-NPS*hez* model demonstrates longer arrival and trailing tails and more rounded concentration peaks consistent with tracer tests results. As such the resultant effects of change in concentration gradients between the storage zone and the overflowing stream is well captured by the proposed model. Hence HCIS-NPS*hez* model can be used in simulation and prediction of pollutant transport in Natural Rivers.

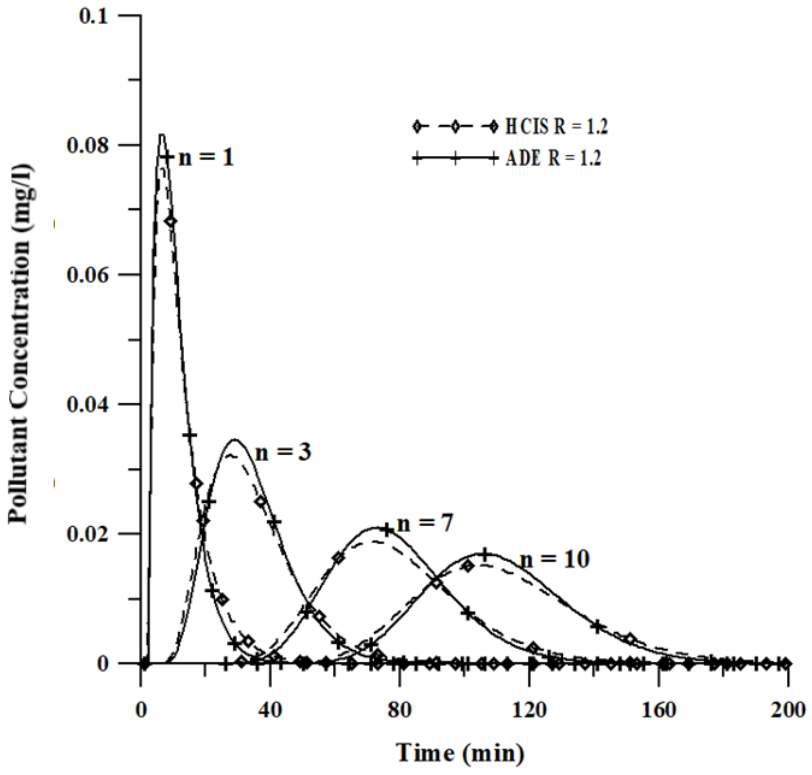

Figure 4. 9: Unit impulse response of ADE-NPS*hez* model and HCIS-NPS*hez* model with Retardation Factors R= 1.2, at the 1st, 3rd, 7th and 10th hybrid units, being downstream locations of 200, 600, 1400 and 2000m respectively from injection source

4.3.4 Validation of Retardation Equation

Results from Knapp et al. (2017) and the proposed model for varying values of porosity is presented in figure 4.10. From the curves obtained in figure 4.10. The retardation factor at 0.39 porosity falls within the range of 1.45 as obtained by Knapp et al. (2017). The trends of both curves are similar. Both curves show that at zero porosity retardation is 1.0 irrespective of river parameters considered. Consequently, retardation effects vary with respect to porosity. Large pores result to decreased retardation due to a reduced adsorbing surface area which results to the main stream flowing right through. However, when the pores are smaller, higher adsorbing surface area per unit volume of solution is present, hence, an increase in retardation. This trend is clearly shown in figure 4.10. Equation (3.35) can be used for estimation of the retardation factor.

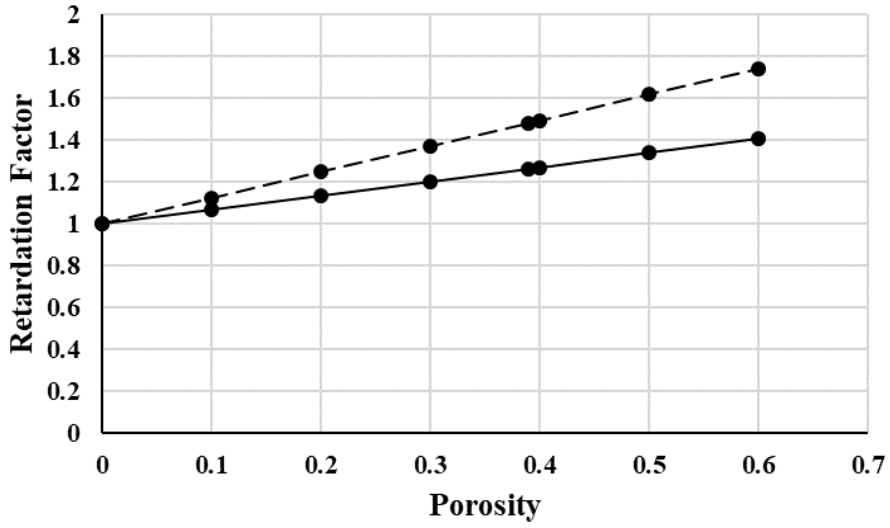

Figure 4. 10: Retardation factor due to varying Porosity values derived from Knapp et al. (2017) (broken lines) and from data used for proposed HCIS-NPS*hez* (Unbroken lines)

4.4 Testing of the Model Component 3 (the HCIS-NPS*k* Model)

4.4.1 Testing of the HCIS-NPSk Model using synthetic data

In testing the proposed model, an artificial situation is considered to demonstrate its potentials for simulating non-conservative pollutants with NPS inflows. A conceptualised 3km river is assumed to have a cross-sectional area of $20m^2$, with a flow rate Q given as $400m^3$/min. The dispersion

coefficient D_L is 1000m^2/min while the flow velocity u is 20m/min. the values for lateral inflow q_L and pollutant concentration from lateral inflow C_L are set at 0.016$m^3min^{-1}m^{-1}$ and 0.08mgl^{-1}. Δx, the size of the hybrid unit is 200m, while the decay rate coefficient k_a is varied between 0, 0.01 and 0.003 per min. The resident time parameters were estimated using equations (3.1 - 3.3). The unit step and unit impulse responses for the first hybrid unit at varying decay rates of 0, 0.01 and 0.003 are clearly presented in figures 4.11 and 4.12. The impulse responses generated for the first, third, seventh and tenth hybrid units with respect to time at different sections of the river from the near field were simulated using equations (3.70 and 3.71). and is presented as figure 4.13. From the figure presented, it is observed that all the graphs illustrate a bell-shaped distribution curve with elongated tails. As the pollutant plume moves downstream the river, attenuation of the C-t curve occurs and peak concentrations and time to peak reduces with increase in hybrid units. The profiles of the impulse response show that with higher decay rate of 0.01 per min, there is a slight reduction in peak concentration within the first hybrid. Which is clearly seen in figure 4.11. However, reduction in peak concentrations is well defined as the plume arrives 600m downstream and further downstream. Within the first hybrid unit, however, the lower decay rate of 0.003 per min was not that obvious as it matched the profile without any decay. It, however, showed a marked decrease in concentration levels in subsequent hybrid units. In general, it is obvious that the C-t profiles with decay show rapid attenuation as the pollutant moves farther downstream when compared with that without decay. Consequently, the higher the decay constant, the lower the pollutant concentration with respect to time becomes. Figure 4.15 shows peak concentration of pollutants in relation to the distance along the river reach at 200, 600, 1400 and 2000m for varied kinetic constants. The response of the model to varying kinetic constants observed from the C-t profiles clearly shows that the model is able to simulate Non- conservative pollutants in streams with inclusion of non-point source pollution.

The model is also tested for varying NPS inputs and decay constants to further demonstrate its response to in-stream conditions. First it is simulated without inclusion of NPS inflows and decay of pollutants occurring. Further simulation, a NPS input of 1.8mg^{-1} of C_L and q_L of 0.16 $m^3min^{-1}m^{-1}$ with a decay constant ka of 0.01 is introduced. Subsequent simulations alternate NPS input and decay reaction. The response of the model to these variations is presented in figure 4.14. The response of the model shown in figure 4.14 is consistent with expected response of model for the varying conditions.

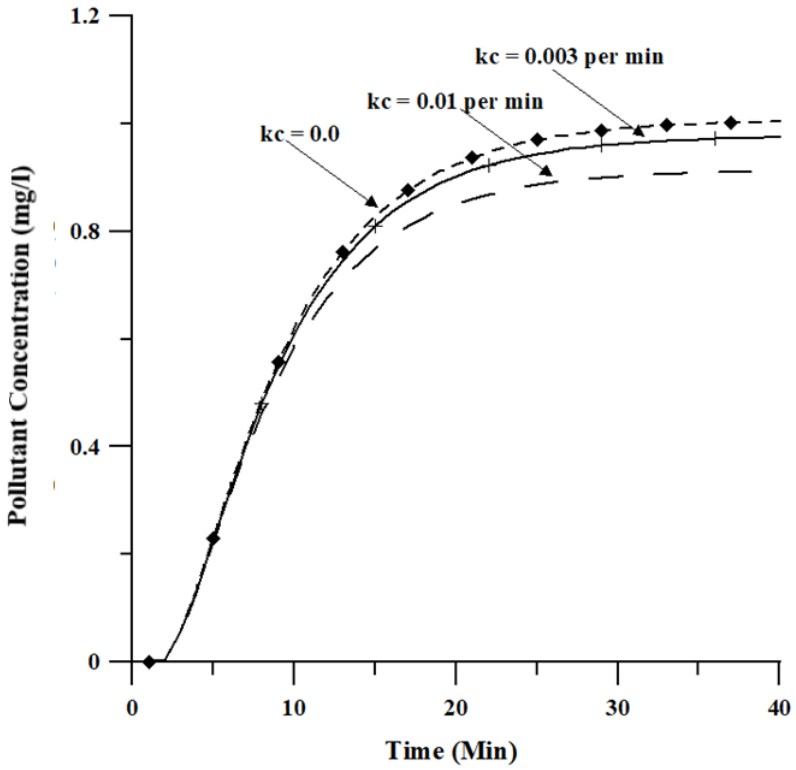

Figure 4. 11: Variation in pollutant concentration in response to unit step impulses of HCIS-NPS*k* model with varied decay rate constants of ka = 0, 0.01 and 0.003 per min, at the end of the first hybrid unit.

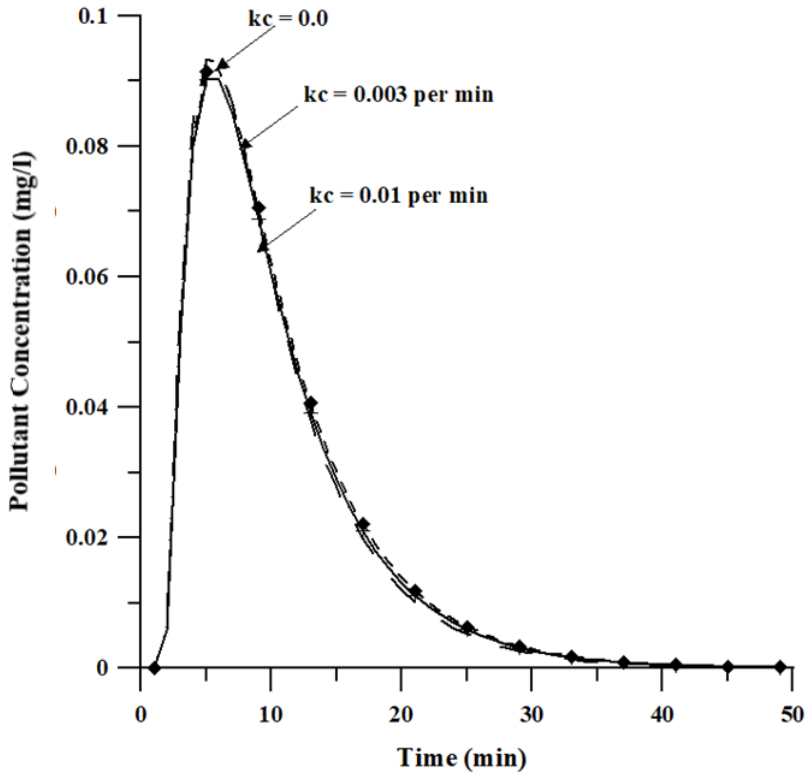

Figure 4. 12: Variation in pollutant concentration in response to unit impulse of HCIS-NPS*k* model with varied decay rate constants of ka = 0, 0.01 and 0.003per min, at the end of the first hybrid unit.

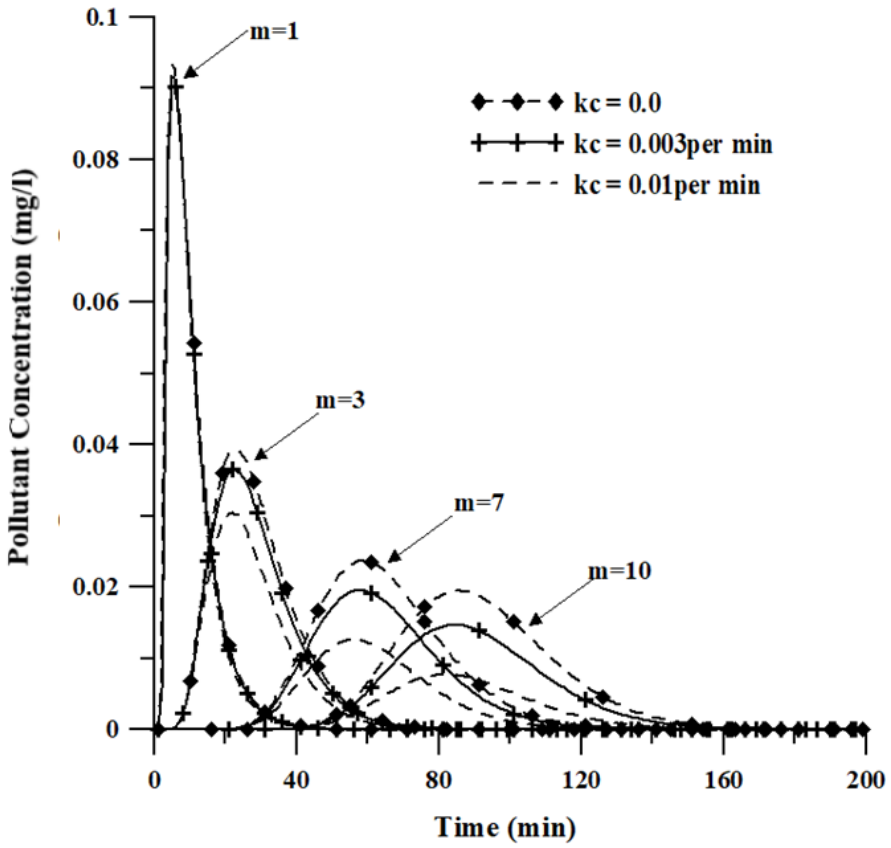

Figure 4. 13: Concentration of pollutants in response to unit impulses of HCIS-NPS*k* model with varied decay constants ka = 0, 0.01 and 0.003 per min, at the 1st, 3rd, 7th and 10th hybrid units, which stands for different points of x at 200, 600, 1400 and 2000m respectively

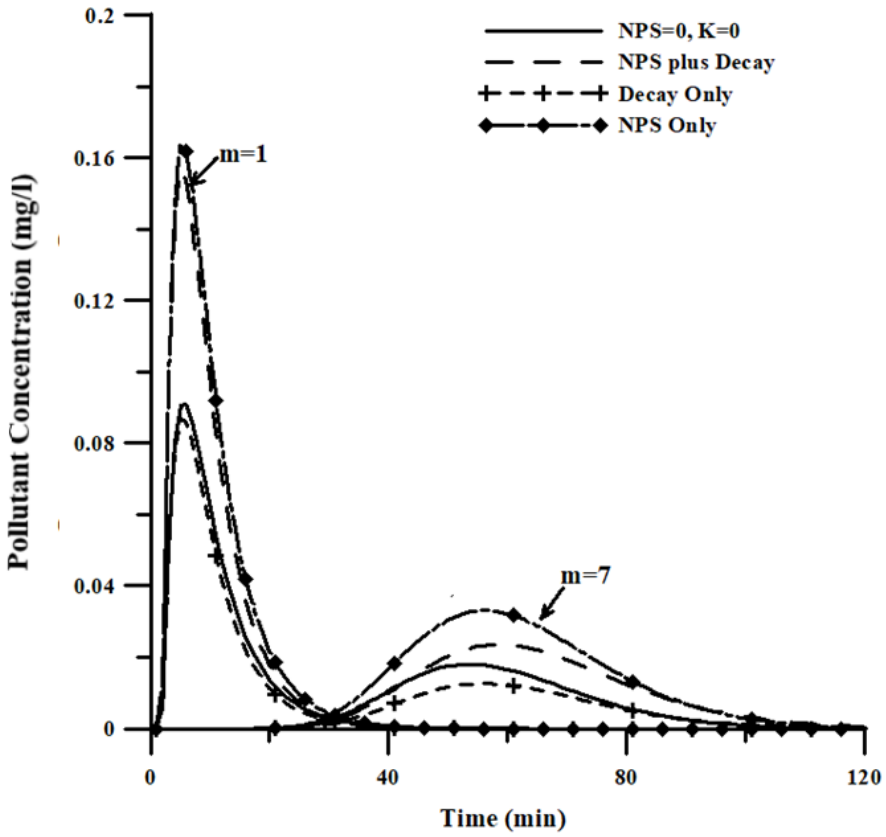

Figure 4. 14: Concentration of pollutants in response to unit impulses of HCIS-NPS*k* model under varying conditions of NPS inputs of C_L=0 mgl^{-1}, q_L=0 $m^3s^{-1}m^{-1}$, and C_L=1.8 mgl^{-1}, q_L =0.16 $m^3s^{-1}m^{-1}$, ka = 0, 0.01 per min, for the 1st and 7th hybrid units.

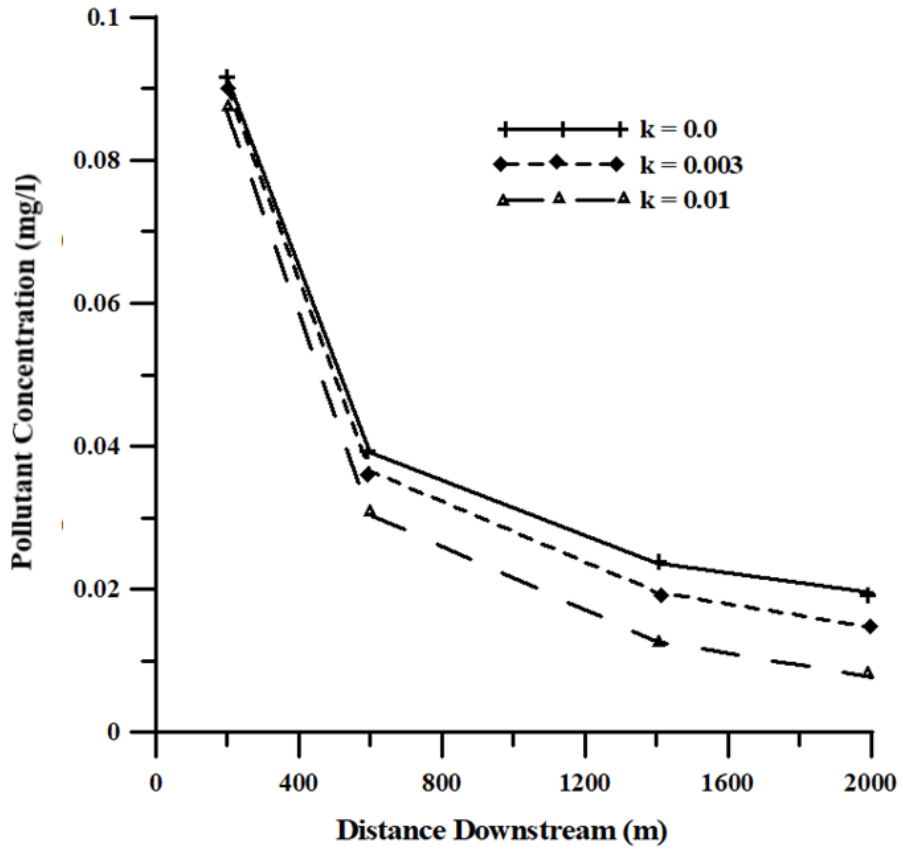

Figure 4. 15: Peak concentration of pollutants along the river reach at x = 200, 600, 1400 and 2000m for varied kinetic constants.

4.4.2 Performance of the HCIS-NPSk in comparison with ADE-NPSk Model

The response of both models at downstream locations of 200m, 600m, 1400m and 2000m for a 3km river reach, represented as 1st, 3rd, 7th and 10th hybrid units is presented in figure 4.16. Both models were simulated in response to first order decay of 0.01per min at the same distance downstream the river. For each simulation run, peak concentration and time to peak were compared. It is noted that both models show a steep rising limb and right-skewness in the first hybrid unit, which subsequently reduces to a normal distribution with an increase in hybrid units. However, the HCIS-NPS*k* model had elongated tails when compared to the ADE-NPS*k* model as the pollutant travelled downstream. Also, with an increase in distance from the location of pollutant release, both models produce C-t Profiles with time to peak occurring at approximately the same time. Differences, however, in peak concentrations of the C-t profiles for ADE-NPS*k* and HCIS-NPS*k* models were observed as the pollutant travelled downstream as seen in figure

4.16. Peak concentrations attenuate more rapidly with the HCIS-NPS*k* model than the ADE-NPS*k*. Hence the response of the HCIS-NPS*k* model is consistent with investigations of solute transport in rivers. At 95% confidence level, the performance of HCIS-NPS*k* to the ADE-NPS*k* was tested. The coefficient of determination (R^2) and the standard error (SE) were within the range of 0.895 to 0.996 and 2.52E-3 to 4.24E-4 respectively. This result is indicative of a good correlation between both models. Both models respond to the effect of the first order kinetic reaction taking place within and down-stream the water channel.

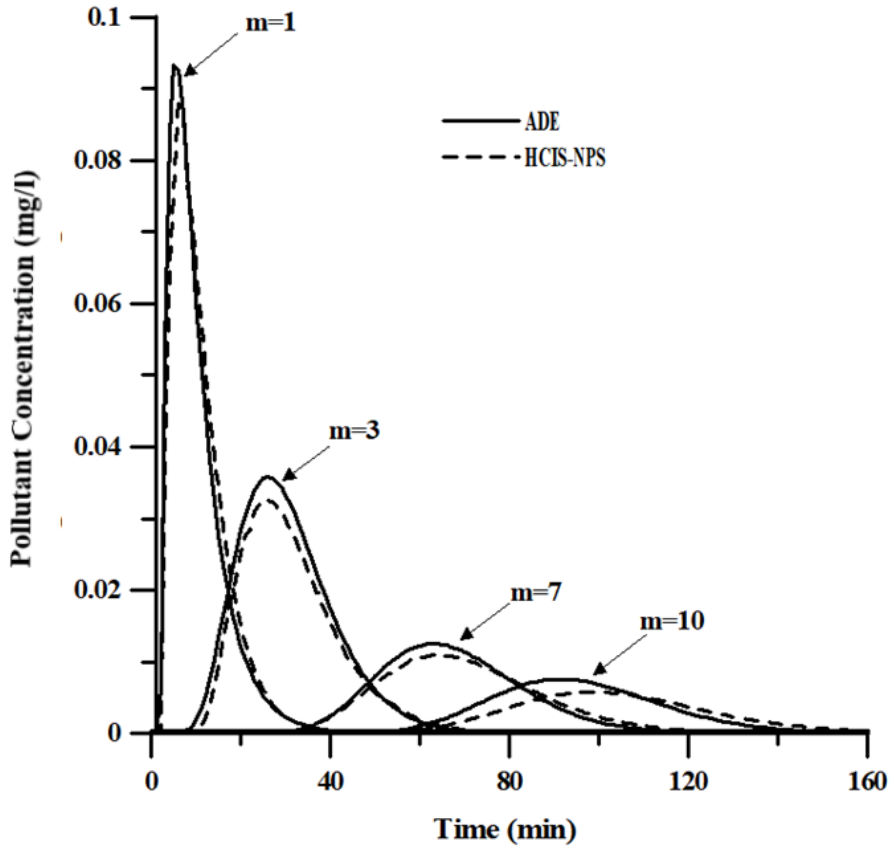

Figure 4. 16: Comparison of pollutants Concentration unit impulse response of ADE-NPS*k* model and HCIS-NPS*k* model with decay rate coefficient ka = 0.01 per min, at the 1st, 3rd, 7th and 10th hybrid units, which stands for different downstream locations of x at 200m, 600m, 1400m and 2000m

4.5 Summary

The proposed HCIS-NPS model is tested with the use of synthetic and field data obtained from Bencala et al. (1990) and directly from Prof Kenneth Bencala and Robert Runkel. The response

of the C-t curves produced for both synthetic and field data are in good relationship. The performance of the model to field data is tested at a 95 percent confidence level for all reaches. And the results show a good correlation between both. Hence the performance of the proposed model shows its ability to effectively simulate pollutant transport in a natural river inclusive of NPS pollution. It also demonstrates its ability to simulate in-stream processes with varying discharge rates. It is concluded therefore, that the simplicity of the HCIS-NPS model, with respect to its ease of operation, parameter estimation and reduced data requirements, makes it suitable, convenient and easy to use. Thus, taking into consideration the difficulties associated with available NPS models, HCIS-NPS model is proven to be a useful tool for predicting pollutant transport in water bodies inclusive of non-point source pollution.

With the inclusion of hyporheic exchange, the proposed HCIS-NPS*hez* model is tested with field data from literature and synthetic data using varying retardation factors representative of non-porous and porous conditions in the hyporheic zone of a river control volume. The model is further compared with the numerical solution of a modified ADE model. In both cases the proposed model proves its ability to capture the behaviour of pollutant fate as observed in field tracer tests. It also matches the numerical response of the Modified ADE model. The equation developed by Kumarasamy, (2011) is also tested and found suitable for estimating the retardation factor for varying medium porosities in the hyporheic zone along natural rivers. The Proposed HCIS-NPS*hez* model has proven its capability of predicting the fate of pollutants along a natural river fed with inflows from non-point sources and affected by mass exchange occurring in the hyporheic zone. And therefore, is considered a useful tool in water quality management.

Considering that most pollutants inflows from agricultural fields are non-conservative in nature, a decay component is introduced in the HCIS-NPS model. And presented as HCIS-NPS*k* model. The proposed model is tested using synthetic data generated based on physical properties of conceptualized river channels, while decay rates are varied. It is seen that with increase in decay rate of the pollutants, there is a visible drop in in-stream concentration. The simulations obtained through the proposed model is compared to that of the numerical solution of ADE inclusive of Non-point source and first-order reaction kinetics components (ADE-NPS*k*). The c-t profiles of the HCIS-NPS*k*, matches that of the ADE-NPS*k* but with a long tail which adequately interprets experimental results as expressed in literature. Thus, the overall response of the proposed model with differing decay rate coefficients, proves its ability to adequately simulate decay in natural

rivers with non-point source inflows. Also, the. simplicity of the HCIS model makes it a useful tool for simulation of decay prone contaminant transport from non-point sources.

CHAPTER 5: CONCLUSION AND RECOMMENDATIONS

5.1 Conclusion

Non-point source pollution has for long been mentioned as a main cause of water pollution, responsible for deterioration in the eco-system and a leading source of a host of water related diseases and infections. Although many developed countries have sought out ways of eradicating or reducing this source of pollution, the attempts have seldom been successful. On the other hand, developing countries are still faced with the enormity of this situation, with depleted water sources due to increased pollutant loads in rivers. Although many models exist and have been developed to simulate non-point source pollution, they have been found to be cumbersome to use as they need extensive calibration and high-level competences in operational skills. They also require large data sets and expensive. Further, they are predominantly watershed based and are incapable of simulating in-stream processes. More so, their use is mainly restricted to areas where they had originally been developed. Thus, their use in other regions would require several changes which could compromise on their accuracy.

The present study stems from the need to develop a simple water quality model capable of simulating in-stream non-point source pollution for diverse rivers. This is to enhance the proper monitoring and remediation of water sources affected by non-point source pollution especially in developing countries with scarce data. The ability to easily predict the water quality status of streams and rivers would ease water quality treatment and management processes which by extension would curb the scarcity of usable water. The model must be user-friendly, have less data requirements, be time-efficient through reduced simulation run time and cost effective.

In this thesis, a hybrid cells in series, non-point source model is developed to predict transport of pollutants from non-point sources in a river, including in-stream point sources. The proposed model is a three-parameter model which consists of three zones, where pure advection through time delay takes place in a plug zone, while advection and dispersion occur in two other thoroughly mixed unequal zones linked in series. The model equations are analytically derived using Laplace transforms and appropriately coded with FORTRAN programming language (Algorithm for programme is presented in Appendix C). Other components such as first order kinetic reaction and hyporheic exchange are incorporated into the proposed model to test is capability to simulate first

order decay and hyporheic exchange in rivers. The capability of the model in simulating non-point source pollution in rivers has been demonstrated using synthetic data and field data from literature.

The overall findings from this research are highlighted thus:

1. This study aimed to answer two questions. Can the hybrid cells in series model be modified to effectively simulate non-point source pollution, and would the developed model be a useful tool for simulation of non-point source pollutants in rivers irrespective of the nature of pollutants? These questions are successfully answered in the affirmative. A Hybrid cells in series, non-point source model is developed and tested for the simulation of conservative pollutants. Also, a first order kinetic equation is added to the equation, and the model adequately simulated non-conservative pollutants. The outcomes of both simulations are positive.
2. The first objective is achieved. A hybrid Cells in Series non-point source model for simulation of conservative pollutants in a river channel is presented. The model is tested for varying non-point source inflows. The response of the model is consistent with expected trends for such inflows.
3. The second objective which seeks to enhance the developed HCIS-NPS model for simulation of hyporheic exchange for conservative pollutants is achieved. The hybrid cells in series, non-point source model adequately simulates the effects of hyporheic zones in a water channel for conservative pollutants. The model is tested for different medium porosities and is compared with the classical advection dispersion model. The presence of hyporheic zones and the exchange that takes place between the zone and the main stream accounts for the long tails observed in breakthrough curves for field tracer tests. This is successfully simulated by the proposed model.
4. The third objective aimed to enhance the model to simulate non-conservative pollutants with inclusion of a first order kinetic equation for no specific pollutant is achieved. The model is seen to respond well to varying decay constants as expected. Further, it is tested with the numerical solution of the classical advection dispersion equation model. The results show that the proposed model adequately presents the breakthrough curves observed in field tracer test better than that produced by the classical advection dispersion model.
5. The fourth objective is achieved. Field data obtained from Bencala et al (1990) is used for the simulation of the developed hybrid cells in series, non-point source model. Simulations are carried out on specific points of the study area. The concentration time profiles generated

by the proposed model is compared to the curves produced from original field data, provided by Prof Ken Bencala and Rob Runkel, for the selected locations. The C-t profiles produced by the proposed model correlates well with the field data. The performance evaluation of the simulated to field data is tested at a confidence level of 95 percent with an average coefficient of determination of 0.932 and Standard error of 2.058E-2 for all four sampled locations.

6. In achieving objective five, the analytical solution of the proposed models as presented in chapter three, are compared with the numerical solution of the classical Advection Dispersion model. In all cases, the proposed models compared well with the classical advection dispersion model but produced better skewness and longer tails as observed in field tracer tests. Therefore, the proposed model can be considered an effective alternative to the classical ADE model.

In general, the breakthrough curves obtained from the proposed model shows its capability to simulate non-point source pollution transport in natural rivers effectively. The simplicity of the hybrid cells in series, non-point source model makes it a practical model for simulating contaminant transport from non-point sources. It can be concluded therefore, that the responses produced by the hybrid cells in series non- point source model, makes it a suitable, reliable and useful tool for predicting the water quality status of a river subject to non-point source inflows. This study has adequately addressed and attempted to develop, validate a new model for simulating non-point source pollutant transport processes in streams and rivers.

5.2 Limitations of the Study

With all research work limitations are confronted. The major limitation encountered in this work is the unavailability of localised field data to test the components of the model. Hence, synthetic data and field data provided by Profs Kenneth Bencala and Robert Runkel of the United States Geological Survey (USGS) was utilised in testing and validating the model.

5.3 Recommendations for Continuation of the Study

The proposed model has been validated using recorded data collected from the field for a specific tracer injection event and considered suitable for simulation of non-point source pollution transport in rivers. Based on this, the following recommendations are made for further study

1. It is imperative to carry out investigation on changes in model time parameters (α, T_1 and T_2) before, during and after storm events.

2. A catchment interface through remote sensing should be added to adequately capture, quantify and characterise the non-point source inflows into the river for effective data collection.
3. A HCIS-NPS*hez* model for the simulation of non-equilibrium mass exchange in streams should be considered.
4. The model should be tested in localised rivers within South Africa in a bid to curb the prevailing water scarcity and pollution problem in the country.

REFERENCES

Abbaspour, K.C., Yang, J., Maximov, I., Siber, R., Bogner, K., Mieleitner, J., Zobrist, J. and Srinivasan, R., 2007. Modelling hydrology and water quality in the pre-alpine/alpine Thur watershed using SWAT. *Journal of hydrology*, *333*(2-4), pp.413-430.

Abon, C.C., Nguyen, T.C., Shams, S., Phan, D.V. and Huong, D.T.T., 2009. River Pollution.

Adu, J.T. and Kumarasamy, M.V., 2018. Assessing non-point source pollution models: a review. *Pol. J. Environ. Stud*, *27*, pp.1913-1922.

Amaya, F.L., Gonzales, T.A., Hernandez, E.C., Luzano, E.V. and Mercado, N.P., 2012. Estimating Point and Non-Point Sources of Pollution in Biñan River Basin, the Philippines. *APCBEE Procedia*, *1*, pp.233-238.

Arnold, J.G., Williams, J.R., Nicks, A.D. and Sammons, N.B., 1995. SWRRB–A watershed scale model for soil and water resources management. *Computer models of watershed hydrology. Water Resources Publications*, pp.847-908.

Bardini, L., Boano, F., Cardenas, M.B., Revelli, R. and Ridolfi, L., 2012. Nutrient cycling in bedform induced hyporheic zones. *Geochimica et Cosmochimica Acta*, *84*, pp.47-61.

Barnwell, T.O. and Johanson, R., 1981. HSPF: A comprehensive package for simulation of watershed hydrology and water quality. In *Nonpoint Pollution Control-- Tools and Techniques for the Future, Proceedings of a Technical Symposium p 135-153, 1981. 10 Fig, 38 Ref.*

Bear, J., 1972. Dynamics of fluids in porous media–American Elsevier pub. *Comp., inc. New York, 764p*.

Beasley, D.B. and Huggins, L.F., 1981. ANSWERS, areal nonpoint source watershed environment response simulation: user's manual. US. EPA-905/9-82-001, Chicago, 111.: U.S. Environmental Protection Agency.

Benaman, J., Shoemaker, C.A. and Haith, D.A., 2005. Calibration and validation of soil and water assessment tool on an agricultural watershed in upstate New York. *Journal of Hydrologic Engineering*, *10*(5), pp.363-374.

Bencala, K.E. and Walters, R.A., 1983. Simulation of solute transport in a mountain pool-and-riffle stream: A transient storage model. *Water Resources Research*, *19*(3), pp.718-724.

Bencala, K.E., 1983. Simulation of Solute Transport in a Mountain Pool-and-Riffle Stream with a Kinetic Mass Transfer Model for Sorption. *Water Resources Research*, *19*, pp.732-738.

Bencala, K.E., 2000. Hyporheic zone hydrological processes. *Hydrological Processes*, *14*(15), pp.2797-2798.

Bencala, K.E., McKnight, D.M. and Zellweger, G.W., 1990. Characterization of transport in an acidic and metal-rich mountain stream based on a lithium tracer injection and simulations of transient storage. *Water Resources Research*, *26*(5), pp.989-1000.

Benedini, M. and Tsakiris, G., 2013. *Water quality modelling for rivers and streams*. Water Science and Technology Library, Vol. 70, p. 290. Dordrecht: Springer Science + Business Media.

Bhuyan, S.J., Koelliker, J.K., Marzen, L.J. and Harrington Jr, J.A., 2003. An integrated approach for water quality assessment of a Kansas watershed. *Environmental Modelling & Software*, *18*(5), pp.473-484.

Bi, E.G., Monette, F. and Gasperi, J., 2015. Analysis of the influence of rainfall variables on urban effluents concentrations and fluxes in wet weather. *Journal of Hydrology*, *523*, pp.320-332.

Bingner, R.L. and Theurer, F.D., 2001. Topographic factors for RUSLE in the continuous-simulation, watershed model for predicting agricultural, non-point source pollutants (AnnAGNPS). In *Soil Erosion* (p. 619). American Society of Agricultural and Biological Engineers.

Boano, F., Harvey, J.W., Marion, A., Packman, A.I., Revelli, R., Ridolfi, L. and Wörman, A., 2014. Hyporheic flow and transport processes: Mechanisms, models, and biogeochemical implications. *Reviews of Geophysics*, *52*(4), pp.603-679.

Bolster, D. and Dentz, M., 2012. Anomalous dispersion in chemically heterogeneous media induced by long-range disorder correlation. *Journal of Fluid Mechanics*, *695*, pp.366-389.

Borah, D.K. and Bera, M., 2003. Watershed-scale hydrologic and nonpoint-source pollution models: Review of mathematical bases. *Transactions of the ASAE*, *46*(6), p.1553.

Borah, D.K. and Bera, M., 2004. Watershed-scale hydrologic and nonpoint-source pollution models: Review of applications. *Transactions of the ASAE*, *47*(3), p.789.

Bottacin Busolin, A., 2010. *Transport of solutes in streams with transient storage and hyporheic exchange*. Ph.D. thesis, University of Padua, Padua, Italy.

Bourke, S.A., Cook, P.G., Shanafield, M., Dogramaci, S. and Clark, J.F., 2014. Characterisation of hyporheic exchange in a losing stream using radon-222. *Journal of hydrology*, *519*, pp.94-105.

Briggs, M.A., Gooseff, M.N., Arp, C.D. and Baker, M.A., 2009. A method for estimating surface transient storage parameters for streams with concurrent hyporheic storage. *Water Resources Research*, *45*(4).

Buragohain, P., Garg, A., Feng, S., Lin, P. and Sreedeep, S., 2018. Understanding the retention and fate prediction of copper ions in single and competitive system in two soils: An experimental and numerical investigation. *Science of The Total Environment*, *634*, pp.951-962.

Cardenas, M.B., 2009. A model for lateral hyporheic flow based on valley slope and channel sinuosity. *Water Resources Research*, *45*(1).

Cardenas, M.B., 2015. Hyporheic zone hydrologic science: A historical account of its emergence and a prospectus. *Water Resources Research*, *51*(5), pp.3601-3616.

Chahor, Y., Casalí, J., Giménez, R., Bingner, R.L., Campo, M.A. and Goñi, M., 2014. Evaluation of the AnnAGNPS model for predicting runoff and sediment yield in a small Mediterranean agricultural watershed in Navarre (Spain). *Agricultural Water Management*, *134*, pp.24-37.

Chapra, S.C., 2008. *Surface water-quality modeling*. Waveland press.

Chen, H., Teng, Y. and Wang, J., 2013. Load estimation and source apportionment of nonpoint source nitrogen and phosphorus based on integrated application of SLURP model, ECM, and RUSLE: a case study in the Jinjiang River, China. *Environmental monitoring and assessment*, *185*(2), pp.2009-2021.

Chen, J.N., 2009. Nonpoint Source Pollution Control—Case Studies in Dianchi Lake Catchments. *China Environmental Science Press, Beijing*.

Cherubini, C., Giasi, C.I. and Pastore, N., 2014. On the reliability of analytical models to predict solute transport in a fracture network. *Hydrology and Earth System Sciences*, *18*(6), pp.2359-2374.

Chinyama, A., Ochieng, G.M., Nhapi, I. and Otieno, F.A.O., 2014. A simple framework for selection of water quality models. *Reviews in Environmental Science and Bio/Technology*, *13*(1), pp.109-119.

Cho, J., Barone, V.A. and Mostaghimi, S., 2009. Simulation of land use impacts on groundwater levels and streamflow in a Virginia watershed. *Agricultural water management*, *96*(1), pp.1-11.

Coles, C.A., 2007. Estimating Retardation from the Freundlich Isotherm for Modeling Contaminant Transport. *Engr. Mun. Ca*, *6*.

Collick, A.S., Fuka, D.R., Kleinman, P.J., Buda, A.R., Weld, J.L., White, M.J., Veith, T.L., Bryant, R.B., Bolster, C.H. and Easton, Z.M., 2015. Predicting phosphorus dynamics in complex terrains using a variable source area hydrology model. *Hydrological processes*, *29*(4), pp.588-601.

Collins, A.L., Zhang, Y.S, M., Inman, A., Jones, J.I., Johnes, P.J., Cleasby, W., Vrain, E., Lovett, A. and Noble, L., 2016. Tackling agricultural diffuse pollution: What might uptake of farmer-preferred measures deliver for emissions to water and air?. *Science of the Total Environment*, *547*, pp.269-281.

Corriveau, J., van Bochove, E., Savard, M.M., Cluis, D. and Paradis, D., 2010. Occurrence of high in-stream nitrite levels in a temperate region agricultural watershed. *Water, air, and soil pollution*, *206*(1-4), pp.335-347.

Crowder, B.M. and Young, C.E., 1985. Modeling agricultural nonpoint source pollution for economic evaluation of the Conestoga Headwaters RCWP project. *ERS staff report-United States Dept. of Agriculture, Economic Research Service (USA)*.

De Aussen, R., Kalita, P.K., Koelliker, J.K. and Mankin, K.R., 1998. Application of AGNPS-ARC INFO interface model to an agricultural watershed of Kansas. *American Society of Agricultural Engineering Paper*, (983139).

De Roo, A.P.J., Hazelhoff, L. and Burrough, P.A., 1989. Soil erosion modelling using 'answers' and geographical information systems. *Earth Surface Processes and Landforms*, *14*(6), pp.517-532.

Dechmi, F. and Skhiri, A., 2013. Evaluation of best management practices under intensive irrigation using SWAT model. *Agricultural water management*, *123*, pp.55-64.

Deng, H., Dai, Z., Wolfsberg, A.V., Ye, M., Stauffer, P.H., Lu, Z. and Kwicklis, E., 2013. Upscaling retardation factor in hierarchical porous media with multimodal reactive mineral facies. *Chemosphere*, *91*(3), pp.248-257.

Dentz, M. and Castro, A., 2009. Effective transport dynamics in porous media with heterogeneous retardation properties. *Geophysical Research Letters*, *36*(3).

Department of Water and Sanitation (DWS). 2016. Water Quality Management Policies and Strategies for South Africa. Report No. 1.3: Water Quality and Water Quality Management Challenges in South Africa. Edition 1. Water Resource Planning Systems Series, DWS Report No.: 000/00/21715/5. Pretoria, South Africa

Diaz-Ramirez, J.N., McAnally, W.H. and Martin, J.L., 2011. Analysis of hydrological processes applying the HSPF model in selected watersheds in Alabama, Mississippi, and Puerto Rico. *Applied Engineering in Agriculture*, *27*(6), pp.937-954.

Dong, Y., Liu, Y. and Chen, J., 2014. Will urban expansion lead to an increase in future water pollution loads?—a preliminary investigation of the Haihe River Basin in north eastern China. *Environmental Science and Pollution Research*, *21*(11), pp.7024-7034.

Drechsel, P., Graefe, S., Sonou, M. and Cofie, O.O., 2006. *Informal irrigation in urban West Africa: An overview* (Vol. 102). IWMI.

Drechsel, P., Keraita, B., Amoah, P., Abaidoo, R.C., Raschid-Sally, L. and Bahri, A., 2008. Reducing health risks from wastewater use in urban and peri-urban sub-Saharan Africa: applying the 2006 WHO guidelines. *Water Science and Technology*, *57*(9), pp.1461-1466.

Dressing, S.A., 2003. *National Management Measures for the Control of Nonpoint Pollution from Agriculture*. US Environmental Protection Agency, Office of Water.

Finn, M.P., Usery, E.L., Scheidt, D.J., Jaromack, G.M. and Krupinski, T.D., 2006. An interface between the agricultural non-point source (AGNPS) pollution model and the ERDAS imagine geographic information system (GIS). *Geographic information sciences*, *12*(1), pp.10-20.

Fischer, H.B., 1968. Dispersion predictions in natural streams. *J. Sanit. Eng. Div., ASCE*, *94*, pp.927–943.

Fischer, H.B., List, E., Koh, R., Imberger, J. and Brooks, N., 1979. Mixing in inland and coastal waters Academic Press. *New York*.

Fu, C. and Kang, W.Y., 2012. Research on spatial characteristics of TN & TP of agricultural non-point source pollution in the surrounding area of the Poyang lake. *Resources and Environment in the Yangtze Basin*, *21*(7), pp.864-868.

Fu, Y.C., Ruan, B.Q. and Gao, T., 2013. Watershed Agricultural Non-Point Source Pollution Management. *Polish Journal of Environmental Studies*, *22*(2).

Fuller, C.C. and Harvey, J.W., 2000. Reactive uptake of trace metals in the hyporheic zone of a mining-contaminated stream, Pinal Creek, Arizona. *Environmental Science & Technology*, *34*(7), pp.1150-1155.

Gao, X.P., Li, G.N., Li, G.R. and Zhang, C., 2015. Modeling the effects of point and non-point source pollution on a diversion channel from Yellow River to an artificial lake in China. *Water Science and Technology*, *71*(12), pp.1806-1814.

Gavrilescu, M., Demnerová, K., Aamand, J., Agathos, S. and Fava, F., 2015. Emerging pollutants in the environment: present and future challenges in biomonitoring, ecological risks and bioremediation. *New biotechnology*, *32*(1), pp.147-156.

Ge, Y. and Boufadel, M.C., 2006. Solute transport in multiple-reach experiments: Evaluation of parameters and reliability of prediction. *Journal of hydrology*, *323*(1-4), pp.106-119.

Ghosh, N.C., 2001. *Study of solute transport in a river.* PhD Thesis, Dept. of Civil Eng., IIT, Roorkee, India.

Ghosh, N.C., Mishra, G.C. and Kumarasamy, M., 2008. Hybrid-cells-in-series model for solute transport in streams and relation of its parameters with bulk flow characteristics. *Journal of Hydraulic Engineering*, *134*(4), pp.497-502.

Ghosh, N.C., Mishra, G.C. and Ojha, C.S.P., 2004. Hybrid-cells-in-series Model for Solute Transport in a River. *Journal of Environmental Engineering*, *130*(10), pp.1198-1209.

Gooseff, M.N., Wondzell, S.M., Haggerty, R. and Anderson, J., 2003. Comparing transient storage modeling and residence time distribution (RTD) analysis in geomorphically varied reaches in the Lookout Creek basin, Oregon, USA. *Advances in Water Resources*, *26*(9), pp.925-937.

Haggerty, R., McKenna, S.A. and Meigs, L.C., 2000. On the late-time behavior of tracer test breakthrough curves. *Water Resources Research*, *36*(12), pp.3467-3479.

Han, L.X., Huo, F. and Sun, J., 2011. Method for calculating non-point source pollution distribution in plain rivers. *Water Science and Engineering*, *4*(1), pp.83-91.

Hansen, S.K. and Vesselinov, V.V., 2018. Local equilibrium and retardation revisited. *Groundwater*, *56*(1), pp.109-117.

Harvey, J. and Gooseff, M., 2015. River corridor science: Hydrologic exchange and ecological consequences from bedforms to basins. *Water Resources Research*, *51*(9), pp.6893-6922.

Harvey, J.W., Drummond, J.D., Martin, R.L., McPhillips, L.E., Packman, A.I., Jerolmack, D.J., Stonedahl, S.H., Aubeneau, A.F., Sawyer, A.H., Larsen, L.G. and Tobias, C.R., 2012. Hydrogeomorphology of the hyporheic zone: Stream solute and fine particle interactions with a dynamic streambed. *Journal of Geophysical Research: Biogeosciences*, *117*(G4).

Harvey, J.W., Wagner, B.J. and Bencala, K.E., 1996. Evaluating the reliability of the stream tracer approach to characterize stream-subsurface water exchange. *Water resources research*, *32*(8), pp.2441-2451.

Hedden, S. and Cilliers, J., 2014. Parched prospects-the emerging water crisis in South Africa. *Institute for Security Studies Papers*, *2014*(11), p.16.

Hester, E.T. and Gooseff, M.N., 2010. Moving beyond the banks: Hyporheic restoration is fundamental to restoring ecological services and functions of streams.

Hofstra, N. and Vermeulen, L.C., 2016. Impacts of population growth, urbanisation and sanitation changes on global human Cryptosporidium emissions to surface water. *International journal of hygiene and environmental health*, *219*(7), pp.599-605.

Hong, Q., Sun, Z., Chen, L., Liu, R. and Shen, Z., 2012. Small-scale watershed extended method for non-point source pollution estimation in part of the Three Gorges Reservoir Region. *International Journal of Environmental Science and Technology*, *9*(4), pp.595-604.

Hornberger, G.M., Bencala, K.E. and McKnight, D.M., 1994. Hydrological controls on dissolved organic carbon during snowmelt in the Snake River near Montezuma, Colorado. *Biogeochemistry*, *25*(3), pp.147-165.

Hu, H. and Huang, G., 2014. Monitoring of non-point source pollutions from an agriculture watershed in South China. *Water*, *6*(12), pp.3828-3840.

Hu, Y. and Cheng, H., 2013. Water pollution during China's industrial transition. *Environmental Development*, *8*, pp.57-73.

Huang, J. and Hong, H., 2010. Comparative study of two models to simulate diffuse nitrogen and phosphorus pollution in a medium-sized watershed, southeast China. *Estuarine, Coastal and Shelf Science*, *86*(3), pp.387-394.

Huo, L., Qian, T., Hao, J., Liu, H. and Zhao, D., 2013. Effect of water content on strontium retardation factor and distribution coefficient in Chinese loess. *Journal of Radiological Protection*, *33*(4), p.791.

Jain, C.K., 2000. Application of chemical mass balance approach to determine nutrient loading. *Hydrological sciences journal*, *45*(4), pp.577-588.

Jha, R., Ojha, C.S.P. and Bhatia, K.K.S., 2007. Non-point source pollution estimation using a modified approach. *Hydrological Processes: An International Journal*, *21*(8), pp.1098-1105.

Jiake, L., Huaien, L.I., Bing, S.H.E.N. and Yajiao, L.I., 2011. Effect of non-point source pollution on water quality of the Weihe River. *International Journal of Sediment Research*, *26*(1), pp.50-61.

Jonsson, K., Johansson, H. and Wörman, A., 2003. Hyporheic exchange of reactive and conservative solutes in streams—Tracer methodology and model interpretation. *Journal of Hydrology*, *278*(1-4), pp.153-171.

Kahil, M. A., 2016. Application of First Order Kinetics for Modeling Chlorine Decay in Water Networks. *International Journal of Scientific & Engineering Research*, 7(11), p.331.

Karikari, A.Y., Bernasko, J.K. and Bosque-Hamilton, E.K.A., 2007. An assessment of water quality of Angaw River in southeastern coastal plains of Ghana. *West African Journal of Applied Ecology*, *11*(1).

Kauppi, L., 1982. Testing the application of CREAMS to Finnish conditions. In *European and United States Case Studies in Application of the CREAMS Model IIASA Collaborative Proceedings Series CP-82-S 11, 1982. p 43-47, 2 Tab, 3 Ref* (Vol. 1982).

Kazezyılmaz-Alhan, C.M. and Medina Jr, M.A., 2006. Stream solute transport incorporating hyporheic zone processes. *Journal of hydrology*, *329*(1-2), pp.26-38.

Ki, S.J., Hwang, J.H., Kang, J.H. and Kim, J.H., 2009. An analytical model for non-conservative pollutants mixing in the surf zone. *Water Science and Technology*, *59*(11), pp.2117-2124.

Kiedrzyńska, E., Kiedrzyński, M., Urbaniak, M., Magnuszewski, A., Skłodowski, M., Wyrwicka, A. and Zalewski, M., 2014. Point sources of nutrient pollution in the lowland river catchment in the context of the Baltic Sea eutrophication. *Ecological engineering*, *70*, pp.337-348.

Kim, H., Lee, K.K. and Lee, J.Y., 2014. Numerical verification of hyporheic zone depth estimation using streambed temperature. *Journal of Hydrology*, *511*, pp.861-869.

Kim, S.B., Shin, H.J., Park, M. and Kim, S.J., 2015. Assessment of future climate change impacts on snowmelt and stream water quality for a mountainous high-elevation watershed using SWAT. *Paddy and water environment*, *13*(4), pp.557-569.

Kliment, Z., Kadlec, J. and Langhammer, J., 2008. Evaluation of suspended load changes using AnnAGNPS and SWAT semi-empirical erosion models. *Catena*, *73*(3), pp.286-299.

Knapp, J.L., González-Pinzón, R., Drummond, J.D., Larsen, L.G., Cirpka, O.A. and Harvey, J.W., 2017. Tracer-based characterization of hyporheic exchange and benthic biolayers in streams. *Water Resources Research*, *53*(2), pp.1575-1594.

Kollongei, K.J., 2015. *Non-point source pollution processes and connectivity modelling in the Mkabela Catchment, South Africa*. Ph.D. thesis, University of Kwa-Zulu Natal, Kwa-Zulu Natal, Durban.

Krause, S., Hannah, D.M., Fleckenstein, J.H., Heppell, C.M., Kaeser, D., Pickup, R., Pinay, G., Robertson, A.L. and Wood, P.J., 2011. Inter-disciplinary perspectives on processes in the hyporheic zone. *Ecohydrology*, *4*(4), pp.481-499.

Krupka, K.M., Kaplan, D.I., Whelan, G., Serne, R.J. and Mattigod, S.V., 1999. Understanding variation in partition coefficient, Kd, values *Volume I: The Kd Model, Methods of Measurement, and Application of Chemical Reaction Codes. EPA*.

Kumar, A. and Dalal, D.C., 2014. Analytical solution and analysis for solute transport in streams with diffusive transfer in the hyporheic zone. *Journal of Hydro-environment Research*, *8*(1), pp.62-73.

Kumarasamy, M., 2011. Simulation of Stream Pollutant Transport with Hyporheic Exchange for Water Resources Management. In *Current Issues of Water Management*. InTech.

Kumarasamy, M., Ghosh, N.C., Mishra, G.C. and Kansal, M.L., 2013. Hybrid model development for the decaying pollutant transport in streams. *International Journal of Environment and Waste Management*, *12*(2), pp.130-145.

Kumarasamy, M., Mishra, G.C., Ghosh, N.C. and Kansal, M.L., 2011. Semianalytical solution for nonequilibrium sorption of pollutant transport in streams. *Journal of Environmental Engineering*, *137*(11), pp.1066-1074.

Kumarasamy, M.V., 2015. Deoxygenation andReaeration Coupled hybridMixing cells Based Pollutant Transport Model to Assess Water Quality Status of a River. *International journal of environmental research*, *9*(1), pp.341-350.

Lam, Q.D., Schmalz, B. and Fohrer, N., 2010. Modelling point and diffuse source pollution of nitrate in a rural lowland catchment using the SWAT model. *Agricultural Water Management*, *97*(2), pp.317-325.

Lee, M., Park, G., Park, M., Park, J., Lee, J. and Kim, S., 2010. Evaluation of non-point source pollution reduction by applying Best Management Practices using a SWAT model and QuickBird high resolution satellite imagery. *Journal of Environmental Sciences*, *22*(6), pp.826-833.

Lee, S.C., Park, I.H., Kim, B.S. and Ha, S.R., 2015. Relationship Between Non-Point Source Pollution and Korean Green Factor. *Terrestrial, Atmospheric & Oceanic Sciences*, *26*(3).

Leeman, W.P., Schutt, D.L. and Hughes, S.S., 2009. Thermal structure beneath the Snake River Plain: Implications for the Yellowstone hotspot. *Journal of Volcanology and Geothermal Research*, *188*(1-3), pp.57-67.

Lees, M.J., Camacho, L.A. and Chapra, S., 2000. On the relationship of transient storage and aggregated dead zone models of longitudinal solute transport in streams. *Water Resources Research*, *36*(1), pp.213-224.

Leon, L.F., Booty, W.G., Bowen, G.S. and Lam, D.C.L., 2004. Validation of an agricultural non-point source model in a watershed in southern Ontario. *Agricultural Water Management*, *65*(1), pp.59-75.

Leon, L.F., Soulis, E.D., Kouwen, N. and Farquhar, G.J., 2001. Nonpoint source pollution: a distributed water quality modeling approach. *Water Research*, *35*(4), pp.997-1007.

Leonard, R.A. and Knisel Jr, W.G., 1986. Selection and application of models for nonpoint source pollution and resource conservation. In *Developments in environmental modelling* (Vol. 10, pp. 213-229). Elsevier.

Li, C., Zheng, X., Zhao, F., Wang, X., Cai, Y. and Zhang, N., 2017. Effects of Urban Non-Point Source Pollution from Baoding City on Baiyangdian Lake, China. *Water*, *9*(4), p.249.

Li, J.K., 2009. *Research on non-point source pollution load quantification for watershed-taking the weihe river basin as an example* (Doctoral dissertation, Doctoral dissertation, Xian: Xi'an University of Technology).

Li, Q.K. and Li, H.E., 2010. The preliminary frame of non point source pollution study in the Yellow River watershed. *Yellow River*, *32*(12), pp.131-135.

Li, S., Zhuang, Y., Zhang, L., Du, Y. and Liu, H., 2014. Worldwide performance and trends in nonpoint source pollution modeling research from 1994 to 2013: A review based on bibliometrics. *Journal of soil and water conservation*, *69*(4), pp.121A-126A.

Lin, J., Ganesh, A. and Singh, M., 2012. *Microbial Pathogens in the Umgeni River, South Africa*. Water Research Commission.

Liu, X., Zhang, L. and Hong, S., 2011. Global biodiversity research during 1900–2009: a bibliometric analysis. *Biodiversity and Conservation*, *20*(4), pp.807-826.

Loague, K. and Corwin, D.L., 2006. Point and nonpoint source pollution. *Encyclopedia of hydrological sciences*.

López, M.E.P., Sanchez-Martinez, M.G., de la Rosa, M.G.V. and Leon, M.T., 2013. Eutrophication Levels through San Pedro-Mezquital River Basin. *Journal of Environmental Protection*, *4*(11), p.45.Loucks, D.P. and van Beek, E., 2017. Water Quality Modeling and Prediction. In *Water Resource Systems Planning and Management* (pp. 417-467). Springer, Cham.

Loucks, D.P. and van Beek, E., 2017. Water Quality Modeling and Prediction. In *Water Resource Systems Planning and Management* (pp. 417-467). Springer, Cham.

Ma, X., Li, Y., Zhang, M., Zheng, F. and Du, S., 2011. Assessment and analysis of non-point source nitrogen and phosphorus loads in the Three Gorges Reservoir Area of Hubei Province, China. *Science of the Total Environment*, *412*, pp.154-161.

Maghrebi, M., Jankovic, I., Fiori, A. and Dagan, G., 2013. Effective retardation factor for transport of reactive solutes in highly heterogeneous porous formations. *Water Resources Research*, *49*(12), pp.8600-8604.

Mamun, A.A. and Salleh, M.N., 2014. Challenges in non-point source pollution-sampling and testing. In Engineering and Technology (BICET 2014), 5th Brunei International Conference, 1-6. IET.

Maringanti, C., Chaubey, I., Arabi, M. and Engel, B., 2011. Application of a multi-objective optimization method to provide least cost alternatives for NPS pollution control. *Environmental management*, *48*(3), pp.448-461.

Marquardt, D.W., 1963. An algorithm for least-squares estimation of nonlinear parameters. *Journal of the society for Industrial and Applied Mathematics*, *11*(2), pp.431-441.

Martin, J.L., Wool, T. and Olson, R., 2002. A dynamic one-dimensional model for hydrodynamics and water quality. *EPDRiv1 Version*, *1*.

McDowell, R. W., N. Cox, and T. H. Snelder., 2017. Assessing the Yield and Load of Contaminants with Stream Order: Would Policy Requiring Livestock to Be Fenced Out of High-Order Streams Decrease Catchment Contaminant Loads? *Journal of environmental quality*, *46*(5), pp.1038-1047.

McKnight, D.M. and Bencala, K.E., 1989. Reactive iron transport in an acidic mountain stream in Summit County, Colorado: A hydrologic perspective. *Geochimica et Cosmochimica Acta*, *53*(9), pp.2225-2234.

Mishra, G.C. and Jain, S.K., 1999. Estimation of hydraulic diffusivity in stream-aquifer system. *Journal of irrigation and drainage engineering*, *125*(2), pp.74-81.

Mohammed, H., Yohannes, F. and Zeleke, G., 2004. Validation of agricultural non-point source (AGNPS) pollution model in Kori watershed, South Wollo, Ethiopia. *International Journal of Applied Earth Observation and Geoinformation*, *6*(2), pp.97-109.

Moolman, J., Quibell, G. and Hohls, B., 1999. A qualitative (GIS-based) model of non-point source areas (modelling suspended sediment in the Olifants River catchment). *Institute for Water Quality Studies, Department of Water Affairs and Forestry, Pretoria, South Africa*. http://www.dwaf.gov.za/iwqs/reports/slopes_olifants/sed_olif.htm (accessed August 2017).

Morin, R.H., Paillet, F.L., Taylor, T.A. and Barrash, W., 1993. *Geophysical logging studies in the Snake River Plain Aquifer at the Idaho National Engineering Laboratory: Wells 44, 45, and 46* (No. DOE/ID/13042--8). Geological Survey.

Mueller-Warrant, G.W., Griffith, S.M., Whittaker, G.W., Banowetz, G.M., Pfender, W.F., Garcia, T.S. and Giannico, G.R., 2012. Impact of land use patterns and agricultural practices on water quality in the Calapooia River Basin of western Oregon. *Journal of Soil and Water Conservation*, *67*(3), pp.183-201.

Muller, A.B., Langmuir, D. and Duda, L.E., 1982. The formulation of an integrated physicochemical-hydrologic model for predicting waste nuclide retardation in geologic media. *MRS Online Proceedings Library Archive*, *15*.

Muthukrishnavellaisamy, K., Mishra, G.C., Kansal, M.L. and Ghosh, N.C., 2009. Estimation of stream water quality parameter using regime channel theory. *Environmental geology*, *57*(4), p.899.

Naidoo, N. and Kumarasamy, M., 2016. Sensitivity Analysis of Model Parameters for Water Quality Simulation. *Polish Journal of Environmental Studies*, *25*(4).

Neitsch, S.L., Arnold, J.G., Kiniry, J.R. and Williams, J.R., 2011. *Soil and water assessment tool theoretical documentation version 2009*. Texas Water Resources Institute.

Neuman, S.P. and Tartakovsky, D.M., 2009. Perspective on theories of non-Fickian transport in heterogeneous media. *Advances in Water Resources*, *32*(5), pp.670-680.

Novotny, V., 1994. *Water quality: prevention, identification and management of diffuse pollution*. Van Nostrand-Reinhold Publishers.

Nuruzzaman, M., Al-Mamun, A. and Salleh, M.N.B., 2017. Experimenting biochemical oxygen demand decay rates of Malaysian river water in a laboratory flume. *Environmental Engineering Research*, *23*(1), pp.99-106.

Nyenje, P.M., Foppen, J.W., Uhlenbrook, S., Kulabako, R. and Muwanga, A., 2010. Eutrophication and nutrient release in urban areas of sub-Saharan Africa—a review. *Science of the Total Environment*, *408*(3), pp.447-455.

Oberholster, P., 2010. The current status of water quality in South Africa. *A CSIR perspective on water–2010. CSIR Report No. CSIR/NRE/PW/IR//2011/0012/A. CSIR, Pretoria*. (accessed August 2017).

O'Connor, D.J., 1976. The concentration of dissolved solids and river flow. *Water Resources Research*, *12*(2), pp.279-294.

Oliveira, B., Bola, J., Quinteiro, P., Nadais, H. and Arroja, L., 2012. Application of Qual2Kw model as a tool for water quality management: Cértima River as a case study. *Environmental monitoring and assessment*, *184*(10), pp.6197-6210.

Olowe, K.O. and Kumarasamy, M., 2017. Development of the hybrid cells in series model to simulate ammonia nutrient pollutant transport along the Umgeni River. *Environmental Science and Pollution Research*, *24*(29), pp.22967-22979.

Olsen, R.L., Chappell, R.W. and Loftis, J.C., 2012. Water quality sample collection, data treatment and results presentation for principal components analysis–literature review and Illinois River watershed case study. *Water research*, *46*(9), pp.3110-3122.

Ongley, E.D., Xiaolan, Z. and Tao, Y., 2010. Current status of agricultural and rural non-point source pollution assessment in China. *Environmental Pollution*, *158*(5), pp.1159-1168.

Ouyang, W., Jiao, W., Li, X., Giubilato, E. and Critto, A., 2016. Long-term agricultural non-point source pollution loading dynamics and correlation with outlet sediment geochemistry. *Journal of Hydrology*, *540*, pp.379-385.

Pegram, G.C. and Bath, A.J., 1995. Role of non-point sources in the Development of a water quality Management plan for the Mgeni river catchment. *Water Science Tech*, *32*(5-6), pp. 175-182.

Pimentel, D., 1993. *World soil erosion and conservation*. Cambridge University Press.

Piniewski, M., Marcinkowski, P., Kardel, I., Giełczewski, M., Izydorczyk, K. and Frątczak, W., 2015. Spatial quantification of non-point source pollution in a meso-scale catchment for an assessment of buffer zones efficiency. *Water*, *7*(5), pp.1889-1920.

Poudel, D.D., 2016. Surface water quality monitoring of an agricultural watershed for nonpoint source pollution control. *Journal of Soil and Water Conservation*, *71*(4), pp.310-326.

Poudel, D.D., Lee, T., Srinivasan, R., Abbaspour, K. and Jeong, C.Y., 2013. Assessment of seasonal and spatial variation of surface water quality, identification of factors associated with water quality variability, and the modeling of critical nonpoint source pollution areas in an agricultural watershed. *Journal of Soil and Water Conservation*, *68*(3), pp.155-171.

Qiu, Z., 2013. Comparative assessment of stormwater and nonpoint source pollution best management practices in suburban watershed management. *Water*, *5*(1), pp.280-291.

Ribarova, I., Ninov, P. and Cooper, D., 2008. Modeling nutrient pollution during a first flood event using HSPF software: Iskar River case study, Bulgaria. *Ecological modelling*, *211*(1-2), pp.241-246.

Runkel, R.L. and Bencala, K.E., 1995. Transport of reacting solutes in rivers and streams. In *Environmental hydrology* (pp. 137-164). Springer, Dordrecht.

Runkel, R.L. and Chapra, S.C., 1993. An efficient numerical solution of the transient storage equations for solute transport in small streams. *Water Resources Research*, *29*(1), pp.211-215.

Runkel, R.L., McKnight, D.M. and Rajaram, H., 2003. Modeling hyporheic zone processes. *Advances in Water Resources*, *26*(9), pp.901-905.

Rutherford, J.C., 1994. *River mixing*. John Wiley & Son Ltd. New York

Sexton, A.M., Shirmohammadi, A., Sadeghi, A.M. and Montas, H.J., 2011. Impact of parameter uncertainty on critical SWAT output simulations. *Transactions of the ASABE*, *54*(2), pp.461-471.

Sharma, D. and Kansal, A., 2013. Assessment of river quality models: a review. *Reviews in Environmental Science and Bio/Technology*, *12*(3), pp.285-311.

Shen, Z., Chen, L., Hong, Q., Qiu, J., Xie, H. and Liu, R., 2013a. Assessment of nitrogen and phosphorus loads and causal factors from different land use and soil types in the Three Gorges Reservoir Area. *Science of the Total Environment*, *454*, pp.383-392.

Shen, Z., Chen, L., Hong, Q., Xie, H., Qiu, J. and Liu, R., 2013b. Vertical variation of nonpoint source pollutants in the Three Gorges Reservoir Region. *PloS one*, *8*(8), p.e71194.

Shen, Z., Hong, Q., Chu, Z. and Gong, Y., 2011. A framework for priority non-point source area identification and load estimation integrated with APPI and PLOAD model in Fujiang Watershed, China. *Agricultural Water Management*, *98*(6), pp.977-989.

Shen, Z., Liao, Q., Hong, Q. and Gong, Y., 2012. An overview of research on agricultural non-point source pollution modelling in China. *Separation and Purification Technology*, *84*, pp.104-111.

Shen, Z., Qiu, J., Hong, Q. and Chen, L., 2014. Simulation of spatial and temporal distributions of non-point source pollution load in the Three Gorges Reservoir Region. *Science of the Total Environment*, *493*, pp.138-146.

Shoemaker, L., Dai, T., Koenig, J. and Hantush, M., 2005. *TMDL model evaluation and research needs*. National Risk Management Research Laboratory, US Environmental Protection Agency.

Strokal, M., Kroeze, C., Wang, M., Bai, Z. and Ma, L., 2016. The MARINA model (Model to Assess River Inputs of Nutrients to seAs): Model description and results for China. *Science of the Total Environment*, *562*, pp.869-888.

Tonina, D. and Buffington, J. M., 2009. Hyporheic exchange in mountain rivers I: Mechanics and environmental effects, *Geography Compass* 3/3: 1063-1086.

Tzoraki, O. and Nikolaidis, N.P., 2007. A generalized framework for modeling the hydrologic and biogeochemical response of a Mediterranean temporary river basin. *Journal of Hydrology*, *346*(3-4), pp.112-121.

Ullrich, A. and Volk, M., 2009. Application of the Soil and Water Assessment Tool (SWAT) to predict the impact of alternative management practices on water quality and quantity. *Agricultural Water Management*, *96*(8), pp.1207-1217.

Van Rooyen J., Van Niekerk P. and Versveld R., 2009. Strategic planning for water resources in South Africa. *Civil Engineering. 17* (5), pp.5-8.

Varol, M. and Şen, B., 2012. Assessment of nutrient and heavy metal contamination in surface water and sediments of the upper Tigris River, Turkey. *Catena*, *92*, pp.1-10.

Voß, A., Alcamo, J., Bärlund, I., Voß, F., Kynast, E., Williams, R. and Malve, O., 2012. Continental scale modelling of in-stream river water quality: a report on methodology, test runs, and scenario application. *Hydrological Processes*, *26*(16), pp.2370-2384.

Wagner, B.J. and Harvey, J.W., 1997. Experimental design for estimating parameters of rate-limited mass transfer: Analysis of stream tracer studies. *Water Resources Research*, *33*(7), pp.1731-1741.

Wang, A., Tang, L. and Yang, D., 2016. Spatial and temporal variability of nitrogen load from catchment and retention along a river network: a case study in the upper Xin'anjiang catchment of China. *Hydrology Research*, *47*(4), pp.869-887.

Wang, Q., Li, S., Jia, P., Qi, C. and Ding, F., 2013a. A review of surface water quality models. *The Scientific World Journal*, *2013*.

Wang, S., He, Q., Ai, H., Wang, Z. and Zhang, Q., 2013b. Pollutant concentrations and pollution loads in stormwater runoff from different land uses in Chongqing. *Journal of Environmental Sciences*, *25*(3), pp.502-510.

Wen, Y., Schoups, G. and Van De Giesen, N., 2017. Organic pollution of rivers: Combined threats of urbanization, livestock farming and global climate change. *Scientific reports*, *7*, p.43289.

Williams, J.R., Nicks, A.D. and Arnold, J.G., 1985. Simulator for water resources in rural basins. *Journal of Hydraulic Engineering*, *111*(6), pp.970-986.

Winter, T.C., 1998. *Ground water and surface water: a single resource* (Vol. 1139). DIANE Publishing Inc.

Wu, L., Liu, X. and Ma, X.Y., 2016. Spatio-temporal variation of erosion-type non-point source pollution in a small watershed of hilly and gully region, Chinese Loess Plateau. *Environmental Science and Pollution Research*, *23*(11), pp.10957-10967.

Wu, L., Long, T.Y., Liu, X. and Guo, J.S., 2012. Impacts of climate and land-use changes on the migration of non-point source nitrogen and phosphorus during rainfall-runoff in the Jialing River Watershed, China. *Journal of Hydrology*, *475*, pp.26-41.

Wu, Y. and Chen, J., 2013. Investigating the effects of point source and nonpoint source pollution on the water quality of the East River (Dongjiang) in South China. *Ecological Indicators*, *32*, pp.294-304.

Xia, J., Zhai, X. and Zhang, Y. 2012. Progress in the research of water environmental nonpoint source pollution models. *Progress in Geography*, *31*(7), pp.941-952.

Xia, J., Zhang, Y.Y., Zhan, C. and Ye, A.Z., 2011. Water quality management in China: the case of the Huai River Basin. *International Journal of Water Resources Development*, *27*(1), pp.167-180.

Xu, H.S., Xu, Z.X. and Liu, P., 2013. Estimation of nonpoint source pollutant loads and optimization of the best management practices (BMPs) in the Zhangweinan River basin. *Huan jing ke xue= Huanjing kexue*, *34*(3), pp.882-891.

Yan, C.A., Zhang, W. and Zhang, Z., 2014. Hydrological modeling of the Jiaoyi watershed (China) using HSPF model. *The Scientific World Journal*, *2014*.

Yanhua, Z., Thuminh, N., Beibei, N. and Song, H., 2012. Research trends in non-point source during 1975-2010. *Physics Procedia*, *33*, pp.138-143.

Young, R.A., Onstad, C.A., Bosch, D.D. and Anderson, W.P., 1989. AGNPS: A nonpoint-source pollution model for evaluating agricultural watersheds. *Journal of soil and water conservation*, *44*(2), pp.168-173.

Yuceer, M. and Coskun, M.A., 2016. Modeling water quality in rivers: a case study of Beylerderesi river in Turkey. *Applied Ecology and Environmental Research*, *14*(1), pp.383-395.

Zaramella, M., Packman, A.I. and Marion, A., 2003. Application of the transient storage model to analyze advective hyporheic exchange with deep and shallow sediment beds. *Water Resources Research*, *39*(7).

Zema, D.A., Denisi, P., Taguas Ruiz, E.V., Gómez, J.A., Bombino, G. and Fortugno, D., 2016. Evaluation of Surface Runoff Prediction by A nn AGNPS Model in a Large Mediterranean Watershed Covered by Olive Groves. *Land degradation & development*, *27*(3), pp.811-822.

Zhai, X., Zhang, Y., Wang, X., Xia, J. and Liang, T., 2014. Non-point source pollution modelling using Soil and Water Assessment Tool and its parameter sensitivity analysis in Xin'anjiang catchment, China. *Hydrological Processes*, *28*(4), pp.1627-1640.

Zhang, H. and Huang, G.H., 2011. Assessment of non-point source pollution using a spatial multicriteria analysis approach. *Ecological Modelling*, *222*(2), pp.313-321.

Zhang, W., 2015. Applying Numerical Models for Water Environments in Watersheds–Case Studies of Tai Lake, Middle and Lower Han River and East Lake in China. In *Research and Practices in Water Quality*. InTech.

Zhang, W., Che, W., Liu, D.K., Gan, Y.P. and Lv, F.F., 2012. Characterization of runoff from various urban catchments at different spatial scales in Beijing, China. *Water Science and Technology*, *66*(1), pp.21-27.

Zhao, Y., Xia, X.H., Yang, Z.F. and Wang, F., 2012. Assessment of water quality in Baiyangdian Lake using multivariate statistical techniques. *Procedia Environmental Sciences*, *13*, pp.1213-1226.

APPENDIX A

List of Publications from this Thesis

1. Adu, J.T. and Kumarasamy, M.V., (2018). Assessing Non-Point Source Pollution Models: A Review. Polish Journal of Environmental Studies, 27, pp.1913-1922. **(Published)**
2. Adu, J.T. and Kumarasamy, M.V., (2018). Development of Mathematical model for Simulation of Non-Point Source Pollutant Transport in Rivers. International Journal of Environmental Research. **(Submitted)**
3. Adu, J.T. and Kumarasamy, M.V., (2018). Analytical Solution of Reactive Solute Transport in Rivers with Diffuse Inflows, Polish Journal of Environmental Studies. **(Submitted)**
4. Adu, J.T. and Kumarasamy, M.V., (2018). Simulation of Non-Point Source Pollutant Transport in Streams with Hyporheic Exchange Processes. Environmental Science and Pollution Research **(Submitted**)

APPENDIX B

B1. Data for Snake River tracer test adopted from Bencala et al (1990)

TABLE 1. Tracer Injection Studies in the Snake River, 1983

Sampling Reach	Tracer	Duration	Injection Rate, mmol s^{-1}	Purpose
		Study 1: August 30, 1983		
Upstream to downstream Injection at "0 m"	LiCl	0900–1500	15.1	Evaluate Li as a tracer compared to Cl and SO_4 and estimate solute transport characteristics of Stream
Upstream to downstream Injection at "0 m"	H_2SO_4	0900–1200	114.7	Control *p*H in the Snake River; permits evaluation of Li with variable *p*H
Downstream Injection into Deer Creek	NaBr	1000–1600	4.6	Evaluate Br as a tracer compared to Li, Cl, SO_4, and Na
		Study 2: September 1, 1983		
Downstream Injection above confluence at "2557 m"	LiCl	0900–1200	12.7	Evaluate Li as a tracer compared to Cl and estimates solute transport characteristics of stream
Downstream Injection into Deer Creek	NaBr	0900–1200	5.1	Evaluate Br as a tracer compared to Li, Cl, and Na
Downstream Injection into Deer Creek	NaOH	0900–1000	34.6	Control *p*H in the lower Snake River; permits evaluation of Li with variable *p*H

Source: Bencala et al., 1990

TABLE 2*a*. Simulation Parameters: Snake River 1983 Injection Experiment

Parameters at Boundary ("0 m")	Value
Discharge Q, $m^3\ s^{-1}$	0.224
Background concentration C, μM	
Lithium	0
Chloride	5
Sulfate	385
Plateau concentration C, μM	
Lithium	68
Chloride	71
Sulfate	867

Source: Bencala et al., 1990

TABLE 2*b*. Simulation Parameters: Snake River 1983 Injection Experiment

Subreach	Stream Cross-Sectional Area A, m^2	Dispersion Coefficient D, $m^2\ s^{-1}$	Volume Inflow q_L, $m^3\ s^{-1}\ m^{-1}$	Storage Cross-Sectional Area A_s, m^2	Exchange Coefficient α, s^{-1}	Solute Inflow C_L, μM		
						Li	Cl	SO_4
Parameters Through Subreaches Upstream of Deer Creek								
0–628 m	0.61	0.75	0.062×10^{-3}	0.10	0.025×10^{-3}	0	5	732
628–1365 m	0.55	0.60	0.083×10^{-3}	0.02	0.050×10^{-3}	0	5	795
1365–1487 m	1.90	0.50	0.131×10^{-3}	1.50	0.500×10^{-3}	0	5	591
1487–1605 m	1.80	0.20	0.161×10^{-3}	0.50	0.100×10^{-3}	0	5	591
1605–2845 m	0.70	0.20	0.028×10^{-3}	0.12	0.200×10^{-3}	0	5	164
*Deer Creek Confluence**								
2845–2913 m	0.80	0.02	3.118×10^{-3}	0.05	0.200×10^{-3}	0	3	80
Parameters Through Subreaches Below Deer Creek								
2913–3912 m	1.08	0.2	0.176×10^{-3}	0.05	0.050×10^{-3}	0	4	194
3912–3889 m	1.21	0.2	0.043×10^{-3}	0.05	0.050×10^{-3}	0	4	686
3889–5231 m	1.60	0.2	0.090×10^{-3}	0.50	0.100×10^{-3}	0	4	387

Source: Bencala et al., 1990

B2. Field tracer test results from Snake River (provided by Profs Kenneth Bencala and Robert Runkel).

The following sets of data from Snake River have been availed from Prof Bencala on request. These sets of data have been used for comparing model simulation as presented in Fig. 4.4, 4.5, 4.6 and 4.8

Data for Lithium Before Confluence
Title Text: Lithium (h) @ 628 m (8/30/83)
X Unit Text: Time [hour]
Y Unit Text: Concentration [mg/l]

S/No	Time of Day (hrs)	Lithium Concentration (mg/l)
1	9.000000	0.000000
2	9.116667	0.000000
3	9.266667	0.000000
4	9.350000	0.012000
5	9.433333	0.223000
6	9.533333	0.372000
7	9.616667	0.384000
8	10.000000	0.391000
9	11.000000	0.391000
10	12.000000	0.412000
11	12.166667	0.397000
12	12.333333	0.397000
13	12.666667	0.403000
14	12.833333	0.412000
15	13.000000	0.397000
16	13.166667	0.412000
17	14.000000	0.384000
18	14.250000	0.405000
19	14.500000	0.391000
20	14.750000	0.385000
21	15.000000	0.398000
22	15.250000	0.398000
23	15.500000	0.015000
24	15.750000	0.012000
25	16.000000	0.012000

Title Text: Lithium (h) @ 2845 m (8/30/83)
X Unit Text: Time [hour]
Y Unit Text: Concentration [mg/l]

S/No	Time of Day (hrs)	Lithium Concentration (mg/l)
1	9.000000	0.000000
2	10.00000	0.000000
3	10.116667	0.000000
4	10.266667	0.000000
5	10.400000	0.000000
6	10.550000	0.000000
7	10.700000	0.009000
8	10.816667	0.048000
9	10.966667	0.119000
10	11.100000	0.158000
11	11.266667	0.190000
12	11.433333	0.206000
13	11.633333	0.225000
14	11.800000	0.229000
15	12.016667	0.229000
16	12.216667	0.245000
17	12.566667	0.253000
18	12.766667	0.253000
19	13.066667	0.253000
20	13.250000	0.261000
21	13.433333	0.261000
22	13.650000	0.270000
23	13.850000	0.261000
24	14.000000	0.269000
25	14.250000	0.269000
26	14.550000	0.269000
27	14.716667	0.206000
28	15.000000	0.277000
29	15.250000	0.269000
30	15.516667	0.237000
31	15.766667	0.269000
32	16.500000	0.258000
33	16.750000	0.239000
34	17.083333	0.104000
35	17.250000	0.080000
36	17.500000	0.055000
37	17.750000	0.037000

Data for Lithium After the Confluence
Title Text: Lithium (h) @ 3192 m (8/30/83)
X Unit Text: Time [hour]
Y Unit Text: Concentration [mg/l]

S/No	Time of Day (hrs)	Lithium Concentration (mg/l)
1	9.000000	0.000000
2	10.500000	0.000000
3	10.666667	0.000000
4	10.833333	0.032000
5	11.166667	0.076000
6	11.333333	0.102000
7	11.533333	0.115000
8	11.666667	0.120000
9	11.833333	0.129000
10	12.000000	0.129000
11	12.166667	0.133000
12	12.333333	0.141000
13	12.533333	0.145000
14	12.666667	0.149000
15	13.000000	0.149000
16	13.533333	0.154000
17	14.000000	0.158000
18	14.500000	0.158000
19	15.000000	0.163000
20	15.500000	0.158000
21	16.000000	0.163000
22	16.500000	0.163000
23	17.000000	0.118000
24	17.500000	0.043000

Title Text: Lithium (h) @ 5231 m (8/30/83)
X Unit Text: time [hour]
Y Unit Text: Concentration [mg/l]

S/No	Time of Day (hrs)	Lithium Concentration (mg/l)
1	10.866667	0.000000
2	11.016667	0.000000
3	11.116667	0.000000
4	11.250000	0.000000
5	11.250000	0.000000
6	11.400000	0.000000
7	11.500000	0.000000
8	11.600000	0.000000
9	11.750000	0.000000
10	11.900000	0.000000
11	12.083333	0.015000
12	12.333333	0.048000
13	12.566667	0.071000
14	12.700000	0.082000
15	12.850000	0.088000
16	13.000000	0.094000
17	13.166667	0.100000
18	13.333333	0.106000
19	13.500000	0.107000
20	13.666667	0.111000
21	13.833333	0.117000
22	14.000000	0.111000
23	14.333333	0.117000
24	14.500000	0.117000
25	14.666667	0.120000
26	14.833333	0.123000
27	15.000000	0.123000
28	15.166667	0.123000
29	15.333333	0.126000
30	15.500000	0.126000
31	15.833333	0.129000
32	16.083333	0.129000
33	17.083333	0.132000
34	17.333333	0.129000
35	17.583333	0.129000

Data for Chloride Before Confluence
Title Text: Chloride (h) @ 628 m (8/30/83)
X Unit Text: time [hour]
Y Unit Text: Concentration [mg/l]

S/No	Time of Day (hrs)	Chloride Concentration (mg/l)
1	9.116667	0.195000
2	9.266667	0.180000
3	9.350000	0.229000
4	9.433333	1.232000
5	9.533333	2.023000
6	9.616667	2.103000
7	10.000000	2.177000
8	11.000000	2.215000
9	12.000000	2.248000
10	12.166667	2.274000
11	12.333333	2.248000
12	12.500000	2.245000
13	12.666667	2.227000
14	12.833333	2.189000
15	13.000000	2.189000
16	13.166667	2.256000
17	14.000000	2.150000
18	14.250000	2.165000
19	14.500000	2.177000
20	14.750000	2.147000
21	15.000000	2.153000
22	15.250000	2.162000
23	15.500000	0.263000
24	15.750000	0.208000

Title Text: Chloride (h) @ 2845 m (8/30/83)
X Unit Text: Time [hour]
Y Unit Text: Concentration [mg/l]

S/No	Time of Day (hrs)	Chloride Concentration (mg/l)
1	9.000000	0.275000
2	10.000000	0.166000
3	10.116667	0.164000
4	10.266667	0.157000
5	10.400000	0.163000
6	10.550000	0.158000
7	10.700000	0.193000
8	10.816667	0.371000
9	10.966667	0.649000
10	11.100000	0.854000
11	11.266667	1.063000
12	11.433333	1.168000
13	11.633333	1.272000
14	11.800000	1.488000
15	12.016667	1.358000
16	12.216667	1.417000
17	12.566667	1.447000
18	12.766667	1.492000
19	13.066667	1.488000
20	13.250000	1.499000
21	13.433333	1.533000
22	13.650000	1.533000
23	13.850000	1.581000
24	14.000000	1.592000
25	14.250000	1.462000
26	14.550000	1.493000
27	14.716667	1.505000
28	15.000000	1.560000
29	15.250000	1.501000
30	15.516667	1.509000
31	15.766667	1.537000
32	16.000000	1.545000
33	16.250000	1.541000
34	16.500000	1.537000
35	16.750000	1.423000
36	17.083333	0.583000
37	17.250000	0.494000

Data for Chloride After Confluence
Title Text: Chloride (h) @ 3192 m (8/30/83)
X Unit Text: Time [hour]
Y Unit Text: Concentration [mg/l]

S/No	Time of Day (hrs)	Chloride Concentration (mg/l)
1	9.000000	0.175000
2	10.500000	0.165000
3	10.666667	0.159000
4	10.833333	0.172000
5	11.000000	0.285000
6	11.166667	0.491000
7	11.333333	0.630000
8	11.500000	0.676000
9	11.683333	0.692000
10	11.833333	0.730000
11	12.000000	0.770000
12	12.166667	0.773000
13	12.333333	0.805000
14	12.500000	0.827000
15	12.666667	0.869000
16	13.000000	0.898000
17	13.500000	0.895000
18	14.000000	0.927000
19	14.500000	0.949000
20	15.000000	0.975000
21	15.500000	0.930000
22	16.000000	0.940000
23	17.000000	0.714000
24	17.500000	0.361000

Title Text: Chloride (h) @ 5231m (8/30/83)
X Unit Text: Time [hour]
Y Unit Text: Concentration [mg/l]

S/No	Time of Day (hrs)	Chloride Concentration (mg/l)
1	10.866667	0.171000
2	11.016667	0.183000
3	11.116667	0.128000
4	11.250000	0.160000
5	11.400000	0.158000
6	11.500000	0.151000
7	11.600000	0.151000
8	11.750000	0.147000
9	11.900000	0.140000
10	11.900000	0.158000
11	12.083333	0.219000
12	12.333333	0.366000
13	12.566667	0.506000
14	12.700000	0.565000
15	13.000000	0.574000
16	13.166667	0.599000
17	13.333333	0.603000
18	13.500000	0.630000
19	13.666667	0.684000
20	13.833333	0.706000
21	14.000000	0.697000
22	14.166667	0.675000
23	14.500000	0.680000
24	14.666667	0.698000
25	14.833333	0.738000
26	15.000000	0.756000
27	15.166667	0.736000
28	15.333333	0.759000
29	15.500000	0.711000
30	15.666667	0.716000
31	15.833333	0.714000
32	16.083333	0.727000
33	16.333333	0.734000
34	16.583333	0.730000
35	16.833333	0.738000
36	17.333333	0.731000
37	17.583333	0.741000
38	17.833333	0.752000
39	18.083333	0.699000

APPENDIX C

Flow Chart of Modelling Process Using FORTRAN

Model components were developed using FORTRAN for all the processes namely NPS, Retardation and decay. Flow chart below shows the model development process steps, model parameters estimation and outputs.